Space and Particles at the Planck Scale

by

Tomasz Konopka

A thesis
presented to the University of Waterloo
in fulfilment of the
thesis requirement for the degree of
Doctor of Philosophy
in
Physics

Waterloo, Ontario, Canada, 2007

I hereby declare that I am the sole author of this thesis.

This is a true copy of the thesis, including any required final revisions, as accepted by my examiners.

I understand that my thesis may be made electronically available to the public.

Abstract

The aim of this thesis is to summarize some results in two approaches to studying how quantum gravity may be relevant for experiments.

The first approach starts off by stating that one of the questions a theory of quantum gravity might address is how a large-scale universe can be constructed from discrete Planck-size elements. Starting from a discussion of the role of causal and foliation structure in causal dynamical triangulations, this approach leads to a formulation of a model based on graphs whose purpose is to uncover what kind organizational principle or structure might be responsible for endowing spacetime with manifold-like properties. Thus in this approach, experimental input used to constrain models for quantum gravity are observations of glaring large-scale properties of the universe such as the dimensionality or total size.

The second approach considers the possible effects of quantum gravity on the propagation of particles. In particular, the focus is on understanding the physics of deformed special relativity when this novel symmetry is seen as a residual effect due to a gauge fixing from a higher dimensional system. Thus here the hope is to connect a proposal for quantum gravity phenomenology with precision experiments of particle properties.

A synthesis of such complementary approaches would represent a consistent model for quantum gravity phenomenology and is the background goal for the work in this thesis. The extent to which such a synthesis can be described today is presented.

Acknowledgments

I would like to thank the Waterloo community for its warm hospitality over the past few years. In physics, I am appreciative of many stimulating discussions with collaborators and other members of the University of Waterloo and Perimeter Institute. Special thanks goes to my supervisor and co-supervisors at UW and PI: Fotini Markopoulou, Lee Smolin, Rob Mann, and Rob Myers.

Contents

List of Figures

1 Introduction

The action for gravity and matter fields is

$$S = \frac{1}{16\pi G}\int d^4x\sqrt{-g}\,(R+2\Lambda) + \int d^4x\sqrt{-g}\,\mathcal{L}_M. \tag{1.1}$$

It describes everything that is familiar in the universe: the Einstein-Hilbert term R defines the properties of spacetime in terms of a metric $g_{\mu\nu}$, Λ is the cosmological constant, and the Lagrangian $\mathcal{L}_M$ describes matter fields that propagate in the spacetime. In this view, matter content usually refers to everything that is not included in the metric field $g_{\mu\nu}$.

This dichotomy between space and matter allowed modern physics to progress very rapidly in the 20th century developing good understanding of the space and matter sectors independently. Within the matter sector, quantum field theory (QFT) provides techniques and interpretations that connect theoretical principles such as gauge invariance, unitarity, and Lorentz symmetry to real phenomena observed in the low-energy condensed matter laboratory as well as the very high-energy elementary particle accelerators. Due to the great successes of quantum field theory in describing non-metric fields, QFT techniques were also applied to quantize possible excitations of the metric, i.e. gravitational waves or gravitons, defined with respect to a fiducial background metric, usually the flat metric $\eta_{\mu\nu} = \text{diag}(-1,1,1,1)$. However, for technical reasons related to renormalization (one of the key techniques of QFT that allows to translate between calculations and the finite quantities recorded in experiments) it was realized that metric-based fields cannot be understood in the same way as the fields describing photons, electrons, quarks, and all the other elementary and composite particles.

The breakdown of QFT in the gravitational sector is usually taken as an indication for new physics related to the interplay between matter and gravity that is not encoded in (1.1). Research on quantum gravity aims to unravel and understand this new physics. Despite of this problem of fundamental nature, the action (1.1) is an extremely accurate description of known phenomena and is thus regarded as the correct low energy limit of the a true (or maybe only 'more true') quantum theory of gravity. The crossover or boundary between where the known description of physics is valid and the quantum gravitational regime is believed to be the 'Planck scale'. In the forms of length and energy, the Planck scale is

$$\ell_P = \sqrt{\frac{\hbar G}{c^3}} \sim 10^{-35}m, \qquad E_P = \sqrt{\frac{\hbar c^5}{G}} \sim 10^{19}GeV. \tag{1.2}$$

These quantities can be obtained through dimensional analysis by naive combinations of the physical constants of gravity (G), relativity (c) and quantum mechanics ($\hbar$).

Although the Planck scale is introduced above in a rather ad-hoc way, this scale does indeed characterize new physical effects in research programs on quantum gravity. One of

these programs, called Loop Quantum Gravity (LQG) [1], is based on the premise that perturbation theory around a fiducial flat spacetime is not an adequate technique to use in a setting where the spacetime geometry is dynamical and is actually expected to be an output to the theory rather than an input. Thus instead of studying quantum gravitational waves on a background, LQG considers an abstract Hilbert space for the gravitational degrees of freedom expressed in a set of variables that resemble those of a standard gauge theory. One of the key results in LQG is that when quantization is carried out in a way that is compatible with the diffeomorphism symmetry of classical general relativity, the kinematical states of the theory at the quantum level are characterized by graphs with labels called spin-networks [1]. These states are expected to correspond to spatial geometry and the discrete labels on the graph edges are directly responsible for the eigenstates of physical volume and area operators acquiring discrete spectra. The spacings in these spectra are proportional to the Planck area (ℓ_P^2) and Planck volume (ℓ_P^3). Thus in LQG geometry can be said to be discrete.

The fact remains that the Planck length ℓ_P is many orders of magnitude smaller than an atomic nucleus ($10^{-15}m$) and that the Planck energy is greater than the energy in a typical collider ($10^4\,GeV$ at the LHC) by a similarly large ratio. This fact is often used to explain why an effective description of reality based on (1.1) can be so successful in low-energy physics familiar from daily life even though it cannot in principle be the final state of our understanding of the world. At the same time, the extreme values of the Planck scale have caused concern that purely quantum gravitational phenomena can only be studied in the realm of thought experiments, thereby disconnecting research in quantum gravity from real experiments. But there is growing optimism regarding quantum gravity phenomenology due to two complementary trends and developments.

The first of these developments has a somewhat indirect impact on quantum gravity phenomenology. Several models have been considered in which the discreteness of geometry, such as found in Loop Quantum Gravity, is taken as indicating that geometry is made up of finite units or 'atoms' of space. For these ambitious models, a first step toward connecting with experiment is showing how a large scale universe might emerge. This step may, but does not have to, involve deriving (1.1) from something more fundamental. Further steps in these models include providing satisfactory explanations for early universe dynamics that are consistent with the growing number of observational constraints.

Second, it has been realized in the late 1990s [2] that certain experiments detecting ultra high energy particles from astrophysical sources (cosmic rays and hard radiation from gamma ray bursts) may be sensitive enough to pose bounds on possible quantum gravity-induced corrections to the matter sector of (1.1). Initial analysis of the particle processes involved were carried out using effective techniques, but more innovative models also now exist. All these models have the aim of describing how quantum gravity effects might leave imprints on particle physics at energies below E_P. Here the basic requirements are therefore to reproduce known physics at collider energies and to predict the results of upcoming experiments.

These two avenues for phenomenologically relevant quantum gravity research, and how they motivate the work in this thesis, are explained in more detail below.

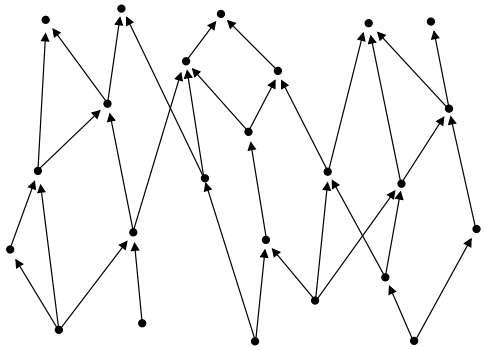

Figure 1: A causal set.

1.1 Discrete Models of Space and Spacetime

What if, instead of studying fields on a manifold, one postulates that space, or even spacetime, is made up discrete units? A theory of space would then have as a goal organizing these units together to make a large-scale universe. Since not even the existence of a manifold with fixed dimension would be presupposed, such a theory would be background independent and geometry would be purely a result of the dynamics between the discrete units. One might speculate that such a theory could be finite without needing renormalization, or that it could resolve the issue of singularities at the Big-bang or within black holes. But before such issues can even be formulated, it must be realized that the postulate of discrete units of space turns most of the notions in familiar physics on their heads: large scale properties of space cannot be assumed, near-continuity of space as seen by low-energy matter modes is unclear, and even the notions of particle or field must be reconsidered and redefined. The study of such a proposal must therefore start at a rather primitive level.

A notable proposal in which spacetime is discrete is the causal set program [3]. There, events in spacetime are represented by points and causal relations between the events are indicated by arrows - an example of a causal set is shown in Figure 1. This minimal body of properties is motivated by the observation that causal structure is sufficient to reproduce the geometry (metric) of a space up to a conformal factor. One of the interesting developments within the causal set program is a reconciliation of Lorentz symmetry and discreteness. However, while there is an accepted process (by Poisson sprinkling) by which a causal set can be generated from a spacetime manifold, it is still unclear how to build an approximation to a spacetime manifold starting only from points and arrows. Thus this research direction so far cannot make the first steps towards confronting experiment in the way discussed above.

A different approach to quantum gravity is through dynamical triangulations [4]. In that program, more complex units of space or spacetime are allowed (tetrahedra instead of points, for example) and the discretized Einstein-Hilbert action of (1.1) is used from the start. Still, only some dynamical triangulation models are able to generate homogenous and large scale structures that are comparable to the observed universe. This further demonstrates the non-triviality, already seen in the discussion of causal sets, of treating space (or spacetime) as being composed of a collection of discrete units. At the same time, the partial successes of a

few of the dynamical triangulation models suggest that the basic idea of discrete space is not entirely hopeless - what is needed is an understanding of what makes some models succeed and others fail, and thus to formulate a principle that explains how or why the observed universe has the large scale structure that it does.

1.2 Particle Phenomenology

A different approach to studying the implications of a Planck scale is to consider its possible effects on the propagation of low energy particles. An appealing property of such an approach is that it immediately offers opportunities to test various proposals experimentally.

Quantum field theory is the accepted description of low energy particle physics (energy low compared to the Planck length). An action principle for a scalar field interacting with itself is, for example,

$$S_\phi = \int \frac{d^4p}{(2\pi)^4}\ \phi(-p)(p^2 - m^2)\phi(p) + \mathcal{L}_{int}[\phi]. \tag{1.3}$$

This is here written in momentum space, m is the mass of the scalar field, and $\mathcal{L}_{int}$ encodes the self-interactions; the signature used in particle physics is $(1, -1, -1, -1)$. The way to describe possible physics characterized by an energy scale E_P in effective field theory is to append to the above action some new interaction terms of the form

$$S_P = \int \frac{d^4p}{(2\pi)^4}\ \left(\frac{1}{E_P}\mathcal{L}_P^{(1)} + \frac{1}{E_P^2}\mathcal{L}_P^{(2)} + \cdots\right), \tag{1.4}$$

where the terms $\mathcal{L}_P^{(1,2)}$ are of mass dimensions five and six so to appropriately cancel the Planck masses in the denominators, and the ellipses denote possible higher order terms which are however suppressed by higher orders of the Planck energy. These terms encode an effective description of Planck scale physics on the scalar field.

For studies of physics at energies low compared to the Planck energy, the higher order terms are often ignored and discussions are focussed on truncated expansions of S_P. Truncated models of this kind, however, usually break Lorentz symmetry. (Lorentz symmetry is unbroken if the new terms are by themselves Lorentz invariant. However, in such cases the new terms can be interpreted as a redefinitions of the mass parameter and are therefore not considered as true Planck scale corrections.) Thus the subject of studying possible Planck-physics effects on particle physics has been tightly correlated with testing Lorentz symmetry (see [33] for a review). The results of extensive studies show that correction terms of the form $\mathcal{L}_P^{(1)}/E_P$ in S_P above are practically ruled out on experimental grounds. This is quite remarkable in itself in a field where the relevant energy scale is as high as the Planck scale. Since then, however, a new question has been posed, namely whether the Planck energy can make an appearance in the Lorentz transformation equations as an invariant scale. The answer seems to be that it is indeed possible to consider such deformed transformation equations - the resulting framework has been called Doubly or Deformed Special Relativity (DSR). The task ahead of DSR is to understand the origins of such a deformed symmetry from a quantum gravity context and to work out its observational consequences.

1.3 Outline

The rest of this thesis explores the two themes described in more detailed. The first theme is the subject of sections 2 and 3, while the second theme is discussed in section 5. Section 4 is a bridge which shows correlations between the two themes.

In more detail, section 2 shows some results on the role of foliation structure within the causal dynamical triangulations program. Section 3 presents a different model in which an extended geometry is built up from discrete atoms of space. In section 4 the subject of discussion changes slightly to the relation between noiseless subsystems and constrained mechanics. This is related to the definition of particles and propagating degrees of freedom in background independent settings, which brings the discussion closer to particle physics phenomenology. Section 5 deals with a particular interpretation of Deformed Special Relativitic particles as solutions to a constrained system in five dimensions. Finally, a brief conclusion and outlook on these themes is presented in section 6.

2 Causal Dynamical Triangulations

Background independent approaches to quantum gravity often rely on the Feynman path integral (partition function). Given boundary conditions in the form of asymptotic past and future space-like slices, the path integral over intermediate geometries provides a means for evaluating the quantum amplitude for the evolution between the two slices. In practice one needs a method for defining and regularizing this integral over geometries - causal dynamical triangulations are a specific prescription for doing this which has recently gained attention [4].

A sum over geometries can be defined with the help of the concept, developed by Regge, that a macroscopic spacetime can be constructed by gluing together a large number of elementary elements. These elementary building blocks in general are called n-simplices, with n denoting the dimensionality; 0-simplices are points, 1-simplices are edges, 2-simplices can be faces of triangles, 3-simplices can be tetrahedra, etc. Although the geometry inside the individual simplices is flat, the way in which they are glued together can create a spacetime that has curvature at the connecting points or areas. A convincing example of how this may be possible is obtained by placing five equilateral triangles side be side so that they share a common vertex - the result is a surface with curvature at the common vertex.

The dimensionality of the model refers to the largest simplex which is deemed as elementary in a model. For example, the building blocks in $2+1$ dimensionsional models are the tetrahedra shown in Figure 2. These $2+1$ dimensional models are the focus of most of the discussion below. It should be stressed, however, that the all approaches to quantum gravity using simplicial methods, including dynamical triangulations, can be defined and studied in any dimension. The main reason for choosing $2+1$ dimensions for detailed studies is that in that case the relevant equations are simpler than in the more observationally relevant $3+1$ dimensions. (The simplification, however, is unrelated to the fact that General Relativity in $2+1$ is a topological theory, which is important in some other approaches. The discussion below does not rely on this topological property in the least.)

Dynamical triangulation models [4] are distinguished from other Regge-calculus based approaches by the fact that the type and geometry of the elementary building blocks is fixed. All the edges making up the tetrahedra are given fixed lengths squared and all the tetrahedra in a triangulation are alike. Interpolating geometries between slices are obtained by changing the gluing configurations of these simplices and not by varying some edge lengths in a fixed configuration. This scheme is advantageous particularly if one has in mind simulating the sum over geometries between given boundaries using a computer monte-carlo. It also allows to visualize variations over geometries by certain moves, sometimes called Pachner moves, that change one set of simplices into a new set that has the same boundary. Examples of such moves involving tetrahedra are shown in Figures 3 and 4.

Since the path integral is well defined (non-oscillatory) and can be evaluated only in

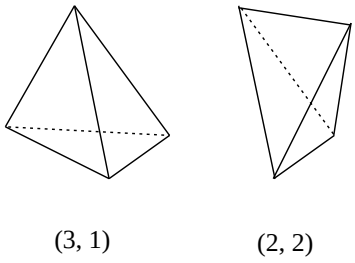

Figure 2: Simplices in 2+1 dimensions. Edges pointing mostly vertically (mostly sideways) are time-like (space-like). Simplices are named after the number of vertices on space-like surfaces.

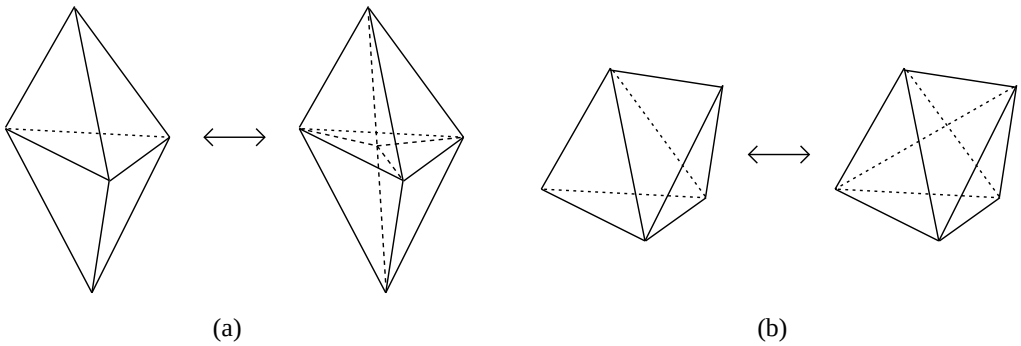

Figure 3: Moves manipulating a triangulation. (a) Two $(3,1)$ change into six $(3,1)$ tetrahedra. (b) A combination of one $(3,1)$ and one $(2,2)$ tetrahedra change into a combination with one $(3,1)$ and two $(2,2)$ tetrahedra.

Euclidean signature when it becomes a proper partition function, attention was initially devoted to purely Euclidean models. In the dynamical triangulation literature, this means that the sum over interpolating geometries was performed without any restrictions beyond those coming from the boundaries. Somewhat surprisingly, it was found that the most likely geometries arising in such models do not resemble at all any large-scale spacetimes [4]. The effective dimension of the likely configurations does not even match the dimensionality of the simplices used in the models. The culprit for the pathological behavior turns out to be the "Euclidean move" shown in Figure 4 (in three dimensions), which has the propensity of bunching too many simplices within a small boundary.

A fix for this problem is to formulate what are now called Causal Dynamical Triangulation (CDT) models [4]. These models retain the main philosophy of the original dynamical triangulation models but impose that every d-simplex should be time-orientable. For example, in $2+1$ dimensions, the elementary building blocks are again the tetrahedra in Figure 2; the lengths squared of the edges, however, are required to be space-like (positive) for some edges and time-like (negative) for others. The assignment of these edge-lengths is suggested in Figure 2: in the tetrahedron called $(3,1)$, for example, the edges of the base have positive length squared while the edges meeting at the peak of the pyramid have negative length

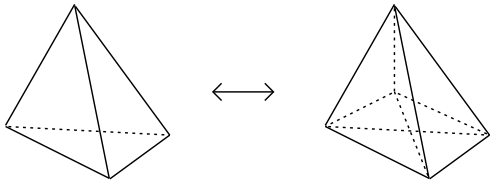

Figure 4: A move allowed in Euclidean triangulation models but not in Lorentzian ones.

squared. These assignments induce a causal order on the vertices in the tetrahedra and the names $(3,1)$ and $(2,2)$ help to encode these causal relations.

It turns out the moves in Figure 3 preserve the 'causal' assignments of edge lengths. The 'Euclidean move' in Figure 4, however, does not. Thus the move that causes difficulties in the Euclidean formulation is eliminated in the causal version. These models have again been studied numerically [4] and simulations (in $2+1$ and $3+1$ dimensions) suggest that causal dynamical triangulations generate large-scale space-times with desirable properties [4]. For example, the space-times appear to have an appropriate Hausdorff dimension on the large scale. They also seem to spontaneously demonstrate expanding and contracting behavior, the first of which is appealing given the current cosmological data.

As a consequence of the 'causal' restrictions, allowed configurations of simplices in CDTs can always be interpreted as foliated space-times in which every layer of simplices is separated from another layer by a space-like hypersurface formed by the faces of the simplices. Hence, there is a clear time-like direction and foliation structure in the macroscopic spacetime. Given the success of causal dynamical triangulations, it is interesting to ask how rigid the structure of the studied Lorentzian models really is: What are the consequences of loosening the assumptions in the original Lorentzian models, and is it possible to build more general models with the same low-energy properties? It is the task of this section to explore some aspects of this question.

The remainder of this section is organized as follows. The next subsection contains some more background material on Euclidean and Lorentzian causal dynamic triangulations models. The presentation of this material is a set up for section 2.2 where a model that includes foliation breaking simplices is introduced and studied. Some comments are presented in 2.3.

2.1 Euclidean and Lorentzian models

In the original Lorentzian (causal) model, all space-like edges have length-squared set to unity, and all time-like edges have length-squared equal to $-\alpha$, where α is a positive constant. Space-times formed by gluing these simplices together always have a layered structure so that the space-like faces of the $(3,1)$ tetrahedra make extended surfaces. These surfaces can be thought of as the discrete analogs of foliation hyper-surfaces.

The Regge Action

The Regge action corresponding to such a configuration is

$$S = k_0 \sum_a \left(-iV(a) \left(2\pi - \sum \theta \right) \right) + k_0 \sum_b \left(V(b) \left(2\pi - \sum \theta \right) \right) - \lambda \sum_c V(c), \qquad (2.1)$$

where the indeces a, b and c run over all space-like edges, time-like edges, and 3− simplices in the triangulation, respectively. k_0 is related to Newton's constant and λ is related to the cosmological constant. The real functions $V(a, b, c)$ denote the lengths of edges or volumes of tetrahedra, and the sums of θ's tally the dihedral angles subtended by faces meeting at an edge.

These volumes and dihedral angles can be computed using the techniques described by Hartle [9] and summarized here for convenience. For each tetrahedron, one first labels the vertices by numbers from 0 to 3. Then, to compute the area A of a face one uses the relation

$$A^2 = \left(\frac{1}{2!} \right)^2 \det \left(e_i \cdot e_j \right), \qquad (2.2)$$

where the entries of the matrix $e_i \cdot e_j$ are expressed in terms of square lengths s_{ij} between points i and j,

$$e_i \cdot e_j = \frac{1}{2} \left(s_{0i} + s_{0j} - s_{ij} \right). \qquad (2.3)$$

To compute the volume V of a tetrahedron, one can use the analogous

$$V^2 = \left(\frac{1}{3!} \right)^2 \det \left(e_i \cdot e_j \right). \qquad (2.4)$$

Dihedral angles θ subtended by two faces with areas A_1 and A_2 at an edge of length $L = \sqrt{s}$ can be obtained using

$$\sin \theta = \left(\frac{3}{2} \right) \left(\frac{LV}{A_1 A_2} \right). \qquad (2.5)$$

All these quantities can be computed explicitly for the two tetrahedra in Figure 2.

Inserting explicit expressions into the action, one obtains

$$\begin{aligned} S \;=\; & k_0 \left(\frac{2\pi}{i} N_1^S - \frac{2}{i} N_3^{(2,2)} \sin^{-1} \frac{-i2\sqrt{2}\sqrt{2\alpha+1}}{4\alpha+1} - \frac{3}{i} N_3^{(3,1)} \cos^{-1} \frac{-i}{\sqrt{3}\sqrt{4\alpha+1}} \right) \\ & + k_0 \sqrt{\alpha} \left(2\pi N_1^T - 4 N_3^{(2,2)} \cos^{-1} \frac{-1}{4\alpha+1} - 3 N_3^{(3,1)} \cos^{-1} \frac{2\alpha+1}{4\alpha+1} \right) \\ & - \lambda \left(N_3^{(2,2)} \frac{1}{12} \sqrt{4\alpha+2} + N_3^{(3,1)} \frac{1}{12} \sqrt{3\alpha+1} \right). \end{aligned} \qquad (2.6)$$

The variables N_1^S, N_1^T, $N_3^{(3,1)}$ and $N_3^{(2,2)}$ count the number of space-like edges, time-like edges, and 3−simplicies of the two kinds, respectively.

Although the model is formulated with Lorentzian signature, in order to put the partition function to good use, one has to perform a Wick rotation and write the model in Euclidean

space. In the present case, this rotation is simply realized by changing the sign of α. With $\alpha = -1$, some simplifications occur - various edge lengths, angles, and volumes related to the $(3,1)$ and $(2,2)$ tetrahedra become equal. It is then possible, by using some combinatorial manipulations, to write S as a function of $N_1 = N_1^T + N_1^S$ and $N_3 = N_3^{(3,1)} + N_3^{(2,2)}$ only. One finds

$$S \to iS_E; \qquad S_E = k_3 N_3 - k_1 N_1 \tag{2.7}$$

where k_1 and k_3 are

$$k_1 = 2\pi k_0, \qquad k_3 = k_A k_0 + \lambda k_V \tag{2.8}$$

and

$$k_A = 6\cos^{-1}\frac{1}{3}, \qquad k_V = \frac{1}{6\sqrt{2}}. \tag{2.9}$$

The Euclidean action can also be rewritten as

$$S_E = k_V N_3(\lambda - k_0\zeta) \tag{2.10}$$

where

$$\zeta = \frac{k_1}{k_0 k_V}\xi - \frac{k_A}{k_V}, \qquad \xi = \frac{N_1}{N_3}. \tag{2.11}$$

The action is traditionally discussed in terms of the dimensionless parameter ξ. The other parameter ζ, obtained from ξ by a re-scaling and a shift, is introduced here because it will be useful in the next subsection.

What is the allowed range for ξ (and consequently, ζ)? The range affects the partition function of the triangulation model in the large volume limit and therefore it is worth sketching how it can be estimated. One can write down an arbitrary configuration of tetrahedra and define a set of moves, i.e. manipulations of the triangulation, that allow to generate other configurations starting from the initial one. The minimal and maximal values of either of these parameters can be estimated from the way these moves change the configuration of simplices.

Interpolating Geometries and Partition Function

It is convenient to keep track of the interpolating configuration via a vector f counting the number of simplices of various kinds,

$$f = f(N_0, N_1^S, N_1^T, N_3). \tag{2.12}$$

Here N_3 is the sum of $(3,1)$ and $(2,2)$ types of $3-$simplices; they can be grouped together because their volumes are equal when $\alpha = -1$.

It is believed that just three types of moves are sufficient to manipulate an initial configuration of simplices into any other one. The moves are given names like $(a \to b)$, indicating that they change a configuration with a tetrahedra into another configuration with b tetrahedra. Two examples are shown in Figure 3. Under these moves, the f vector also changes as follows

$$\begin{aligned} \Delta_{(2\to 6)} f &= (1,\ 3,\ 2,\ 4), \\ \Delta_{(2\to 3)} f &= (0,\ 0,\ 1,\ 1). \end{aligned} \tag{2.13}$$

Starting with a triangulation consisting of N_1 edges and N_3 tetrahedra, one can construct another configuration by performing x moves of the $(2 \to 6)$ kind and z moves of the $(2 \to 3)$ kind. The total change in the f vector in such a transaction would be

$$\Delta f = (x,\, 3x,\, 2x + z,\, 4x + z), \tag{2.14}$$

giving a resulting ratio ξ of

$$\xi = \frac{N_1 + 5x + z}{N_3 + 4x + z}. \tag{2.15}$$

In the limit of large x and z, which corresponds to constructing triangulations of large volume,

$$\lim_{x\to\infty} \xi = \frac{5}{4}, \qquad\qquad \lim_{z\to\infty} \xi = 1. \tag{2.16}$$

These are in fact the upper and lower bounds for the parameter ξ after many substitutions, so the range for ξ is

$$1 \le \xi \le \frac{5}{4}. \tag{2.17}$$

Using (2.8) and (2.11), this can be translated into a range for ζ

$$-9.356 < \zeta < 3.973. \tag{2.18}$$

Note that after the Wick rotation, the 'Lorentzian' model does not appear different from what one could have started with for a 'Euclidean' model. For example, the Wick rotated $(3,1)$ simplex has the same properties as an equilateral tetrahedron in Euclidean space. What distinguishes the models, however, is the fact that in a a purely Euclidean model, a move of the type $(1 \to 4)$ shown in Figure 4 would be allowed. The Δf corresponding to that move would be

$$\Delta_{(1\to4)} f = (1, (4), 3), \tag{2.19}$$

where (4) denotes that there are four new edges created (their interpretation as time-like or space-like is unclear.) With this new move, the maximum parameter ξ would be pushed to $\xi \to 4/3$, correspondingly ζ would be pushed to $\zeta \to 8.416$.

As ζ (equivalently, ξ) appears in the action S_E, its range plays an important role in determining the partition function of the triangulation model [8]. The partition function is

$$Z(k_0, N_3) = \sum_T W(k_0, N_3, T) e^{-k_V N_3 (\lambda - k_0 \zeta)} \tag{2.20}$$

where $W(k_0, N_3, T)$ is a weighting function that depends on the symmetry of a configuration T and the sum is over all possible configurations having a fixed volume. (In the present situation, since all simplices have equal volume, the sum can be equally constrained by the total number of simplices N_3.) In the limit of a large fixed volume $k_V N_3$, the expression for the partition function can be considerably simplified. Up to an overall factor, Z can be written as

$$Z(k_0, N_3) \sim \sum_T W(k_0, N_3, T) e^{k_V N_3 k_0 \zeta}. \tag{2.21}$$

The number of triangulations is known to be asymptotically bounded from above by an exponential function [7]. This allows to rewrite the weighting function as

$$W(k_0, N_3, T) = f(k_0, N_3) e^{k_V N_3 s(\zeta)} \tag{2.22}$$

where $f(k_0, N_3)$ is a function that grows sub-exponentially with N_3, and $s(\zeta)$ is some function that can (in principle) be found using combinatorics. As a result of this substitution, the partition function becomes

$$Z(k_0, N_3) \sim \sum_T f(k_0, N_3) e^{k_V N_3 (s(\zeta) + k_0 \zeta)}. \tag{2.23}$$

Still working in the large $k_V N_3$ regime, the sum can be replaced by an integral; the integration variable can be taken to be ζ so that

$$Z \sim \int_{\zeta_{min}}^{\zeta_{max}} f(k_0, N_3) e^{k_V N_3 (s(\zeta) + k_0 \zeta)} \, d\zeta. \tag{2.24}$$

The limits on the integral indicate the minimum and maximum values that the parameter ζ can take. The integral is dominated by the configurations for which the expression $s(\zeta) + k_0 \zeta$ in the exponential is maximized in the allowed range $\zeta_{min} < \zeta < \zeta_{max}$. The position of the maximum depends on the precise form of $s(\zeta)$, but for k_0 large enough, it should occur at ζ_{max}. Contributions to the partition function at other values of ζ are exponentially smaller, so the partition function can be simplified further to

$$Z \sim \int_{\zeta_{min}}^{\zeta_{max}} f(k_0, N_3) e^{k_V N_3 (s(\zeta) + k_0 \zeta)} \delta(\zeta - \zeta_{max}) \, d\zeta = f(k_0, N_3) e^{k_V N_3 (s(\zeta_{max}) + k_0 \zeta_{max})}. \tag{2.25}$$

The final result is that the macroscopic properties of space-time are determined by the triangulations with the maximal value of ζ, namely $\zeta = 3.973$ (alternatively, with $\xi = 5/4$). These configurations are formed by repetitively applying the $(2 \to 6)$ move in (2.13).

It is worth comparing again the Lorentzian and Euclidean versions of the dynamical triangulation models. These models differ in that the partition function of the Euclidean version includes a sum over more configurations than the Lorentzian version, which is reflected by the different ranges for ζ or ξ. The extra configurations counted in the Euclidean models are those that do not respect the foliation structure present in the Lorentzian models and are generated by the $(1 \to 4)$ moves. Numerical studies of these models show that the Euclidean and Lorentzian versions have very different properties [4]. The Lorentzian version produces well behaved spacetimes whereas the Euclidean one does not. Those results suggest to treat the parameter ζ as an indicator to the large scale behavior of a model. In the next subsection, a modified Lorentzian model is introduced with the goal of studying the robustness of the original Lorentzian model.

2.2 Role of foliation structure

A different model is now presented in which the foliation is 'punctured' in the sense that a new type of simplex is allowed to probe multiple layers of tetrahedra. There are several

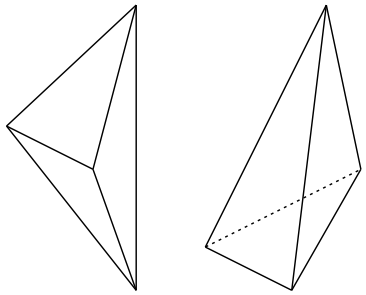

Figure 5: Simplices in 2+1 dimensions that span two foliation layers.

types of tetrahedra that can puncture the foliation in this way: two of them are shown in figure 5. In the $(1, 2, 1)$ simplex, for example, two vertices are spatially separated from each other but are at the same time in the causal future of the third vertex and in the causal past of the fourth; the notation $(1, 2, 1)$ again denotes the number of the vertices on distinct and consecutive causality levels. The foliation, in the sense of the original triangulation model, is punctured by the $(1, 2, 1)$ tetrahedron because it does not have a space-like face that passes through the spatially separated vertices. Thus, when these simplices are present, it is generically impossible to construct space-like hyper-surfaces that span all of the space-time.

The presence of (1,2,1) tetrahedra may affect the large volume behavior of dynamical triangulations. To investigate this possibility, consider a simple model in which there are $(3, 1)$, $(2, 2)$ and $(1, 2, 1)$ simplices, all space-like edges have length-squared equal to 1, all time-like edges of the $(3, 1)$ and $(2, 2)$ tetrahedra and the shorter sides of the $(1, 2, 1)$ simplex have length-squared $-\alpha$, and the longer time-like edges of the $(1, 2, 1)$ tetrahedron have length-squared $-\beta$.

The Action

The action for this model is an extension of $S_{original}$ in (2.6) by terms specific to the new simplex type,

$$\begin{aligned} S =& S_{original} - k_0 \left(\frac{1}{i} N_3^{(1,2,1)} \cos^{-1} \frac{(4\alpha - 2\beta + 1)}{4\alpha + 1} \right) \\ & - \sqrt{\alpha} k_0 \left(4 N_3^{(1,2,1)} \cos^{-1} \frac{\sqrt{\beta}}{\sqrt{4\alpha + 1}\sqrt{\beta - 4\alpha}} \right) \\ & + \sqrt{\beta} k_0 \left(2\pi N_1^L - N_3^{(1,2,1)} \cos^{-1} \frac{4\alpha + 2 - \beta}{4\alpha - \beta} \right) \\ & - \lambda \left(N_3^{(1,2,1)} \frac{1}{6} \sqrt{\frac{1}{4}\beta^2 - \frac{1}{4}\beta + \alpha\beta} \right). \end{aligned}$$

The variable N_1^L counts the number of the 'long' time-like edges that have length-squared $-\beta$. The meaning of $N_3^{(1,2,1)}$ is as expected the number of tetrahedra of the new kind. Expressions for volumes and dihedral angles for the $(1,2,1)$ tetrahedron are computed using the methods described before.

To study the statistical properties of this model, the action should be Wick-rotated into Euclidean space. For the current purposes, this merely means choosing negative values for α and β such that the action becomes purely imaginary. For the part of the action depending on the $(3,1)$ and $(2,2)$ simplices, this can be done by taking $\alpha \to -1$ as before. As for the part of the action specific to the new simplex, a value of β in the range between -4 and -1 satisfy the required $S \to iS_E$ and S_E is real.

After the Wick rotation, the general form of the action is

$$S_E = (k_A k_0 + \lambda k_V)\, N_3^{(3,1)+(2,2)} + (k'_A k_0 + \lambda k'_V)\, N_3^{(1,2,1)} - \left(k_1 N_1^{S+T} + k'_1 N_1^L\right), \tag{2.26}$$

where k_1, k_A, and k_V are the same as in (2.8). The primed variables can be computed from (2.26) by fixing β. Now, S_E can be written in a form similar to (2.10) by factorizing the volume terms. The result is

$$S_E = V\,(\lambda - k_0 \zeta') \tag{2.27}$$

where

$$V = k_V N_3^{(3,1)+(2,2)} + k'_V N_3^{(1,2,1)} \tag{2.28}$$

and

$$\zeta' = \frac{k_1}{k_0}\frac{N_1^{S+T}}{V} - k_A \frac{N_3^{(3,1)+(2,2)}}{V} + \frac{k'_1}{k_0}\frac{N_1^L}{V} - k'_A \frac{N_3^{(1,2,1)}}{V}. \tag{2.29}$$

Here ζ' is a generalization of ζ in (2.11).

The Partition Function

Since the form of the action S_E is the same as (2.10), the study of the statistical mechanics of this new model can be carried out along similar lines as previously. The partition function for the new model,

$$Z'(k_0, N_3) = \sum_T W'(k_0, N_3, T) e^{-k_V N_3 (\lambda - k_0 \zeta')}, \tag{2.30}$$

is like in (2.20). The summation is still restricted by the total volume but is now over all possible triangulations that may include the new simplex type - thus there are now more triangulations to sum over. As before, however, W' should be asymptotically bounded by an exponential in the large-volume limit. By the same reasoning as before, the sum can therefore be replaced by an integral over ζ,

$$Z' \sim \int_{\zeta'_{min}}^{\zeta'_{max}} f(k_0, N_3) e^{V(s(\zeta') + k_0 \zeta')}\, d\zeta'. \tag{2.31}$$

The dominant contribution to the integral comes from the values of ζ' that maximize the exponent. Under the same assumptions as before, one concludes that for k_0 large enough,

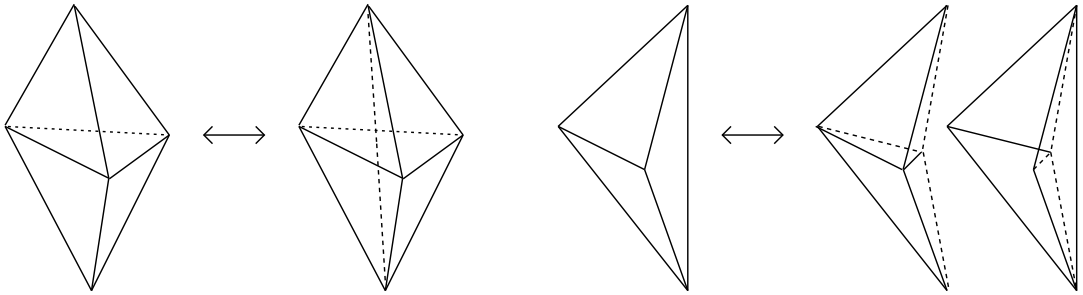

Figure 6: New moves manipulating $(1,2,1)$ simplices. (a) Two $(3,1)$ change into three $(1,2,1)$ tetrahedra. (b) One $(1,2,1)$ changes into two $(1,2,1)$ and two $(3,1)$ tetrahedra. The $(3,1)$ simplices appear distorted in the diagram.

the partition function should be dominated by maximal values of ζ'. Thus, in that approximation,

$$Z' \sim \int_{\zeta'_{min}}^{\zeta'_{max}} f'(k_0, N_3) e^{V(s(\zeta')+k_0\zeta')} \delta(\zeta' - \zeta'_{max})\, d\zeta' = f'(k_0, N_3) e^{V(s(\zeta'_{max})+k_0\zeta'_{max})}, \qquad (2.32)$$

which is completely analogous to (2.25).

What is left to explore is how ζ'_{max} differs from ζ_{max}. The governing assumption is that the new parameter ζ'_{max} can serve as an indicator of large-volume behavior just like ξ in the case of the original Euclidean and Lorentzian models. If this assumption is correct, and if the two values ζ_{max} and ζ'_{max} are the same, then the partition functions of the models would differ only by a multiplicative factor and the physics of the two models would be similar. To investigate the range of ζ', one can once again explore how various moves affect configurations of tetrahedra.

Because ζ reduces to ξ in the limit $N_3^{(1,2,1)} \to 0$, the moves defined in (2.13) suggest that values for ζ' within the range (2.18) should be allowed in the extended model as well. But new moves are now possible as well. In particular, it is important to consider moves that change the number of $(1,2,1)$ tetrahedra. Two such moves are shown in figure 6. The first move is of limited applicability since it cannot be used repeatedly. It does, however, show how to introduce the foliation puncturing simplices into a triangulation that initially contains only $(3,1)$ and $(2,2)$ tetrahedra. The second move can be applied repeatedly and may therefore have an effect on the maximum value of ζ'. It is worth noting that other moves that rearrange simplices while keeping a boundary surface fixed are also possible. However, the two moves shown in the figure are sufficient to discuss the large-scale behavior of the extended model.

The state of the configuration can be described by the vector

$$f' = f'(N_0, N_1^S, N_1^T, N_1^L, N_3^{(3,1)}, N_3^{(2,2)}, N_3^{(1,2,1)}). \qquad (2.33)$$

The two moves shown in the figure, denoted as $(2 \to 3)'$ and $(1 \to 4)'$, change this vector by

$$\begin{aligned} \Delta_{(2\to 3)'} f' &= (0,\, 0,\, 0,\, 1,\, -2,\, 0,\, 3), \\ \Delta_{(1\to 4)'} f' &= (1,\, 2,\, 2,\, 0,\, 2,\, 0,\, 1). \end{aligned} \tag{2.34}$$

After a large number of moves of the $(1 \to 4)'$ type, ζ' would be

$$\zeta' = \frac{k_1}{k_0}\frac{4}{2k_V + k'_V} - k_A \frac{2}{2k_V + k'_V} - k'_A \frac{1}{2k_V + k'_V}. \tag{2.35}$$

The numerical value of expression (2.35) depends on the value of β, the length-squared of the long edge of the $(1, 2, 1)$ simplex, which should be between -4 and -1. Such values of β give ζ' in the range

$$6.42 < \zeta' < 8.4 \tag{2.36}$$

and take ζ'_{max} above the Lorentzian level (2.18), but still keep it below the Euclidean level.

Implications

What does this result mean in the context of previous work on Euclidean and Lorentzian dynamical triangulation models? Unfortunately, the meaning of this result is not entirely clear because the behavior of dynamical triangulation models as a function of ζ has never been studied. However, if the parameter ζ is indeed a good indicator for the low energy behavior, as assumed, then the behavior of the extended model should be intermediate between the purely Euclidean and the original Lorentzian cases. More generally, one can say that this extended Lorentzian model is likely to have a different low energy behavior than either the Euclidean model or the original Lorentzian model. The strength of the deviation from either model is difficult to judge and one may still hope that some of the desirable properties of the original Lorentzian model are preserved. To make more precise statements about the low energy behavior, one would need to simulate the extended model on a computer similarly as done for the original models.

One should note, that the result the analysis could have yielded a different answer had the new moves in Figure 6 not caused a significant change in the vector f. If one were to restrict the new moves to the type shown in Figure 6(a) and disallow the move shown in Figure 6(b), the bounds on ζ in the extended model would have been exactly as in (2.18), and the conclusion of this section would have been that the extended model behaved equivalently to the original Lorentzian model. While such restrictions could be artificially introduced, it seems more natural to consider all kinds of configurations compatible with the simplices to be present in the sum over triangulations. The ambiguous result should thus been seen as a hint that there are still important issues to be understood about dynamical triangulations models and the conditions under which they exhibit a good low-energy behavior.

2.3 Discussion

Dynamical triangulations models aim at constructing likely geometries between boundary slices. The known discrepancies between the results of the Euclidean and Lorentzian versions

demonstrate that obtaining smooth interpolating geometries is non-trivial and cannot be easily grasped by a quick inspection of the simplex geometry or the action. The apparent success of the Lorentzian models suggests that causal structure may be of importance in making dynamical triangulations a candidate for a successful formulation of quantum gravity. Thus the role of causal structure is a very interesting and relevant one to study.

An aspect of the original model is connected with the types of simplices used as the primary building blocks of space-time. The existence of global hyper-surfaces constructed from the space-like faces of simplices can be compromised by introducing new types of simplices into the triangulation. Introducing new types of simplices that puncture the hyper-surfaces foliating the space-time causes triangulation models to generally behave differently than the original models. (The extended models can, in principle, reproduce the familiar behavior if additional constraints are introduced to restrict the number of foliation-puncturing simplices that appear in the triangulations. Alternatively, a similar effect may be achievable by tuning k_0. Such restrictions, however, seem ad-hoc and are not very appealing.) Thus, the extended model suggests that giving each simplex a clear internal arrow-of-time might not be sufficient to reproduce the results of the original Lorentzian CDTs. It might be the case that those results found in simulations actually require the presence of hyper-surfaces in addition to causal structure. This may have important implications on the kind of discretizations that are consistent with a well-behaved classical limit of quantum gravity.

Another important aspect of the original Lorentzian model is the requirement for all time-like edges to have equal length-squared, which can be thought of as a 'lapse' constraint. In $1+1$ dimensions, it has been shown that this requirement on the individual simplices can be removed, allowing their shapes and sizes to fluctuate, as long as a global constraint on the ensemble of simplices in the entire space-time is enforced instead [5]. As shown in [6], a generalization to higher dimensions is also possible: analogous global constraints can be interpreted as specifying average volume and/or curvature contributions for the simplices in the triangulation. This holds in $2+1$ as well as higher dimensions. Adopting this point of view, the dynamical triangulation models are brought closer to other simplicial gravity models in which the simplices are non-fixed. The fact that the properties of the dynamical triangulation models under these extended conditions are largely unchanged further suggests that foliation plays a crucial role in stabilizing these models.

3 Quantum Graphity

Given that some dynamical triangulation models are successful at constructing a large-scale universe while others are not puts forth the question: what kind of organizing principle is needed for the notion of a discrete universe to make sense? This issue can also be seen in the light of the causal sets program in which, as mentioned in the introduction, it is yet not understood how to assemble a universe from just points and causal relations. A method for studying this is therefore relevant for several research areas.

To motivate the "quantum graphity" proposal [11], it is worth comparing and merging a few selected features from the causal dynamical triangulations and causal programs. On the one hand, the idea behind causal sets is minimal, simple, and elegant: there are only points and causal relations as the basic objects. However, the nature of the approach is perhaps too minimal since there is no known way of writing a Lagrangian or Hamiltonian for causal sets. Thus, despite some work on growth algorithms [10], there is no accepted way of discussing kinematics or dynamics in causal sets. In other words, it is unknown how to generate a causal set that approximates a manifold. On the other hand, dynamics is well-defined (if not well understood) in the causal dynamical triangulation program through the Einstein-Hilbert action and the Regge calculus. For this to be possible, however, CDTs introduce higher-dimensional building blocks and require complex and restricted evolution rules (moves). Also, even though CDT models are dubbed as Lorentzian, practical calculations are nonetheless performed after Wick rotation to Euclidean signature.

Since, as in CDTs, path integrals are manageable only in Euclidean form, it is natural to start with a Euclidean model. Thus, the proposal is to study a model that is as minimal as possible in which nonetheless an emergent geometry might occur. The name "quantum graphity" is a play on the words "gravity," i.e. a theory of the spacetime, and "graph" which is the primary object discussed in the model. By formulating the model in the Hamiltonian language also allows to bring this line of research close to condensed matter physics, towards which one can look for inspiration to write an explicit form of the Hamiltonian.

A relatively recent development in condensed matter physics has been the discovery of a new type of matter phase dubbed as string-net condensate [12, 13]. Driven by the experimental discovery of the fractional quantum Hall effect in the 1980s and the subsequent theoretical efforts to understand the phenomenon, research on string-net condensates shows that quantum superpositions of one-dimensional objects on a lattice can give rise to surprising collective behavior and a new kind of phase transitions. In particular, a model in which links between lattice sites are given rotor-like states can exhibit gauge-theory particle excitations in the thermodynamic limit [13]. For the purposes of the quantum graphity model, the Hamiltonian of this rotor model is interesting because it can be formulated in a combinatorial manner by using only the connectivity between sites. Furthermore, the interpretation and implications of the terms of the rotor Hamiltonian are known. Therefore, the Hamiltonians

of string-net condensates can be used as guides for a model aiming to implement emergence of classical geometry.

The remainder of this section is organized as follows. The defining structures of the quantum graphity model are presented in the next subsection. Two versions of the model are presented, called 'classical' and 'quantum;' it is the quantum version which is ultimately of physical interest although the classical model is the easier one to understand and study. Next, the high and low temperature phases of the model are studied in section 3.2. The discussion includes an explanation of the emergence of a gauge theory at low temperature and a possible cosmological scenario. Finally, section 3.3 mentions some possible extensions and/or changes to the basic model described which could be considered; some of these inessential modifications have aesthetic appeal but their main purpose is to highlight which features of the basic model are flexible and which are not.

3.1 Model Definition

A complete graph with N nodes is a collection of N points that are all connected to each other by edges - there are thus

$$M = \frac{N(N-1)}{2} \tag{3.1}$$

edges in total. For convenience, the points (nodes) can be labeled by lower-case Latin letters $a, b, \ldots = 1, 2, \ldots$; edges can be identified by stating their end points.

Graphs are very abstract objects and can be defined and studied irrespectively of any background geometry or embedding space. Starting from a complete graph, however, one can remove certain edges and form less symmetric networks which in some cases may be assigned some geometric interpretations. Two such examples are shown in Figure 7. Therefore, a complete graph is a reasonable starting point for constructing a background independent model which might exhibit emergent geometry. What is necessary is to make the notion of erasing edges more precise and to give a systematic principle for which edges should be thus removed.

Hilbert Space and Operators

Since the edges of the graph must be assigned at least the properties of being "on" or 'off," it seems natural to associate to each edge in the graph a Hilbert space of states. For the purpose of this model, this Hilbert space $\mathcal{H}_{edge}$ is taken to be spanned by four states,

$$\mathcal{H}_{edge} = \text{span}\,\{|0,0\rangle, |1,-1\rangle, |1,0\rangle, |1,+1\rangle\}. \tag{3.2}$$

The interpretation of the state $|0,\, 0\rangle$ is that there is no link between two points; thus this state is called an "off" state. The remaining states, of which there are three and all have 1 in their first entry, are called "on" states. More generally the states can be referred to with the notation $|j,\, m\rangle$.

Several operators can be defined acting on the Hilbert space of each edge. The first two operators, J and M, are eigen-operators of the states $|j,\, m\rangle$ such that

$$\begin{aligned} J\,|j,\, m\rangle &= j\,|j,\, m\rangle \\ M\,|j,\, m\rangle &= m\,|j,\, m\rangle. \end{aligned} \tag{3.3}$$

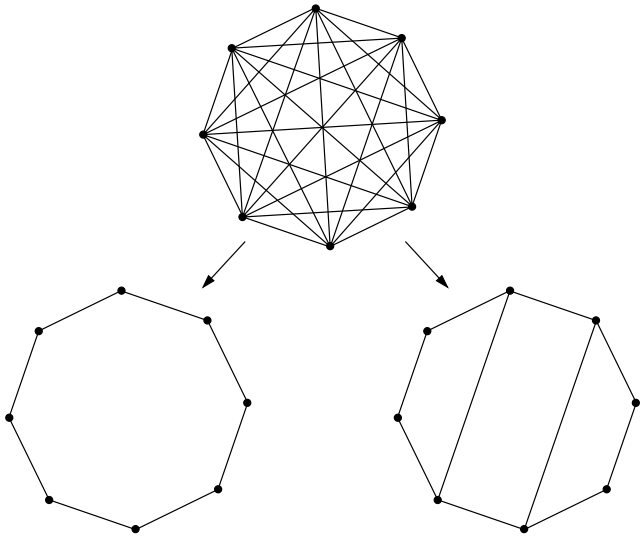

Figure 7: A complete graph with 8 nodes (top) can be transformed into a $1d$ chain (left) or $2d$ sheet (right) by erasing selected edges.

The remaining operators are not eigen-operators of $|j,\, m\rangle$. Two operators J^+ and J^- alternate between "off" on "on" states; their definitions are best stated by listing their actions on all the states,

$$\begin{aligned} J^+ |j,\, m\rangle &= \begin{cases} |1,\, 0\rangle & j = 0,\, m = 0 \\ 0 & \text{otherwise} \end{cases} \\ J^- |j,\, m\rangle &= \begin{cases} |0,\, 0\rangle & j = 1,\, m = 0 \\ 0 & \text{otherwise} \end{cases} \end{aligned} \tag{3.4}$$

The next two operators are M^+ and M^- are raising and lowering operators among the m states. Their definitions can be succinctly written as

$$\begin{aligned} \sqrt{2}\, M^+ |j,\, m\rangle &= \sqrt{(j-m)(j+m+1)}\, |j,\, m+1\rangle \\ \sqrt{2}\, M^- |j,\, m\rangle &= \sqrt{(j+m)(j-m+1)}\, |j,\, m-1\rangle. \end{aligned} \tag{3.5}$$

The commutation relations between these operators can be derived from these definitions. A few facts of particular interest are worth pointing out explicitly. The operator J commutes with M and $M^\pm$,

$$[J, M] = [J, M^\pm] = 0. \tag{3.6}$$

These M and $M^\pm$ in turn form a closed algebra among themselves

$$[M^+,\, M^-] = M, \qquad [M,\, M^\pm] = \pm M^\pm. \tag{3.7}$$

An important fact is also that all operators J, M, $M^\pm$, annihilate the "off" state

$$J\, |0,\, 0\rangle = M\, |0,\, 0\rangle = M^\pm\, |0,\, 0\rangle = 0. \tag{3.8}$$

Finally, if the $|j,\, m\rangle$ have unit normalization

$$\langle j,\, m|j',\, m'\rangle = \delta_{jj'}\, \delta_{mm'}, \tag{3.9}$$

then all matrix elements for these operators are either zero or have unit magnitude.

As an aside, note that there is a close resemblance between these definitions and standard quantum mechanics. The Hilbert space $\mathcal{H}_{edge}$ is the same as the space of states of a spin 1 particle, and the above-defined operators J, M, and $M^{\pm}$ are closely related to the familiar angular momentum operators J^2, J_z, $J^{\pm}$. However, these similarities should be viewed more as a coincidence rather than as carriers of deep insight. To emphasize this point, note the fact that there are three "on" states with $m = 0, \pm 1$ is not a consequence of or associated in any way with the dimensionality of any background space. A related issue is that analogs of operators such as J_x, J_y, and J_z from standard quantum mechanics, although can be defined here, do not have the interpretation of measuring components of a spin in certain spatial directions because, in this model, there is no ambient space and hence no notion of x, y, or z. A possible way to remember this distinction is perhaps to note that the operators defined here differ from the familiar ones in quantum mechanics by several factors of $\sqrt{j_{max}(j_{max}+1)} = \sqrt{2}$. The true purpose of these factors, and what may be perceived as strange definitions (3.3),(3.5), is to give these operators straight-forward interpretations from the graph-theoretic perspective. This will become clearer in the discussion of the system Hamiltonian.

Returning to the discussion of the present model, define the full Hilbert space of the system of the complete graph with N points and $N(N-1)/2$ edges as the tensor product

$$\mathcal{H}^{(N)} = \otimes^{N(N-1)/2}\, \mathcal{H}_{edge}. \tag{3.10}$$

The normalization of states in this large Hilbert space follows from (3.9). The operators acting on this large Hilbert space are constructed from the local operators defined above. For example, an operator J_{ab} acts non-trivially on the Hilbert space $\mathcal{H}_{edge}$ of the edge between nodes labeled a and b, and as an identity on the other parts of $\mathcal{H}^{(N)}$. Several kinds of extensions to $\mathcal{H}^{(N)}$ are possible. For example one can consider associating a Hilbert space to the nodes of the graph, or connecting two nodes by more than one edges. Other extensions and variations are mentioned briefly at the end of this section. The remainder of this section, however, deals with the basic definition of the total Hilbert space that appear in (3.10).

The Hamiltonian

The proposed Hamiltonian for the model is

$$\hat{H} = \hat{H}_V + \hat{H}_C + \hat{H}_D + \hat{H}_B^{(c/q)}(+\hat{H}_{hop} + \hat{H}_{LQG}) \tag{3.11}$$

where the individual terms are

$$\hat{H}_V = V \sum_a \left(v_0 - \sum_b J_{ab} \right)^2 , \tag{3.12}$$

$$\hat{H}_C = C \sum_a \left(\sum_b M_{ab} \right)^2 \tag{3.13}$$

$$\hat{H}_D = D \sum_{ab} M_{ab}^2 , \tag{3.14}$$

$$\hat{H}_B^{(c)} = - \sum_{\text{loops}} B(L) \prod_{i=1}^{L} M_i, \tag{3.15}$$

$$\hat{H}_B^{(q)} = - \sum_{\text{loops}} B(L) \prod_{i=1}^{L} M_i^{\pm}. \tag{3.16}$$

The terms in parenthesis, denoted H_{hop} and H_{LQG}, need not be specified explicitly but are discussed below qualitatively.

The notations in these terms deserve some explanations and may need some getting used to. Physical interpretations of each term is given further below.

In the first term, $\hat{H}_V$, V is a positive coupling constant, v_0 is a fixed number, and the sums are over all points in the graph. The object inside the parenthesis is the difference between a fixed number v_0 and the number of "on" links adjacent to a node labeled a. This difference is raised to an even power to make it a positive quantity. This positive quantity, times the coupling constant V, is the energy associated with the node a due to the links adjacent to it. There is one such contribution for each node a in the graph. Because of the even power, the minimum of H_V occurs when the number of "on" links adjacent to every node in the graph is exactly v_0.

The remaining listed terms depend on operators M and $M^{\pm}$ and not on J. Thus they only contribute when they act along links that are "on."

The interpretation of the sums in $\hat{H}_C$ is similar to that of $\hat{H}_V$. This time, however, the term is minimized when the m values on the edges adjacent to each vertex add up to zero (the coupling constant is taken $C > 0$). That is, this term is minimized when either all m values at a node are exactly equal to zero, or if there is an equal number of edges with $m = +1$ as there are edges with $m = -1$. The term $\hat{H}_D$, however, gives preferences to configurations in which exactly all edges have $m = 0$ (again, the coupling constant satisfies $D > 0$).

The next terms in the Hamiltonian are $\hat{H}_B^{(c)}$ and $\hat{H}_B^{(q)}$; the understanding is that only one of these two kinds of terms will be considered in a model at a time (see however section 3.3). The sums in each terms are over loops - closed paths that begin and end at the same node. The products of operators are defined over a closed sequence of edges as follows

$$\prod_{i=1}^{L} M_i \; = \; M_{ab} \, M_{bc} \, \ldots \, M_{yz} \, M_{za} \tag{3.17}$$

and

$$\prod_{i=1}^{L} M_i^{\pm} \;=\; M_{ab}^{+} M_{bc}^{-} \ldots M_{yz}^{+} M_{za}^{-}. \tag{3.18}$$

The parameter L in each product is the length of the loop, i.e. the number of edges that go into the closed path defining the loop. In each case, the product instructs to multiply the edge from node a to node b by an operator, then multiply the edge from node b to node c by another operator, and so forth until the path is closed back at node a. In the $\hat{H}_B^{(q)}$ version of this product, the operators alternate between M^+ and M^-, and hence the length L of the considered loops must be even. For simplicity, the same restriction can be imposed (by hand) on the loops of $\hat{H}_B^{(c)}$. Note that a given on graph defined by an assignment of "on" links can have loops of varying lengths.

For these loop terms, the coupling is taken to be dependant on the loop length L. The explicit form of the coupling is a choice in the model, and can is taken here to be

$$B(L) = \frac{1}{L!} B_0 B^L \tag{3.19}$$

where B_0 is a positive coupling constant and B is dimensionless. The separation of B from B_0 is useful because B can be now associated with each instance of M (or $M^{\pm}$) in the loop products. The factor $L!$ in the denominator is a combinatorial contribution. This choice of $B(L)$ has the property that it can be small at very low and at very high lengths L and have a maximum value at some particular length L_*,

$$\frac{B^{L_*}}{L_*!} > \frac{B^{L'}}{L'!} \qquad \forall L' \neq L_*. \tag{3.20}$$

This loop length L_* is called the preferred loop length.

The last two terms in the Hamiltonian are H_{hop} and H_{LQG}. These need not be specified in detail, but a brief description is in order. The description of $\hat{H}_{hop}$ is deferred to the discussion of the 'quantum version' of the model below. The final term $\hat{H}_{LQG}$ is such that allows certain edges to turn between their "on" and "off" states; thus it would have to be formulated in terms of operators J^+ and J^-. Some examples of suitable actions for the graph-changing term are illustrated in Figure 8. They appear as local moves changing the connectivity between nodes in the graph, and their role is precisely to allow the system to sample the configuration space by morphing one arrangements of j assignments into another one. For the most part of the analysis and discussion below, these terms are assumed not to alter significantly the equilibrium and ground state of the model.

Definition of Loops

Before discussing the physical interpretation of the terms in the Hamiltonian and the model as a whole, some more remarks on the definitions of loops are in order.

In the products (3.17) and (3.18), the repeated indices a, b, etc. are summed over. However, two restrictions should be imposed. First, the loops should not be self-intersecting - this means that a closed path from point a back to point a should traverse intermediary

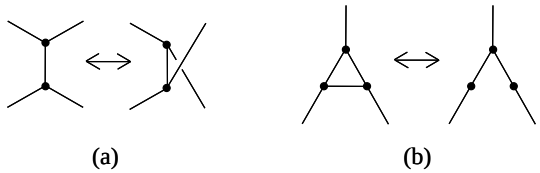

Figure 8: Examples of terms in Hamiltonian H_{LQG} that acts on j variables. (a) Exchange of neighboring links. (b) Addition or subtraction of an edge.

points only once. Second, it is also helpful if two loops ℓ_1 and ℓ_2 are allowed into the Hamiltonian only if their intersection is either null, a single node or one or two edges. Loops which intersect overlap on more than two edges seem to be problematic, at least the first stages of thinking of the model. Perhaps the role of intersecting loops can be worked out in the future, but at the present stages of the model's development, it is best to avoid them.

The first restriction may be implemented, for example, by carefully summing over points b to avoid the base point a, to avoid nodes a and b when summing over nodes c, etc. There is also another way in which a similar effect can be achieved. It is more involved, but it does have the attractive feature of being also able to deal with the second restriction.

Suppose that a two dimensional Hilbert space (qubit) is introduced

$$\mathcal{H}_{qubit} = \text{span}\,\{|0\rangle,\, |1\rangle\} \tag{3.21}$$

and suppose that n such qubits are associated with each node

$$\mathcal{H}_{node} = \otimes^n \mathcal{H}_{qubit}. \tag{3.22}$$

(The full Hilbert space for the quantum graphity system would be suitable enlarged.) Next introduce raising and lowering operators on each of the qubits, which act as

$$\begin{aligned} a_\mu^\dagger|0_\mu\rangle &= |1_\mu\rangle, \qquad a_\mu|0_\mu\rangle = 0, \\ a_\mu^\dagger|1_\mu\rangle &= 0, \qquad a_\mu|1_\mu\rangle = |0_\mu\rangle; \end{aligned} \tag{3.23}$$

Here the subscript μ labels which copy of $\mathcal{H}_{qubit}$ the states belong to. Such operators could be introduced into the loop products as follows

$$\prod_{i=1}^{L} M_i^{\pm} \to \prod_{i=1}^{L} M_i^{\pm}(a, a^\dagger) \;=\; M_{ab}^{+} a_a^\dagger \, M_{bc}^{-} a_b^\dagger \, \ldots M_{yz}^{+} a_y^\dagger \, M_{za}^{-} a_z^\dagger \, + h.c.. \tag{3.24}$$

There should be a distinct set of operators a and $a^\dagger$ for each of the n copies of $\mathcal{H}_{node}$.

Because the Hilbert space of the qubits is fermionic ($a^\dagger a^\dagger = 0$ acting on the same Hilbert space), such loop terms would not contribute to the Hamiltonian unless all the points visited by the loop would be distinct. Also, since the number of qubit species is fixed at n, only a maximum number of n loop operators could possibly give non-trivial contributions at a particular node, hence implementing an upper bound on the number of loops supported at a node.

This method with an auxiliary fermionic Hilbert space is useful to show that the said restrictions on the loop operators can actually be consistently implemented. In the following, the rather cumbersome notation with the node operators a and $a^\dagger$ will be avoided but the restrictions will nonetheless be assumed to hold whenever a sum over loops is invoked.

Classical Version

A simplified version of the Hamiltonian $\hat{H}$ in (3.11) is

$$\hat{H}_{VB} = \hat{H}_V + \hat{H}_B^{(c)} (+\hat{H}_{LQG}). \tag{3.25}$$

Ignoring the last term $\hat{H}_{LQG}$, this Hamiltonian $\hat{H}_{VB}$ can be called 'classical' because the operators in $\hat{H}_V$ and $\hat{H}_B^{(c)}$ commute with each other. The last, graph-changing, term formally does not commute with the others but if attention is restricted only to static or equilibrium configurations, the discussion here should be valid.

What is the meaning of $\hat{H}_{VB}$ and why should it be of interest? It should be considered as a simple model, leading up to the full version, that might have the important property of selecting a classical geometry in its ground state.

To see this, consider the first term $\hat{H}_V$. It is minimized when the valence of each node in the graph is set to the preferred value v_0. Now there are many possible configurations of "on" links that satisfy this broad constraint: some of the configurations resemble regular structures but most of them do not. Thus if $\hat{H}_V$ were the only term in the Hamiltonian, the state with minimal energy would be highly degenerate.

The role of the second term $\hat{H}_B^{(c)}$ is exactly to break this degeneracy. This term assign an energy $B(L)$ to every loop of length L present in the graph. Since the sign of the term is negative, this term can lower the overall energy if the m values along the loops all multiply to unity. Thus, $\hat{H}_B^{(c)}$ gives preference to graphs in which loops are present. Moreover, since the coupling $B(L)$ is maximized at a particular loop length L_*, this term actually favors the presence of loops of that particular length. Combining the two effects, one can expect the configuration of "on" links that would be assigned minimal energy to resemble a regular lattice as shown in Figure 9.

There are several caveats, however, to the argument about the lowest energy state being a regular structure. They are related to some interesting trade-offs that must be understood between the valence and the loops.

The Hamiltonian for the system depends on the valence of nodes and on the lengths of closed loops that are present in the graph. As bookkeeping tools, introduce two sets $\{n_v(v)\}$ and $\{n_L(L)\}$ to denote the number of nodes with particular valence v and the number of loops of length L, respectively. (The subscripts are only labels intended to distinguish the two distributions; they are not indices and are not meant to be summed over.) From a given graph, these sets can be constructed in a straightforward manner and from them the Hamiltonian can be written as

$$\hat{H}_{VB} = V \sum_v n_v(v)\,(v - v_0)^2 - \sum_L n_L(L)\,B(L). \tag{3.26}$$

Information about the connectivity of various nodes is hidden as that is a property of a given state and not of the Hamiltonian.

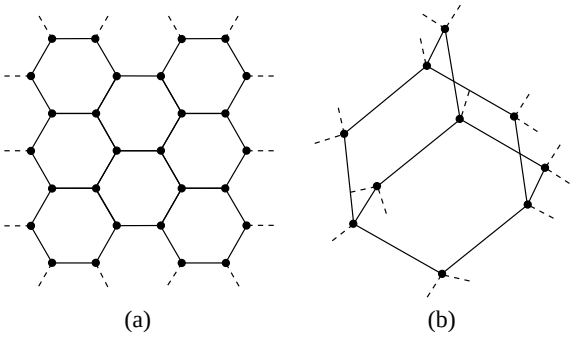

Figure 9: Sample lattice formations. Solid lines represent "on" links and dashed lines designate how the fragments shown fit inside a larger lattice. "Off" links are not shown.

A crucial feature of the system is that the sets $\{n_v(v)\}$ and $\{n_L(L)\}$ are constrained and correlated in several ways. First, the numbers $\{n_v(v)\}$ must add up to the fixed number of nodes N in the system. This is expressed as

$$N = \sum_v n_v(v) \tag{3.27}$$

Second, the numbers of loops of length L is limited by the size of the system N as well as the valence of the nodes. To see this, note that a node with valence v can subtend at most $v(v-1)/2$ different loops; we can say that such a node allows $v(v-1)/2$ 'arcs.' The total number of arcs A in a graph is fixed by valences $\{n_v(v)\}$. Since a loop of length L is made up of L arcs, a system of a given A will only be able to support a limited number of loops of a particular kind. Hence there is a constraint on $\{n_L(L)\}$ as follows

$$A = \sum_v n_v(v) \frac{v(v-1)}{2} = \sum_L n_L(L) L. \tag{3.28}$$

This relation correlates the two sets $\{n_v(v)\}$ and $\{n_L(L)\}$. In particular it implies that, for fixed valence, the total number of loops must decrease as their average length increases. Increasing the valence, meanwhile, necessarily increases the number of loops in the graph.

There are further constraints on the sets $\{n_v(v)\}$ and $\{n_L(L)\}$ which come about from the requirement that a graph can actually be realized given two such distributions obeying the above constraints. Such constraints "due to graph construction" are ignored in the rest of this section, even though one can expect them to become significant in some cases. What is important is that the minimal energy state may be described by a homogenous graph with all nodes having valence v_0 and all loops being of length L_* only when the couplings V and $B(L)$ are in certain parameter ranges. That such parameter ranges exist should be straight-forward; the evaluation of these ranges is quite difficult however, and some work in that direction is presented in subsection 3.2.

Given a candidate for a minimal energy state, one can naturally ask about what other states lie in its neighborhood. These state would correspond to excitations in the spatial

geometry. Two kinds of such excitations can be distinguished. The first is the kind of link configuration that can be obtained from the minimal energy state by a (relatively) small number of local moves such as those shown in Figure 8. Such excitations could take the form of the minimal energy lattice with a few edges removed or added - the latter might be a manifestation of non-locality in the underlying geometry. The second kind of excitation is the kind that has an energy close to the minimum but that cannot be built by manipulating the true minimum state with only a few moves. For example, increasing the size of one plaquette could produce a graph with an energy close to the minimum, but in enlarging one plaquette one actually has to reconfigure connections between a macroscopic number of nodes in the graph. Some more comments on these considerations can be found toward the end of this section.

Quantum Version

The quantum, or full, version of the model is given by

$$\hat{H} = \hat{H}_V + \hat{H}_C + \hat{H}_D + \hat{H}_B^{(q)}(+\hat{H}_{hop} + \hat{H}_{LQG}). \tag{3.29}$$

Before discussing the novel features of this model that differentiate it from the "classical" H_{VB} model, note that this Hamiltonian still contains a term that depends on the valence and a term that depends on loops of various sizes. Although the loop term $\hat{H}_B^{(q)}$ is actually different from $\hat{H}_B^{(c)}$, this model can be expected to exhibit a similar kind of competition between valence and loop contributions as discussed in the context of the simpler model. In particular, these terms should again be instrumental in shaping the graph into a regular structure.

In the following discussion of the role of the different terms in the Hamiltonian, it will be helpful to think of the configuration of links as frozen in a regular lattice-like pattern at low temperatures. The exact arrangement of links is not important but a square, cubic, or diamond lattice are good base patterns to keep in mind. At the end, the discussion will return to dynamical configurations and will be geared to understanding which one of the frozen configurations is in fact more likely.

Once the link assignments (j values) freeze, the remaining degrees of freedom are the m values of the "on" links. By construction, the terms of the Hamiltonian that deal with these degrees of freedom, $\hat{H}_C + \hat{H}_D + H_B^{(q)}$, reproduce the rotor model introduced by Levin and Wen [12, 13]. Thus, the physics of these m degrees of freedom is the same as one would expect from a rotor model Hamiltonian on a fixed lattice.

Because the loop term $\hat{H}_B^{(q)}$ does not commute with the other terms $\hat{H}_C$ and $\hat{H}_D$, eigenstates of the Hamiltonian generically will have to be superpositions of states involving different m configurations. In the $|j, m\rangle$ basis introduced so far, the precise form of the ground state will therefore appear non-trivial. Insight into the nature of the ground state can still be obtained, however, by considering a variational approach: One can start from a fiducial configuration of m values and see the effect of each term in the Hamiltonian on this state.

A good fiducial state to start with is the one in which all m values on all links in the graph take the value $m = 0$. In the absence of the loops term (i.e. if $B_0 = 0$), this configuration would be the exact ground state since, as discussed below (3.11), it would minimize both the

C and D terms of $\hat{H}$. Still ignoring the loop term, excitations on top of the ground state with all $m = 0$ would take the form of closed or open chains of alternating $m = +1$ and $m = -1$ links. These excitations are called closed and open strings, respectively. The energy of the closed strings would be proportional to D times the number of segments forming the string; on a regular lattice with plaquettes of length L_*, the shortest and least energetic closed loops would have energy DL_*. For this reason, the $\hat{H}_D$ term in the Hamiltonian can be called a string tension term. The energy of open strings would come from two sources. For a string with length L, the string tension term would contribute an energy DL. In addition, the $\hat{H}_C$ term would detect the two open ends of the string and contribute an energy $2C$. Thus the minimal energy associated with an open string would be $2C + D$ for a string that spanned only one segment of the graph. In the parameter regime where $C \gg D$, open strings would feel a much greater energy barrier than closed strings and so the latter would be dominant at low temperatures.

Now consider the effect of the loop term $\hat{H}_B^{(q)}$ on the fiducial state. Given a graph with all "on" edges labeled by $m = 0$, a loop operator acts as to create a closed string of alternating $m = +1$ and $m = -1$ links. The string will acquire tension through the $\hat{H}_D$ term. However, since the sign of the loop term is negative, the overall energy of the state may increase or decrease and this creates the possibility of two distinct scenarios.

In one scenario, the tension in a string is greater than the contribution from the loops term, so the overall effect of creating a string is to increase the energy of the system. If this is the case, then the string represents an excited state over the vacuum in which all m values are zero. The situation is not very different from the case above where the loop term was ignored altogether albeit the energy of the shortest possible string here is somewhat lower than DL_* due to the negative contribution of $\hat{H}_B^{(q)}$.

The second scenario is actually the more interesting one. If the tension of a string is small compared to the contribution from $\hat{H}_{loops}$, creating a string decreases the energy. It follows that creating another string also decreases the energy, and so on. Thus the true ground state of the model consists of a superposition of a large number of strings: a string condensate. The precise form of the string-condensed ground state is difficult to write down, but it can be done in some simple situations [12, 13]. It is also difficult to predict the precise value of the B_0 and D couplings which would give rise to the condensate. Reasonable estimates for the division between the two scenarios, however, can be made by comparing the number of edges and the number of plaquettes in a lattice. In a three dimensional cubic lattice, there is on average one edge per plaquette, so the condition for string condensation would be roughly,

$$D - \frac{1}{4!} B_0 B^4 < 0. \tag{3.30}$$

In a diamond lattice characterized by hexagonal plaquettes, there are two edges per plaquette, so the requirement of condensation would be

$$2D - \frac{1}{6!} B_0 B^6 < 0. \tag{3.31}$$

A concise way of parametrizing these conditions is to introduce a parameter $\gamma > 1$ and require the couplings to satisfy

$$24\gamma D = B_0 B^4 \tag{3.32}$$

for the cubic lattice and similarly for the diamond lattice.

Since the string condensate has lower energy than the fiducial state, one can worry about negative energy states and whether the energy is bounded from below. In fact there is no problem because the graph has a finite number of nodes. Also, the m values on each edge only take three possible values so that the loop term can only act on an edge a limited number of times. Thus the Hamiltonian is bounded from below. It also follows that the Hamiltonian can be redefined by adding a constant so that the total energy for the ground state is either exactly zero or is positive.

What are the excitations on top of the string-condensed state? Since the lattice is assumed fixed so that the $\hat{H}_V$ term is minimized and since for the moment open strings are ignored, the relevant terms in the Hamiltonian are $\hat{H}_D$ and $\hat{H}_B^{(q)}$. If the graph is furthermore assumed to be a square lattice in three dimensions so that all loop operators have exactly four sides, then $\hat{H}$ effectively becomes

$$H_{lowT} \sim D \sum_{ab} M_{ab}^2 - \frac{1}{4!} B_0 B^4 \sum_a \prod_{i=1} M_i^{\pm}. \tag{3.33}$$

Since the lattice is regular, the sum over loops can be thought of as a sum over plaquettes. One can define a plaquette operator $W_{a'}$ anchored at a point a' as

$$W_{a'} = M_{a'b}^{+} M_{bc}^{-} M_{cd}^{+} M_{da'}^{-}. \tag{3.34}$$

The points $a', \ldots d$ are now fixed by a convention of labeling plaquettes given their base point so that there is no summation over repeated indices. With the help of this operator, the Hamiltonian can be written as follows

$$H_{lowT} \sim D \sum_{ab} M_{ab}^2 - \frac{1}{3!} B_0 B^4 \sum_{a'} (W_{a'} + h.c.) \tag{3.35}$$

where $h.c.$ stands for the Hermitian conjugate of $W_{a'}$, i.e. a loop operator with M^+ and M^- interchanged on each link. The sum in the second term is over plaquettes. It turns out that this Hamiltonian correspond to $U(1)$ gauge theory in axial $A_0 = 0$ gauge. In fact, the Kogut-Susskind Hamiltonian [16] for a gauge field on a cubic lattice in three spatial dimensions is

$$H_{KS} = \frac{g^2}{2a} {\sum_{ab}}' M_{ab}^2 - \frac{2}{ag^2} \sum_{a'} (W_{a'} + h.c.). \tag{3.36}$$

The sum in the first term is shown primed because it is only over nearest neighbors connection in the lattice. The variables a and g denote the lattice spacing and the coupling constant, respectively. Comparing coefficients of the gauge theory Hamiltonian with (3.35) gives the identifications

$$g^2 \sim \sqrt{\frac{4!D}{B_0 B^4}}, \qquad \frac{1}{a^2} \sim \frac{1}{3!} D B_0 B^4. \tag{3.37}$$

Thus the excitations of the quantum graphity model, which is by construction related to the rotor model of Levin and Wen, describe photon-like particles. In the limit of infinite lattice, these particles become massless, propagate at the speed of light, and have two polarizations.

What is particularly interesting is that these particles appear as collective excitations of the m degrees of freedom in the edges' Hilbert spaces.

To be sure, the correspondence between H_{lowT} and H_{KS} is not exact because in the pure gauge theory, the edges connecting lattice sites can carry arbitrary representations of $U(1)$ whereas the m labels in the graphity model can only take three values $-1, 0$, and 1. Nonetheless, the string condensed phase of H_{lowT} should exhibit features of $U(1)$ theory, such as the presence of photon-like excitations, even in this crude approximation [17]. The correspondence could be improved by allowing a wider range of m values on each edge. This is not in principle an obstacle for the model, but the present setup is kept for simplicity.

Recall that string-net condensation, and thus the possibility of emergent $U(1)$ theory, only occurs when certain conditions such as (3.32) are satisfied. Inserting (3.32) into the expression (3.37) for g^2 above gives

$$g^2 = (2\gamma)^{-1/2}. \tag{3.38}$$

Recall that $\gamma > 1$, so that the coupling g^2 of the emergent gauge field is weak. Furthermore, if the inverse lattice spacing is set on the order of the Planck energy, $a^{-1} \sim E_P$, then it follows from (3.37) and (3.32) that

$$B_0 B^4 \sim E_P g^{-2}, \qquad D \sim g^2 E_P. \tag{3.39}$$

After discussing string condensation and the emergence of $U(1)$ gauge theory, one must return to the original issue of determining a likely graph structure in the ground state. It is seen that the string tension term $\hat{H}_D$ to some degree opposes the tendency of the loop term $\hat{H}_B^{(q)}$ to lower energy and to create strings. Hence the appearance of a graph structure with a large number of short loops can only be expected to be a low energy state if the loop term is dominant. In other words, the possible emergence of a regular graph is directly correlated with string condensation.

The Universe Today

To summarize, the proposed quantum model contains four dimensionful coupling constants (V, C, D, and B_0) and three dimensionless numbers (N, B and v_0). Following the given line of thinking, one can estimate the magnitude of the coupling constants in order for the emergent physics to describe the observed universe. Taking g^{-2} to be of the order of 10^2 for electromagnetism, then

$$B_0 B^{L_*} \sim 10^2 E_P. \tag{3.40}$$

For the graph to cover the visible universe with radius $R \sim 10^{20} m$, the required number of nodes and the number of edges must be at least

$$N > 10^{180}, \qquad M > 10^{360}. \tag{3.41}$$

Finally, the temperatures for which the system should exist in a lattice-like configurations should span the range that is relevant for classical cosmology and particle experiments. As

a conservative number, one can require the lattice to be consistent with the existence of particles at energies of $10^{20}eV$. Thus a safe inverse temperature to consider is

$$\beta = 10^8 E_P^{-1}; \tag{3.42}$$

This also comparable to temperatures associated with the universe at very early times.

3.2 Phases

The aim of this section is to study the statistical mechanics of a graph based model and find the conditions when the system might form a regular low-dimensional structure. For simplicity, the analysis is restricted to the simpler classical model based on the Hamiltonian H_{VB} of (3.25). It is imagined that the system graph is coupled to a bath with inverse temperature β. The partition function is therefore

$$Z_{VB} = \sum_{\text{configs}} e^{-\beta H_{VB}}, \tag{3.43}$$

where 'configs' stands for distinct configurations of links. Much of the difficulties and interesting features of the model are hidden in exactly how these configurations can be identified and enumerated. The calculation below therefore does not aim to solve the model but to offer a reasonable case (subject to a particular set of approximations) that the model can exhibit at least two very distinct types of behaviors or phases.

Homogenous Node Approximation

The Boltzman factor in (3.43) can be reorganized to give

$$Z_{VB} = \sum_{config} \prod_a e^{-\beta V\left(v_0 - \sum_b J_{ab}\right)^2 + \beta \sum_{loops\, at\, a} B(L)} \tag{3.44}$$

so that contributions based on nodes labeled a are grouped together. The task of enumerating configurations is no less complicated now, but this formulation prompts the idea of using a particular approximation. Motivated by naive expectation that the graphs of interest should be homogenous so that every node's neighborhood is similar, the partition function could be approximated by

$$Z_{VB} \simeq (Z_1)^N \tag{3.45}$$

where Z_1 is now a partition function attributed to a single node (the right hand side may have to be divided by $N!$ since the nodes are indistinguishable.) The task at hand is thus simplified: it is now to parametrize only the single-node partition function. The expectation is that the function $(Z_1)^N$ would be a first rough approximation to and would yield some useful information about Z_{VB}.

As already discussed in the previous subsection, configurations of the whole graph may be characterized by distributions such as $\{n_v(v)\}$ and $\{n_L(L)\}$ subjected to the constraints (3.27) and (3.28). By assuming that the nodes are homogenous, the distribution $\{n_v(v)\}$

becomes irrelevant (all nodes have the same valence). The analog of the constraint (3.28) becomes

$$\frac{v(v-1)}{2} = \sum_L n_L(L)L \tag{3.46}$$

where now $n_L(L)$ refer to the number of loops at a particular node. Using this notation, Z_1 becomes

$$Z_1 = \sum_{v=0}^{N} {\sum_{\{n_L(L)\}}}' g\{v, n_L(L)\}\, e^{-\beta V(v_0-v)^2}\, e^{\beta \sum_L n_L(L)B(L)}. \tag{3.47}$$

The sums are over the valence and the loop distribution. The second sum is shown as primed to emphasize that it is constrained by the fact that the numbers of loops $\{n_L(L)\}$ must be such that the total number of loops is compatible with the valence through (3.46). The function $g\{v, n_L(L)\}$ counts the number of distinct configurations that give a node the same values of v and $\{n_L(L)\}$.

The scaling of $g\{v, n_L(L)\}$ with v and $n_L(L)$ can be expected to be rather complicated in general. If, however, the goal of $g\{v, n_L(L)\}$ is to account for the entropy contribution to the partition function, it is reasonable to chose a particular form or ansatz for this function that in fact overcounts the number of configurations of a given kind. Taking this approach, the scaling of the counting function with v and $n_L(L)$ is assumed to be independent so that function factors

$$g\{v, n_L(L)\} \to g\{v\}g\{n_L(L)\}. \tag{3.48}$$

The dependence on v should reflect the number of ways of connecting the node under consideration with v of the other nodes in the graph. In a 'classical' counting scheme, this can be encoded in the binomial coefficient

$$g\{v\} = {}^N C_v; \tag{3.49}$$

the number of ways to chose v 'on' links out of order N possibilities. As for loops, the appropriate factor is

$$g\{n_L(L)\} = 1 \tag{3.50}$$

because the individual arrangements are taken into account explicitly in the sum $\sum'_{\{n_L(L)\}}$. The counting scheme based on this $g\{v, n_L(L)\}$ is conservative in the sense that the contribution of the loops is effectively counted twice. Loops are counted once when the $g\{v\}$ as above is included for all single nodes in the system (all the Z_1 factors in (3.45)) - this effectively counts all possible ways of connecting nodes together with 'on' links, including forming loops of all possible kinds. Loops are counted a second time explicitly through $\{n_L(L)\}$. Furthermore, $g\{v, n_L(L)\}$ is conservative because it does not recognize graph isomorphisms.

Although the constrained sum can be evaluated in straight-forward manner in certain limited cases for example when N and the average valence are small, it would be more useful to have an expression for it that is valid in all cases. To this end, introduce a grand canonical ensemble in which A (the number of arcs at the node) is allowed to vary and write a grand partition function

$$\mathcal{Z}_1 = \sum_{A=0}^{\infty} \left[e^{-\alpha A} \sum_v {\sum_{\{n_L\}}}' g\{v\}\, e^{-\beta V(v_0-v)^2}\, e^{\beta \sum_{n_L(L)} n_L(L)B(L)} \right]. \tag{3.51}$$

Here α is a chemical potential that must be adjusted at the end to satisfy (3.46). Since A depends on both v and the loop distribution $n_L(L)$, the potential is split as follows

$$\alpha A = \alpha\xi\frac{v(v-1)}{2} + \alpha(1-\xi)\sum_L n_L(L)L \tag{3.52}$$

where ξ is a free real parameter. Inserting this into (3.51) gives

$$\mathcal{Z}_1 = \sum_{A=0}^{\infty}\left[\sum_{\{n_L\}}{}' \sum_v g\{v\}\, e^{-\beta V(v_0-v)^2 - \alpha\xi v(v-1)/2} \prod_L \left(e^{\beta\sum_{n_L(L)} n_L(L)B(L) - \alpha(1-\xi)n_L(L)L}\right)\right]. \tag{3.53}$$

Now the constrained sum over $n_L(L)$ together with the sum over A is equivalent to a product of unconstrained sums over $n_L(L)$ for each L. Thus this partition function factorizes,

$$\mathcal{Z}_1 = \mathcal{Z}_{1V}\mathcal{Z}_{1B} \tag{3.54}$$

with

$$\mathcal{Z}_{1V} = \sum_v {}^N C_v\, e^{-\beta V(v_0-v)^2 - \alpha\xi v(v-1)/2} \tag{3.55}$$

$$\mathcal{Z}_{1B} = \prod_L \left[1 - e^{\beta B(L) - \alpha(1-\xi)L}\right]^{-1}. \tag{3.56}$$

The first factor $\mathcal{Z}_{1V}$ is a straight-forward partition function with an energy and potential dependence and a counting function. In principle it is ready to be evaluated but unfortunately the exact solution is not known. The second factor $\mathcal{Z}_{1B}$ resembles the partition function for a gas of Bose particles albeit with an unusual energy function and chemical potential. Still, the average number of loops of a particular length is

$$\langle n_L(L)\rangle = \frac{1}{e^{-\beta B(L)}e^{+(1-\xi)\alpha L} - 1} \tag{3.57}$$

in direct relation with the standard result. This number should be positive for all values of α, β and L if this method is to make sense.

What is the advantage of these manipulations? The main reason for rewriting the system in this language is that the arc constraint (3.46) is now eliminated. This comes at the cost of two parameters α and ξ. The first parameter α can be interpreted as a chemical potential and must be fixed using constraint equation (3.46). The second parameter ξ has no physical interpretation - it just paremetrizes the relative importance of valence and loops in the total grand partition function. Thus the grand partition function $\mathcal{Z}_1$ should be maximized with respect to this parameter. There are three interesting ranges in the parameter ξ: $\xi < 0$, $0 < \xi < 1$, and $\xi > 1$. These ranges give the effective potentials in the partition functions different signs and thus produce very different kinds of behaviors.

$\xi = -1$. The case that will be discussed in most detail is when $\xi = -1$ (or, more generally, $\xi < 0$.) Here, the potential encourages the formation of high-valence nodes and at

the same time promotes short loops. There will be some β for which the system will exhibit condensation of loops into a single type of length L_*:

$$\begin{aligned} \langle n_L(L_*)\rangle &= \frac{A}{L_*}, \\ \langle n_L(L \neq L_*)\rangle &\ll 1. \end{aligned} \tag{3.58}$$

For this to happen ($v > 1$ is required), one needs

$$\begin{aligned} \alpha &\simeq \frac{1}{(1-\xi)}\left[\beta\frac{B(L_*)}{L_*} + \frac{1}{L_*}\ln\left(1+\frac{L_*}{A}\right)\right] \\ 1 &\ll \beta\left(\frac{L}{L_*}B(L_*) - B(L)\right) + \frac{L}{L_*}\ln\left(1+\frac{L_*}{A}\right), \qquad \forall L \neq L_*. \end{aligned} \tag{3.59}$$

The first line verifies that the potential α is positive as required. The second line can be satisfied by taking a large β as long as the quantity in the first set of parenthesis is positive; this constraint on the function $B(L)$ can be satisfied by choosing the coupling constants B and B_0 appropriately.

This solution for α can be now inserted into $\mathcal{Z}_{1V}$ (with $\xi = -1$). The exact evaluation of this partition function and related observables is difficult analytically. (The difficulty lies in the complicated dependence of the Boltzman factor on v in both the V and α terms.) However, some of the expected physics can be described qualitatively by approximating the whole partition function by one dominant term corresponding to valence v. In this approximation, one can set $A = v(v-1)/2$ and thus obtain

$$\mathcal{Z}_{1V} \simeq {}^{N}C_v \exp\left(-\beta V(v-v_0)^2 + \beta\frac{1}{2L_*}B(L_*)v(v-1)\right)\left(1+\frac{2L_*}{v(v-1)}\right)^{\frac{v(v-1)}{2L_*}}. \tag{3.60}$$

The last factor is ill-defined for $v = 0, 1$ but this is not a problem as we are interested in $v = v_0$ or higher anyway. Moreover, this factor has a modest growth with v and hence will be treated as a constant (and ignored).

What value of v should be used to best approximate $\mathcal{Z}_{1V}$? A useful comparison is between the cases $v = v_0$ and $v = v_0 + 1$,

$$\frac{\mathcal{Z}_{1V}|_{v=v_0}}{\mathcal{Z}_{1V}|_{v=v_0+1}} \simeq \left[\frac{{}^{N}C_{v_0}}{{}^{N}C_{v_0+1}}\exp\left(-\beta\frac{B(L_*)}{L_*}v_0\right)\right]\exp(\beta V). \tag{3.61}$$

The first factor in square brackets is less than unity and indicates that the entropic drive of the system is toward higher valence. The second factor on the other hand is greater than unity and reflects the preference of the V term in the Hamiltonian for valence $v = v_0$. These two factors compete and either can prevail depending on the parameters chosen. By approximating the ratio of combinatorial factors as

$$\frac{{}^{N}C_{v_0}}{{}^{N}C_{v_0+1}} \sim \frac{1}{N} \sim e^{-\log N}, \tag{3.62}$$

one sees that configuration with $v = v_0$ is dominant if

$$\beta V > \frac{\beta B(L_*)}{L_*} v_0 + \log N. \tag{3.63}$$

Note that for couplings of order unity in Planck units, N and β on the order of (3.41) and (3.42), the second term on the right hand side of this inequality is not large at all compared to βV. In any case, the main point is that for high enough βV, the second factor can dominate in (3.61) and hence the term with $v = v_0$ term would be preferred over $v = v_0 + 1$ as an approximation of $\mathcal{Z}_{1V}$. Similarly, for high enough βV, the choice $v = v_0$ can be made optimal over any other choice of v. As βV drops below a critical level, however, in this approximation scheme, the partition function $\mathcal{Z}_{1V}$ should rather be approximated by one of the other terms in the series with $v > v_0$. Hence there is a hint for two distinct regimes that depend on the combination of parameters βV. The type of the transition that occurs between these two regimes when β varies should be a very interesting subject for further study.

$\xi = \frac{1}{2}$. The next case is when $\xi = \frac{1}{2}$ (or, more generally, $0 < \xi < 1$.) Then the potential in $\mathcal{Z}_{1B}$ acts to suppress long loops just as in the previous case. Thus, it can be expected that there will be some β for which the system will exhibit condensation of loops into a single type of length L_*. The conditions are identical to (3.59). The major difference from the $\xi = -1$ case is in the function $\mathcal{Z}_{1V}$ where the potential now suppresses high valence configurations. Thus we expect a behavior that is qualitatively similar to that described in the previous case with $\xi = -1$. Again it is difficult to evaluate the partition function and the observables analytically.

$\xi = 2$. The third case is $\xi = 2$ (or more generally, $\xi > 1$.) With this choice, the potential encourages long loops and small valences. Thus the system should form a sparse network in its ground state. This region of the parameter space does not seem to be of direct physical significance.

Back to the general discussion, note that similar analysis can be performed in the high temperature regime. For now, however, it is sufficient to remain at a qualitative level: the above partition functions indicate that at high temperature (low β) the valence of the nodes can be high. This is described for example by the discussion below (3.63). Also, at high temperatures, the distribution of loops can be quite diverse. Thus the typical graph might look more like a random graph than a regular lattice and may be characterized by a probability p that each of the $(N-1) \sim N$ edges adjacent to a node are excited. This probability can be estimated by

$$p = \frac{v}{N} \sim \frac{T}{V} \sim \frac{1}{\beta V} \tag{3.64}$$

for each edge. Thus when the temperature T is on the order of V, a macroscopic number of edges in the complete graph will be "on."

Implications for Cosmology

Based on the descriptions of the high and low temperature behavior of the quantum graphity model, one can propose the following scenario for the evolution of the universe. It is presented 'in reverse' - starting from current times and tracing back to the beginning.

At low temperatures, i.e. $T \ll V$ or $\beta \gg V$ as in (3.42), the graph is in an ordered state characterized by nodes of a fixed valence and loops of preferred length L_*. A candidate for the state of the graph in this regime is a regular lattice-like pattern. As time goes back, the temperature T increases and β decreases. This is imagined to occur because the temperature in the heat reservoir is tuned up, but more thoughts on this are described in section 3.3. When β becomes comparable to V or the other couplings, defects in the graph can start to appear due to thermal fluctuations: some loops may grow larger or smaller, and some nodes may change valence. The effect of these defects on the overall structure of the graph, such as its effective dimension or excitation spectrum, depend very much on the interaction terms $\hat{H}_{hop}$ and $\hat{H}_{LQG}$, which have not been studied in this work. Possibilities range from smooth changes in the dimension to abrupt changes in the connectivity similar to what could be expected in a phase transition. As time goes back further and T becomes much larger than the couplings, $T \gg V$, the graph ends up in a very disordered state and the average valence of each node is large. The diameter of the graph, or the distance measured in "on" links between any two points, is very short in this phase so that the degrees of freedom can be considered to be highly interacting and can quickly come into thermal equilibrium. Running time in the forward direction, the transition from the high temperature phase where there is no notion of geometry to the low temperature ordered phase may be termed "geometrogenesis."

Even if this is a simplified model of the emergence of space, it suggests insights for physical cosmology. The horizon problem is the statement that distant parts of the universe appear to be in thermal equilibrium despite universe's evolution, modeled by standard FRW dynamics, suggesting that these parts could not have interacted during the course of the universe's estimated lifetime. This is deemed to be a puzzle because its most straight-forward resolution by positing special initial conditions lacks physical justification. The graphity model provides such a justification because it suggests that the spins were interacting and were part of a thermal ensemble before the temperature fell sufficiently for the system to enter a phase of extended classical geometry. Thus the model shows the horizon problem may be avoided if geometry is emergent. In this sense, the model also provides an explicit example of a broader idea that a distinction between micro-locality (locality between fundamental degrees of freedom) and macro-locality (locality between emergent degrees of freedom) may be important for understanding quantum gravity and the physics of the very early universe [14].

Again, the cosmological scenario of the graphity model is only a tentative description of the early universe. Given the vast amount of data from observational cosmology that is now available, it should be tested and scrutinized in much more detail. This is particularly important if the model is to be fruitfully and meaningfully compared with the standard inflation-based paradigm for the early universe. Among the issues that should be addressed are the following. Constraints on the variation in time of the gravitational constant G indicate that the dimensionality of the spatial slices of the universe is three up to very early times - these observations should pose bounds as to when and how the transition from regular to complete graph can occur in the graphity model. The spectrum of inhomogeneities in the cosmic microwave background radiation is nearly scale invariant with an indication of a small red tilt - it should be checked whether a transition from a highly connected graph to a low dimensional structure can generate such a spectrum and the required small ratio

of anisotropies $\delta T/T \sim 10^{-5}$ in the CMB. Some interesting work on holographic phase transitions [28] has appeared that is relevant to this last issue, but more analysis is needed in the particular graphity scenario proposed here.

The cosmological scenario needs to be worked out in much more detail. This should be a promising line of research given that the model is well-defined and there is now a lot of experience and interest in describing cosmological models. If the model is found to be successful, it would be a concrete example of a model which demonstrates both emergent geometry and relevance for astrophysical observations.

3.3 Variations, Extensions, Open Issues

When considering a new model such as quantum graphity, it is sometimes unfeasible to attack the whole problem directly. Instead it is useful to study certain variations or simplifications as warm-up exercises as in the analysis of the "classical" version of the model using tools of statistical mechanics in the previous subsection. There are variations and extensions that one can naturally consider to the proposed model. Some of these are quickly reviewed below. Open issues that are left to be studied are mentioned as well.

Removing the Heat Bath

In the statistical analysis of the model in the previous subsection, a prominent role is played by the canonical ensemble and the inverse temperature β - the model can exhibit regularity features such as fixed valence mainly thanks to the very high value of β (in Planck units) associated with the universe today. Temperature is often related to the average energy per degree of freedom in a system. In usual condensed matter physics, it is a parameter that can be controlled by coupling the system to an environment. In a model like quantum graphity where the system is supposed to describe the universe and its matter content, what is the meaning of a heat bath or an environment? Moreover, what does a changing temperature parameter imply about energy conservation in the system (universe)? These are interesting questions that could be addressed in the context of quantum graphity. At this stage, the approach to the model is a practical one in which β is regarded as a useful parameter that allows one to tame entropy in the partition function and favor low-energy configurations which are regular. Thus the temperature parameter is found to be a very useful asset that, for example, is not available in the approach of causal dynamical triangulations. In future works, it would be very interesting to try to understand the temperature parameter intrinsically without reference to an external heat source or sink.

Geometrical Interpretation

The results on the classical model in the previous subsection give evidence that the ground state of the system is regular but do not technically prove that the ground state of the system is a regular lattice. In fact, at this stage of the model's development, the dimensionality of the structures formed is not known either; a dimension operator and its expectation value have not been computed. However, given the results on condensation and the definition of

non-overlapping loops, it is reasonable to expect that the ground state for the cases discussed at least locally resemble the honeycomb or diamond lattices shown in Figure 9.

Also, the calculations do not prove that the ground state is composed of a unique graph - in principle, the ground state could be a superposition of configurations. For example, it is conceivable for the elements in the superposition to represent discretizations of manifolds with different topologies. The question of interpreting such a superposition is not addressed here. A possibility worth mentioning, however, is that the dynamics of the transition between a high temperature phase to a low temperature one could play a role in the reduction of the superposition to one dynamically selected ground state. In particular, the graph changing moves of $\hat{H}_{LQG}$ in Figure 8, do not allow an initially connected graph to evolve into two or more disconnected components. Thus the superposition making up the ground state can already be said to dynamically select graphs which have the same number of connected pieces.

Residual Matter Entropy

When thinking of entropy and stability, the matter content should be taken into account. It is, in fact, a very important part of the model as it motivates the loop term in the Hamiltonian. A gas of photons in three spatial dimensions carries an entropy

$$S_{gas} \simeq NT^3 \tag{3.65}$$

where the number of nodes N has been substituted for volume, and T is the temperature. This is a residual entropy that must be present even when the graph does freeze into a lattice configuration. In the microcanonical ensemble, this translates into a multiplicity of states on the order of

$$\Omega_{gas} \simeq \exp(NT^3). \tag{3.66}$$

This demonstrates that the the existence of matter in principle halts the break-up of the regular lattice into a non-geometric graph with high valence or large loops. The extent of this effect should also be studied in more detail.

Scaling

A very important issue that should be addressed in the graphity context is that of scaling, i.e. the question of how the model behaves as the number of degrees of freedom changes. In the context of lattice gauge theories, this question can be either associated with the limit of the lattice spacing going to zero, or the lattice size going to infinity. Since the motivation for the graphity model is that space is fundamentally composed of discrete units, the scaling issue should be thought of in the latter sense. The issue is of theoretical interest because it addresses the stability of the model, but it also has a practical side because current observations suggest that the universe is expanding (and accelerating) and thus the number of nodes N seems to be increasing.

Thus it would be interesting to define a related model to graphity in which the number of nodes and edges in the system is not fixed. This could be achieved for example by defining

a Fock Hilbert space of the form

$$\mathcal{H}_{Fock} = \mathcal{H}^{(1)} \oplus \mathcal{H}^{(2)} \oplus \cdots \oplus \mathcal{H}^{(N)} \oplus \cdots \tag{3.67}$$

where $\mathcal{H}^{(X)}$ are Hilbert spaces for complete graphs with number of nodes ranging from $X = 1$ to $X = \infty$. Some work on growing lattices is available and could serve as background for future work on graphity [29]. But even before attempting to define a Hamiltonian acting on such a space, some insights might be gained by just considering the graph connectivity structure and the partition functions already studied.

In terms of graph structure, a fixed lattice seems problematic in the context of an expanding universe. This is because when a new node is connected arbitrarily to somewhere in the lattice, a large number of edges must be reconfigured so that the new graph configurations is again a regular lattice. Hence it seems that the connections between nodes in a graphity model should in fact be quite malleable and movable. On the same vein, it has been suggested that a lattice structure might be too rigid to allow gravitons to propagate as fluctuations in the geometry [17].

In terms of the partition function, note that that a characteristic term in the sum over configurations can be written (ignoring the chemical potential) as

$${}^{N}C_v \exp\left(-\beta V(v - v_0)^2\right) < \exp\left(v \log N\right) \exp\left(-\beta V(v - v_0)^2\right). \tag{3.68}$$

As N grows, the importance of the counting function ${}^{N}C_v$ increases as well; this is exaggerated by the $v \log N$ in the exponent on the right hand side of the above relation. However, in an expanding universe, the inverse temperature also changes with N. Since T is inversely proportional to the scale factor a when the universe is filled with radiation [19], and taking the scale factor a as the radius of the $3 + 1$ dimensional universe so that $a^3 \sim N$, then $\beta \sim N^{1/3}$. For large N, β increases faster than the entropy factor as the universe expands. In other words, the importance of the ${}^{N}C_v$ factor actually diminishes with growing N with respect to the other terms. It also follows that the combinatorial factor is relatively more important at early times when N is smaller and the temperature is large than today. This supports the proposed cosmological scenario wherein the high temperature phase is very different (perhaps non-geometrical) from the low temperature phase.

Diffeomorphisms

The formulation of the quantum graphity model in terms of a complete graph may be dubbed "background independent" because it does not presuppose any manifold structure. But can one see "background independence" in the low energy states? Suppose that the ground state of a $v_0 = 3$, $L_* = 6$ model is a honeycomb lattice as suggested above. The lattice possesses only some discrete translation and rotation symmetries and thus in the strict sense it cannot be said to accommodate diffeomorphism invariance either. However, in a looser sense, the discreteness of the lattice is not a very big problem. After embedding the lattice in a manifold with metric $g_{\mu\nu}$, the nodes of the lattice are assigned coordinate positions. Smooth symmetries such as rotations, or more generally diffeomorphisms, can act on this manifold in the usual manner; their effect is to assign new coordinate values to the nodes of the lattice. The action of a particular diffeomorphism is portrayed in Figure 10. Its action

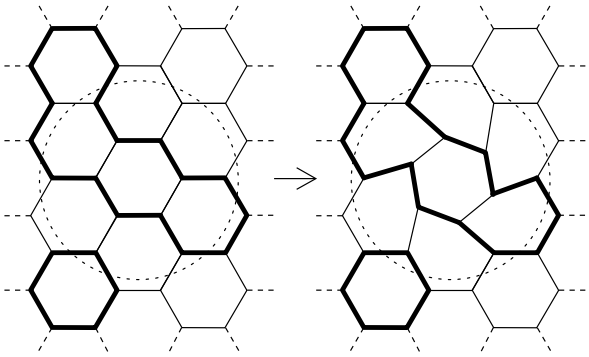

Figure 10: The action of a diffeomorphism on the honeycomb lattice. The map is trivial outside the dotted region and is a twirl or rotation inside that region. Bold lines indicate strings.

changes the coordinate position of some of the nodes and the coordinate distance between some of the nodes. However, since expectation values for observables in the underlying graphity model must be defined and computed using the underlying linking structure and the Hamiltonian that makes no reference to the embedding or the metric, all quantities that are computable in the model will take the same values whether evaluated using the graph on the left or the right of Figure 10. In this sense then, the model can be said to be background independent and to respect diffeomorphism symmetry. This feature, however, should be demonstrated explicitly for example by defining and computing two point functions for the emergent gauge field in the low temperature regime.

Removing One Parameter

Note that the conditions for fixing the valence of nodes in the graph in (3.59) essentially determine the relative strengths of the V and B terms in the Hamiltonian. This suggests a modification of the model Hamiltonian that would eliminate the parameter v_0. Suppose the V term in H_{VB} is replaced by

$$\hat{H}'_V = V \sum_a \left(\sum_b J_{ab} \right)^4 \tag{3.69}$$

so that the energy scales as the fourth power of the a node's valence instead of the second power. A consequence of this would be that, in the homogenous node approach, the grand partition function $\mathcal{Z}_{1V}$ would become

$$\mathcal{Z}'_{1V} = \sum_v {}^N C_v \, e^{-\beta V v^4 - \alpha \xi v(v-1)/2}. \tag{3.70}$$

Now it is possible to chose the couplings V and B such that it is advantageous for the system to create v_0 'on'-links on each node (since this would allow the formation of loops). Hence the emergence of a preferred valence v_0 would be a result of a dynamical process (a

balance between the valence and loop formation) and would not be an explicit input in the Hamiltonian. This certainly has an aesthetic appeal although for practical purposes it might be more straight-forward to work within the original model.

Outlook

The outlook for the graphity model looks promising at this stage. Despite the model's lengthy Hamiltonian, it is nevertheless possible to study fragments of it analytically as shown in the subsection on phases. As such, the model can be viewed both as an interesting problem in statistical mechanics and as a physically relevant model for Planck scale physics and early universe cosmology. Given the recent interest in cosmological evolution, it would be very interesting to see whether a discrete model of this kind can reproduce the successes of the standard inflationary theory. Simultaneously, it would be useful to connect the model back to general relativity - a possible route for this would be to construct dual triangulations to the graphs (in the low temperature limit) and map the various terms to a dynamical triangulation model. In short, many open questions remain but answers to them appear to be within reach. An honest evaluation of the model will be possible once these issues are worked out.

4 Noiseless Subsystems

In the situation where space and geometry are dynamical, perhaps evolving according to the moves of causal dynamical triangulations (section 2) or changing linking patterns as in quantum graphity (section 3), one would still like to be able to identify particle-like excitations and interpret them in the familiar way. Since these particle excitations are supposed to be detectable and measurable at human time-scales, the information carried by particles must be preserved despite the microscopic changes in the structure of space. Following this line of thought, it has been proposed that the objects of familiar physics, particles and fields, must be resistant to various interactions that one can expect to take place at the Planck scale [15, 18]. To analyze this proposal, it is useful to look at quantum information processing.

Quantum information processing is a relatively young field of research compared to, for example, the study of thermodynamics, field theories, or gravity. Current interest and the large amount research in this new field is largely due to its possible exciting applications in computation and communication [20]; these potential uses for quantum mechanics have only been observed quite recently in the 1980s and 1990s. Some quantum information processing techniques may inspire new ways to look at some old problems related to quantum gravity and physics of the Planck scale [18]. In particular, one set of tools dubbed by the name of noiseless subsystems (NS) or passive error correction codes has been argued to provide an intuitive picture for the emergence of particles and space-time from a fully quantum background-independent system [15].

Originally, the framework of noiseless subsystems was developed as a tool to preserve fragile quantum information against decoherence [21]. When a quantum register (a Hilbert space) is subjected to an interaction with an external and uncontrollable environment, information stored in the register is, in general, degraded. However, when the source of decoherence exhibits some symmetries, certain subsystems of the quantum register are unaffected by the interactions with the environment and are thus noiseless. These subsystems are therefore potentially very natural and robust tools that can be used for quantum information processing.

In this work, it is shown how the framework of noiseless subsystem can provide a basis for thinking about any (quantum) mechanical system that is subject to constraints [22]. The next section 4.1 contains a review of the details of noiseless subsystems and discusses how they may be related to constrained mechanics. Then, in section 4.2, this relationship is demonstrated through several examples. Implications of the proposed way of thinking of constrained systems are summarized in section 4.3.

4.1 Background

Quantum information science studies how quantum resources can be manipulated to transmit messages or perform computations. It does not add any new postulates to standard quantum mechanics, but in viewing quantum mechanics as a theory about information, it sometimes shifts the focus of discussion onto aspects of computer science. From this different perspective, the field of quantum information processing can contribute new ideas for other topics such mechanics.

NS in Quantum Information Processing

Consider a quantum system S coupled to an environment (bath) B. The full Hilbert space is given by the tensor product

$$\mathcal{H}_{full} = \mathcal{H}_S \otimes \mathcal{H}_B \tag{4.1}$$

where $\mathcal{H}_S$ and $\mathcal{H}_B$ are Hilbert spaces of the two components. It is helpful to assume that both of these Hilbert spaces are compact and discrete. The full Hamiltonian describing evolution can generically be decomposed as

$$H_{full} = H_S \otimes I_B + I_S \otimes H_B + H_I, \tag{4.2}$$

where H_S and H_B are operators acting on the system and bath, I_S and I_B are unit operators on S and B, and H_I encodes the interactions between S and B. This last term can be expanded as

$$H_I = \sum_\alpha N_\alpha \otimes B_\alpha, \tag{4.3}$$

where N_α and B_α are a set of operators acting only on the system and bath respectively.

It is worth pointing out that the terms $H_S \otimes I_B$ and $I_S \otimes H_B$ that are singled out in H_{full} are only special cases of interactions and could in principle be included in the expansion of H_I. In the following, these terms will be set to zero. Alternatively, one can say that the following discussion will apply in the interaction picture, i.e. when the evolution according to $H_S \otimes I_B + I_S \otimes H_B$ is absorbed into the definition of operators.

Operators H_S, I_S and N_α, i.e. the parts of the Hamiltonian that act on the system S, generate an algebra which is usually called $\mathcal{A}$. The interpretation of $\mathcal{A}$ is that it comprises all the possible operations (as part of the system or the interaction Hamiltonians) that change the state of the system. It follows from the fact that the Hamiltonian is hermitian that $\mathcal{A}$ is a †-closed, unital algebra. It can be decomposed as

$$\mathcal{A} = \bigoplus_J I_{n_J} \otimes M_{d_J}, \tag{4.4}$$

where the tensor sum is over independent algebras M_{d_J} of $d_J \times d_J$ matrices, each occurring with multiplicity n_J. Following through, the Hilbert space of the system can similarly be decomposed as

$$\mathcal{H}_S = \bigoplus_J C_{n_J} \otimes C_{d_J}. \tag{4.5}$$

An operator $N_\alpha \in \mathcal{A}$ acts on $|a\,b\rangle$, where a and b denote states according to the above decomposition (4.5), to give

$$N_\alpha |a\,b\rangle = \sum_{b'} M^\alpha_{b\,b'} |a\,b'\rangle. \tag{4.6}$$

The matrix $M^\alpha_{b\,b'}$ rotates the states labeled by b but does not depend on or change the label a. One sees that the subspaces labeled by states a in C_{n_J} are acted upon with the unit operator by elements of $\mathcal{A}$ so that they are therefore left unchanged during evolution - these subspaces are said to be 'noiseless.'

Another terminology for the noiseless states is 'decoherence free.' This name can be appreciated when the situation is studied from a different point of view. Consider the density matrix $\rho_0 = |a\,b\rangle\langle a\,b|$. The action of the operators N_α on ρ is

$$N_\alpha \rho N^\dagger_\alpha = \sum_{b',\,b''} M^\alpha_{b,b'} |a\,b'\rangle\langle a\,b''| M^{\alpha\,\dagger}_{b,b''}. \tag{4.7}$$

Tracing out the subsystem spanned by the $|b\rangle$ states gives

$$\begin{aligned} \mathrm{Tr}_B N_\alpha \rho_0 N^\dagger_\alpha &= \sum_{b'''} \langle b'''| \sum_{b',\,b''} M^\alpha_{b,b'} |a\,b'\rangle\langle a\,b''| M^{\alpha\,\dagger}_{b,b''} \, |b'''\rangle \\ &= \sum_{b'''} \sum_{b',\,b''} \delta_{b'\,b'''} M^\alpha_{b,b'} |a\,b'\rangle\langle a\,b''| M^{\alpha\,\dagger}_{b,b''} \, \delta_{b''\,b'''} \\ &= |a\rangle\langle a| = \mathrm{Tr}_B \rho_0 \end{aligned} \tag{4.8}$$

after using the identity

$$\sum_{b'} MM = 1. \tag{4.9}$$

This shows that the subspace spanned by states $|a\rangle$ (or, density matrices of the form $|a\rangle\langle a|$) is left invariant by the noise operations. Note that if a density matrix ρ is not initially in the special product form $|a\,b\rangle\langle a\,b|$, then $\mathrm{Tr}_B N_\alpha \rho N^\dagger_\alpha \neq \mathrm{Tr}_B \rho$, giving the appearance of non-unitary evolution. Examples of these effects are given in the next section.

There is an interesting specialization of noiseless subsystems in the event where the algebra $\mathcal{A}$ decomposes so that all the matrix algebras M_{d_J} are one-dimensional. In this case, the form of operators N_α is

$$N_\alpha |a, b\rangle = p_{\alpha\,b} |a\,b\rangle, \tag{4.10}$$

where the phases $p_{\alpha\,b}$ replace the rotations $M^\alpha_{b\,b'}$ of (4.6). The phases cancel out when using the density matrix formalism,

$$N_\alpha |a, b\rangle\langle a, b| N^\dagger_\alpha = p_{\alpha\,b} |a, b\rangle\langle a, b| p^\dagger_{\alpha\,b} = |a\,b\rangle\langle a\,b|. \tag{4.11}$$

In such special cases, the operators N_α are called 'stabilizer' elements and the invariance is apparent without having to trace out a particular subsystem.

Now, recall that the system Hilbert space is coupled to an environment. Thus a full state can be written as $\rho = |\psi\,\phi\rangle\langle\psi\,\phi|$ where ψ is a state of the system Hilbert space and ϕ is a state

of the environment. Evolution is generated by the unitary operator $U_{full} = \exp(i\tau H_{full})$. In time τ, dropping the subscripts, the density matrix changes as follows

$$\rho \to U\rho U^\dagger \sim \rho + \frac{\tau^2}{2}\left(2H\rho H - H^2\rho - \rho H^2\right). \tag{4.12}$$

The approximation being made is valid in the limit of short evolution times. For the case of the interaction Hamiltonian (4.3), consider the operators N to act as $N|\psi\rangle = |\psi'\rangle$ and $N|\psi'\rangle = |\psi''\rangle$. Then, after a short evolution and after tracing out states of the environment, one has

$$|\psi\rangle\langle\psi| \to |\psi\rangle\langle\psi| + \frac{\tau^2}{2}\left(2|\psi'\rangle\langle\psi'| - |\psi''\rangle\langle\psi| - |\psi\rangle\langle\psi''|\right). \tag{4.13}$$

The nature of the resulting state depends on the type of initial state. In the special case where the original state is noiseless and obeys (4.10) with unit phase, i.e. $|\psi'\rangle = |\psi''\rangle = |\psi\rangle$, the terms in the parenthesis cancel and the evolution is trivial. In other cases, the interpretation of the resulting state is less self-evident. For example, when the original state $|\psi\rangle$ is noiseless and obeys (4.6), the evolution appears to be trivial only after tracing out a subsystem similarly as in (4.8) (the b component of $|\psi\rangle$.) A different situation arises when the original state does not satisfy any of the noiselessness conditions. Then, the result of the evolution is a state that is, generically, mixed and whose 'extent' of mixture grows as the evolution progresses (the new terms in the density matrix are proportional to τ). Thus, from the point of view of the system, noisy states evolve according to a dissipative and non-unitary dynamics.

Decoherence-free states are of importance for quantum information processing because they can reliably store information for long periods of time. For information processing, however, it is also very important to be able to manipulate or change information in order to perform computations. To this end, it is interesting to define the possible operations that can be applied to a noiseless states without ruining its noiseless feature. These operations are elements of the algebra $\mathcal{A}'$ of all elements that commute with the interaction algebra $\mathcal{A}$ [21]. That is, an operator $A' \in \mathcal{A}'$ can be used to safely manipulate a noiseless state if and only if $[A, A'] = 0$ for all $A \in \mathcal{A}$. The algebra $\mathcal{A}'$ is called the commutant of $\mathcal{A}$; for more details on identifying noiseless subsystems via the commutant of the algebra of operators on the system, see [21].

Map to Constrained Mechanics

Shifting slightly to review the standard method of dealing with quantum constrained systems (see, for example, [1]), consider the kinematical Hilbert space $\mathcal{H}_{kin}$ of an unconstrained system. Constraints are represented by operators C_a acting on this Hilbert space. The kind of constraints considered here are those that form a closed, first-class algebra $[C_a, C_b] = f_{ab}{}^c C_c$ for some structure constants $f_{ab}{}^c$. Physical states of the system are defined to be those that satisfy the constraint equations $C_a|\psi\rangle_{phys} = 0$; the span of these states forms the physical Hilbert space, $\mathcal{H}_{phys}$. An important aspect of understanding constrained systems is the construction of the algebra $\mathcal{D}$ of Dirac observables. Operators in this algebra commute with the constraints and thus measure physical (invariant) properties of physical states. In other words, $D \in \mathcal{D}$ is an observable if and only if $[D, C_a] = 0$ for all C_a.

There are significant similarities in the algebraic structures that are relevant to the constrained systems and that appear in the discussion of noiseless subsystems. Specifically, in each case one has two distinct algebras that commute. The aim of the present work is to probe this similarity and establish a connection between constrained systems and noiseless subsystems. This is accomplished by constructing a mapping from a constrained system to a noiseless subspace.

Consider a system subject to a set of first-class constraints C_a. Consider also an identity operator I on the kinematical Hilbert space $\mathcal{H}_{kin}$ and define new operators $N_{\alpha\,\lambda} = (I + \lambda C_\alpha)$. Then if $C_\alpha|\psi\rangle_{phys} = 0$, operators $N_{\alpha\,\lambda}$ stabilize physical states for all λ, i.e. $N_{a\,\lambda}|\psi\rangle_{phys} = |\psi\rangle_{phys}$. Thus, an alternative description of the constrained system starts to develop in which $\mathcal{H}_{kin}$ can be identified with $\mathcal{H}_S$ and the new stabilizer elements $N_{a\,\lambda}$ generate the algebra $\mathcal{A}$. Recall that elements of $\mathcal{A}$ have the interpretation of being operations that couple the system to an environment. Thus, this approach suggests $\mathcal{H}_{kin}$ should be coupled to a new Hilbert space $\mathcal{H}_B$ representing an environment or bath.

The interaction Hamiltonian (4.3) for the constrained system and environment will have the form

$$H_I = \sum_\alpha N_\alpha \otimes B_\alpha = \sum_\alpha \left(1 \otimes B_\alpha + \lambda C_\alpha \otimes B_\alpha\right), \tag{4.14}$$

for some operators B_a acting on the environment. Incidentally, the decomposition of the interaction terms on the right hand side make the first term appear as operators acting on the environment only, i.e. being part of $1 \otimes H_B$ of (4.2). Only the terms proportional to the constraints are therefore part of the 'true' interaction Hamiltonian,

$$H_I \to \sum_\alpha C_\alpha \otimes B_\alpha. \tag{4.15}$$

In short, there is now a new quantum system with a full Hilbert space $\mathcal{H}_{full} = \mathcal{H}_{kin} \otimes \mathcal{H}_B$ governed by a Hamiltonian of the form (4.3) with H_S given by the Hamiltonian of the constrained problem, H_B given by the operators B_α, and H_I given by (4.15).

The noiseless states of this new system are, by construction, solutions to the constraints C_α. They therefore exhibit all the physical properties that the solutions to the constrained problem do. Since the environment in the quantum information theoretic description is not really of interest from the point of view of the constrained dynamics problem, it should be traced out. As a result, the noiseless states evolve unitarily under the full Hamiltonian while the noisy states, which do not satisfy the constraint equations, decay non-unitarily and as such are not of physical interest.

The commutant $\mathcal{A}'$ in the noiseless subspace picture is the set of all operators that commute with the constraints C_α. Thus, there is also a close correspondence between $\mathcal{A}'$ and $\mathcal{D}$, up to the status of the unit operator. The unit is always a Dirac observable and is thus in $\mathcal{D}$. On the noiseless subsystem side, however, the unit operator is also included in the algebra $\mathcal{A}$ (recall that $\mathcal{A}$ is assumed unital). The interesting correspondence, therefore, should be made between the non-trivial elements of $\mathcal{A}'$ and the non-trivial Dirac observables.

4.2 Examples

This section demonstrates the mapping between noiseless subspaces and solutions to constraints through several examples. The first example is the standard case used to demonstrate noiseless subsystems in the quantum information processing literature [21]. The other examples apply the concepts to situations more familiar from mechanics and field theory. One of these, involving a scalar field, is worked out in detail, while the other examples are focussed on discussing the conceptual implications of adopting the noiseless subsystems viewpoint.

Strong Collective Decoherence and Angular Momentum

The first example is a system well studied in the literature on fault-tolerant computation. It consists of a group of qubits subjected to strong collective decoherence due to a coupling to an environment. For concreteness, the number of qubits in the following discussion is set to three as that is the minimal number that can give rise to a non-trivial noiseless subsystem under the stated conditions. The system Hilbert space is

$$\mathcal{H}_S = \mathcal{H}_1 \otimes \mathcal{H}_2 \otimes \mathcal{H}_3 \tag{4.16}$$

where each of $\mathcal{H}_i$ on the right hand side are spaces spanned by two states $|0\rangle$ and $|1\rangle$. The interaction Hamiltonian for strong collective decoherence is of the form (4.3) with noise operators

$$N_\alpha = \sigma_\alpha \otimes 1 \otimes 1 \,+\, 1 \otimes \sigma_\alpha \otimes 1 \,+\, 1 \otimes 1 \otimes \sigma_\alpha; \tag{4.17}$$

here the index α takes one of the values x, y, and z. The σ_α are the Pauli matrices

$$\sigma_x = \begin{bmatrix} 0 & 1 \\ 1 & 0 \end{bmatrix}, \qquad \sigma_y = \begin{bmatrix} 0 & i \\ -i & 0 \end{bmatrix}, \qquad \sigma_z = \begin{bmatrix} 1 & 0 \\ 0 & -1 \end{bmatrix} \tag{4.18}$$

and satisfy the algebra $[\sigma_i, \sigma_j] = 2i\epsilon_{ijk}\sigma_k$ when they act on the same qubit. The important feature of these noise operators is that they act symmetrically on all the qubits; hence the word "collective" in the name of the model. The term "strong" refers to the fact that all three Pauli operators appear in three noise operators N_α.

From standard quantum mechanics, it is known that three qubits (which are effectively spin 1/2 particles) combine to form a system with total angular momentum equal to either $J = 3/2$ or $J = 1/2$. In fact, there is a unique way of aligning the spins to produce $J = 3/2$ and there are two distinct ways of producing $J = 1/2$. The Hilbert space $\mathcal{H}_S$ described above can therefore be also written in the form

$$\mathcal{H}_S = (C_2 \otimes C_2) \,\oplus\, (C_1 \otimes C_4)\,; \tag{4.19}$$

the total dimension is still 8 $(= 2 \cdot 2 + 4.)$ just as in (4.16). This is a decomposition of the total Hilbert space of the form (4.5), and since there are two copies of the the C_2 space (angular momentum $J = 1/2$) that degeneracy can encode a noiseless subsystem.

The states of $\mathcal{H}_S$ which have $J = 1/2$ can be computed with the help of Clebsch-Gordan coefficients. In this case they are [21]:

$$\begin{aligned} |\phi_0\rangle &= \frac{1}{\sqrt{2}}\left(|010\rangle - |100\rangle\right) \\ |\phi_1\rangle &= \frac{1}{\sqrt{2}}\left(|011\rangle - |101\rangle\right) \end{aligned} \tag{4.20}$$

for the first copy of $J = 1/2$ and

$$\begin{aligned} |\psi_0\rangle &= \frac{1}{\sqrt{6}}\left(-2|001\rangle + |010\rangle + |100\rangle\right) \\ |\psi_1\rangle &= \frac{1}{\sqrt{6}}\left(2|110\rangle - |101\rangle - |011\rangle\right) \end{aligned} \tag{4.21}$$

for the second copy. The subscripts 0 and 1 denote the $m = -1/2$ and $m = 1/2$ values, respectively. The $J = 3/2$ states will not be needed below.

None of the states in (4.20) or (4.21) are exactly invariant under the action of any of the N_α operators. However, one finds curious properties. For example, if N_x acts on an arbitrary superposition of $|\phi_0\rangle$ and $|\phi_1\rangle$, then one has

$$N_x\left(a|\phi_0\rangle + b|\phi_1\rangle\right) = b|\phi_0\rangle + a|\phi_1\rangle. \tag{4.22}$$

Thus the coefficients of the $|\phi_0\rangle$ and $|\phi_1\rangle$ in the initial state are rotated into each other ($a \to b$, $b \to a$). This corresponds to the general formula (4.6). One can check that the other noise operators N_y and N_z perform similar rotations, so that the subspace spanned by these two states is invariant under the action of arbitrary combinations of noise operators. Similarly, the noise operators rotate superpositions of $|\psi_0\rangle$ and $|\psi_1\rangle$ into each other but do not take a superposition of these states outside of the subspace spanned by them.

The two subspaces, one spanned by $|\phi_0\rangle$ and $|\phi_1\rangle$ and the other spanned by $|\psi_0\rangle$ and $|\psi_1\rangle$, define two noiseless states. In summary, the three qubit system contains two noiseless states which can be relied on to preserve encoded information despite there being a constant interaction with the environment. Since there are two noiseless states, the system is said to encode one qubit of information in a noiseless subsystem. The word subsystem is used (as opposed to subspace) because neither state can be decomposed as a fixed superposition of states in the computational ($|0\rangle$ and $|1\rangle$) basis of the original three spins.

The goal is now to see the same states turn out as solutions to some constraints. To do this, one interprets the noise operators N_α as related to constraint operators C_α. They form a first class algebra $[N_i, N_j] = 2i\epsilon_{ijk}N_k$ and thus satisfy the criteria for the method outlined before. In the kinematical Hilbert space $\mathcal{H}_{kin} = \mathcal{H}_S$, one finds after group averaging over the orbits of N_α that two states

$$\begin{aligned} |\Phi\rangle &= \frac{1}{\pi}\int_0^1 dr \int_0^{2\pi} d\theta \ \left(r|\phi_0\rangle + e^{i\theta}\sqrt{1-r^2}|\phi_1\rangle\right) \\ |\Psi\rangle &= \frac{1}{\pi}\int_0^1 dr \int_0^{2\pi} d\theta \ \left(r|\psi_0\rangle + e^{i\theta}\sqrt{1-r^2}|\psi_1\rangle\right) \end{aligned} \tag{4.23}$$

satisfy

$$(N_\alpha - 1)|\Phi\rangle = (N_\alpha - 1)|\Psi\rangle = 0. \tag{4.24}$$

Thus these states can be interpreted as physical states which solve the constraints $C_\alpha = N_\alpha - 1$. They span the physical Hilbert space $\mathcal{H}_{phys}$ that one is interested in when dealing with the constrained system. The group averaging in this presentation is equivalent to having to trace out the b subsystem in the general noiseless subsystems framework, as in (4.8). The example also illuminates the role of the unit operator in the relationship between the noise operators N_α and the constraints C_α.

The summary and conclusion is that the same two states, denoted by $|\Phi\rangle$ and $|\Psi\rangle$, become the objects of study either in the perspective of noiseless states for fault-tolerant computation or in the viewpoint of physical states in constrained mechanics.

Momentum Constraint for a Scalar Field

Consider a system composed of a field ϕ in 4d subject to a constraint. A general Lagrangian density for such a system is

$$\mathcal{L} = \frac{1}{2}\phi\nabla_\phi^2\phi - V_0(\phi) - \chi C(\phi) \tag{4.25}$$

where $\nabla_\phi^2 = \partial^2 - m_\phi^2$ is the quadratic D'Alambertian operator for the field ϕ, $V_0(\phi)$ is a potential or self-interaction term, and χ is a Lagrange multiplier whose equation of motion imposes the constraint $C(\phi) = 0$. In what follows, the self-interaction potential is set $V_0(\phi) = 0$ because the discussion is focussed on implementing the constraint on external (free) particle states. The presence of such a potential, however, does not affect the main issues and it can be easily added and treated perturbatively using standard methods.

According to the noiseless subsystems paradigm, one can avoid writing theories such as (4.25) which explicitly contain Lagrange multiplier field and constraints. Instead, one can write down alternative theories which have a larger number of fields, fewer symmetries, but wherein the constraints on the physical degrees of freedom are implemented dynamically. In the present case, one can introduce a scalar field χ and write a new Lagrangian density as follows

$$\mathcal{L}' = \frac{1}{2}\phi\nabla_\phi^2\phi + \frac{1}{2}\chi\nabla_\chi^2\chi + \chi(\mu + \lambda C(\phi)). \tag{4.26}$$

Now χ appears as a standard scalar field with its own kinetic operator; the mass of the field will be denoted m_χ. The final interaction term in $\mathcal{L}'$ establishes a link between this theory and the constrained system (4.25). There appear two new constants μ and λ in this interaction term. The first constant μ has dimensions $4 - D(\chi) = 3$; it will turn out that it does not play a big role in the theory. The second constant λ is more important and has appropriate dimensions so that the term $\lambda\chi C(\phi)$ has total dimension 4. For the Lagrangian to be real, the constraint $C(\phi)$ must be real.

The interaction term is linear in χ, so the whole Lagrangian can be diagonalized to absorb all the dependence on χ into the quadratic kinetic piece. To do this, make the following shift

$$\chi(x) = \chi'(x) - i\int d^4y\ D_\chi(x,y)(\mu + \lambda C(\phi(y))) \tag{4.27}$$

where $D_\chi(x,y)$ is the Greens' function (Feynman propagator) of the operator ∇^2_χ, i.e. $\nabla^2_\chi D_\chi(x,y) = -i\delta(x,y)$. After this shift, the Lagrangian becomes

$$\mathcal{L}' = \frac{1}{2}\phi\nabla^2_\phi\phi + \frac{1}{2}\chi'\nabla^2_\chi\chi' - V^{NL}(\phi) \tag{4.28}$$

where V^{NL} is a new non-local potential

$$V^{NL}(\phi) = i\frac{1}{2}\big(\mu + \lambda C(\phi(x))\big)\int d^4y\; D_\chi(x,y)\big(\mu + \lambda C(\phi(y))\big). \tag{4.29}$$

Now, consider the functional integral

$$Z = \int \mathcal{D}\phi\mathcal{D}\chi' \exp\left(i\int d^4x\; \mathcal{L}'\right). \tag{4.30}$$

Since the χ' field only has a quadratic part in the action, the integral $\int \mathcal{D}\chi'$ is gaussian (in Euclidean signature) and just gives an overall determinant factor which does not affect any correlation functions nor expectation values for observables in the field ϕ. The resulting functional integral for the ϕ field is therefore given by

$$Z \sim \int \mathcal{D}\phi \exp\left(i\int d^4x\; \frac{1}{2}\phi\nabla^2_\phi\phi - V^{NL}(\phi)\right). \tag{4.31}$$

The non-local potential consists of four terms, but it turns out that only one of them is important. One of the terms, $\mu D(x,y)\mu$, is independent of ϕ and can therefore be ignored. To analyze the remaining terms, it is useful to define a new function $C(p)$ as a Fourier transform as follows

$$C(p) = \int d^4y\; C(\phi(y))e^{ip\cdot y} \tag{4.32}$$

and to represent the Green's function as the integral

$$D_\chi(x,y) = \int \frac{d^4p}{(2\pi)^4}\,\frac{i}{p^2 - m^2_\chi + i\epsilon}\,e^{ip\cdot(x-y)}. \tag{4.33}$$

In these notations, another one of the terms of the potential can be expressed as

$$\frac{i}{2}\lambda\mu\int d^4y\; D_\chi(x,y)C(\phi(y)) = \frac{i}{2}\lambda\mu\int \frac{d^4p}{(2\pi)^4}\frac{i}{p^2 - m^2_\chi + i\epsilon}\,C(p)e^{-ip\cdot x}. \tag{4.34}$$

When this potential is inserted into an action, there will be a factor of the form $\int d^4x\; e^{-ip\cdot x}$. This can be set to zero because it is an integral over an oscillating function. Thus, the second term of the potential V^{NL} can also be ignored. The third term in the potential is

$$\frac{i}{2}\lambda\mu C(\phi(x))\int d^4y\; D_\chi(x,y) = \frac{i}{2}\lambda\mu C(\phi(x))\int \frac{d^4p}{(2\pi)^4}\frac{i}{p^2 - m^2_\chi + i\epsilon}e^{-ip\cdot x}\int d^4y\; e^{ip\cdot y}. \tag{4.35}$$

Again, this term can be ignored because the last integral can be set to vanish. The fourth term in the potential is the important one. To see how this term contributes to the action, integrate over all of space to obtain

$$\frac{i}{2}\lambda^2 \int d^4x d^4y \; C(\phi(x)) D_\chi(x,y) C(\phi(y)) = \frac{i}{2}\lambda^2 \int \frac{d^4p}{(2\pi)^4} \; \frac{i}{p^2 - m_\chi^2 + i\epsilon} C(-p)C(p). \quad (4.36)$$

The objects $C(p)$ on the right hand side are again defined by (4.32).

After all these simplifications, the total resulting action in momentum space notation becomes

$$S = \int \frac{d^4p}{(2\pi)^4} \; \left(\frac{1}{2}\phi(-p)(p^2 - m_\phi^2)\phi(p) + \frac{\lambda^2}{2} C(-p) \frac{1}{p^2 - m_\chi^2 + i\epsilon} \, C(p) \right). \quad (4.37)$$

Note that all dependence on the mass parameter μ is removed.

Now it might be helpful to consider a concrete form of $C(\phi(x))$ or $C(p)$ to demonstrate the effect of the formalism. A simple example is the momentum constraint

$$C(\phi(x)) = \partial_3 \phi(x), \qquad\qquad C(p) = -ip_3 \phi(p). \quad (4.38)$$

In the original Lagrangian formulation, this constraint effectively requires the modes of the field ϕ to have momentum only in the p_1 and p_2 components but not in the p_3 component. With this explicit function C, the resulting action is quadratic

$$S = \int \frac{d^4p}{(2\pi)^4} \; \left(\phi(-p)(p^2 - m_\phi^2)\phi(p) + \frac{\lambda^2}{2} \phi(-p) \frac{p_3^2}{p^2 - m_\chi^2 + i\epsilon} \, \phi(p) \right) \quad (4.39)$$

and the corresponding equation of motion is

$$\left(p^2 - m_\phi^2 + \frac{\lambda^2}{2} \frac{p_3^2}{p^2 - m_\chi^2} \right) \phi(p) = 0. \quad (4.40)$$

Despite its simple form, the propagator in the last term reveals that the field is governed by non-local dynamics; this is due to interactions with the χ field which has been integrated out. The inverse of the equation of motion gives the momentum space propagator,

$$D_F(p) = \frac{p^2 - m_\chi^2}{(p^2 - m_\phi^2)(p^2 - m_\chi^2) + \frac{\lambda^2}{2} p_3^2}. \quad (4.41)$$

Since the denominator is quartic, $D_F(p)$ has four poles at $p_0 = \pm (E_\pm^2)^{1/2}$. An interesting special case is when the masses are equal $m_\phi = m_\chi$ so that $\Delta m^2 = 0$. In that case, the propagator simply becomes a sum of two terms

$$D(p) = \frac{1}{2} \left[\frac{1}{p_0^2 - E_+^2} + \frac{1}{p_0^2 - E_-^2} \right] \quad (4.42)$$

where now

$$E_\pm^2 = p_i^2 + m^2 \pm \frac{1}{2} \sqrt{-2\lambda^2 p_3^2}. \quad (4.43)$$

The last term is imaginary since both λ and p_3 are real.

There is a known correspondence between an imaginary mass in a propagator, such as in

$$D(p) = \frac{1}{p^2 - m^2 + im\Gamma} \tag{4.44}$$

and the decay rate of a particle Γ. In the present case, the scalar particle is unstable and decays with

$$\Gamma \propto \frac{\lambda p_3}{m}. \tag{4.45}$$

The decay rate Γ depends explicitly on p_3 and vanishes when $p_3 = 0$ so that free particles which do not carry p_3 momentum are long-lived. Particles which do carry p_3 momentum, decay. Since the parameter λ is a dimensionful coupling in this setup, it can be expected to grow large via the renormalization group flow in the infra red - this implies that the transition in Γ between the $p_3 = 0$ and $p_3 \neq 0$ situations will be fairly sharp. (This statement, however, is not general and the transition would have to be studied in other situations where a coupling analogous to λ had different dimension. A fast decay rate can also be achieved by increasing the number of environment fields and thereby opening more decay channels.)

What does the particle ϕ decay into? From the original Lagrangian (4.25), one can conclude that it decays into a χ particle. However, the noiseless subsystems picture can be sustained even if the content of the environment is unknown because all that is required is that there is an explicit coupling between the constrained field and the environment. In the above calculation, the Hilbert space of the environment was chosen explicitly and the coupling was rather special, but other choices could have been made as well. The results for the exact decay rate formula would then have been different. What is of interest here, however, is that the modes that do not satisfy the constraint are unstable and decohere.

The next few examples are designed to bring out conceptual issues that arise when adopting the noiseless subsystems viewpoint.

Relativistic Particle

A familiar example of a constrained system is the relativistic particle moving in a flat background (metric $\eta_{\mu\nu} = diag(-1, 1, 1, 1)$). Its Lagrangian is given by

$$L = -m\sqrt{-\eta_{\mu\nu}\dot{q}^\mu \dot{q}^\nu}. \tag{4.46}$$

The overdot denotes time derivatives ∂/∂_τ. The conjugate momenta to q_μ are

$$p_\mu = \frac{\partial L}{\partial \dot{q}^\mu} = m^2 \frac{\dot{q}_\mu}{L}, \tag{4.47}$$

and the standard Hamiltonian

$$H = p_\mu \dot{q}^\mu - L = 0 \tag{4.48}$$

vanishes due to time-reparametrization invariance of the Lagrangian. The system is instead characterized by the constraint

$$C = -p_0^2 + p_i^2 + m^2, \tag{4.49}$$

which puts the relativistic particle on-shell. The total Hamiltonian therefore actually consists of this constraint,

$$H = \beta C, \tag{4.50}$$

where β is a Lagrange multiplier.

The kinematical Hilbert space $\mathcal{H}_{kin}$ for the particle is the space of wavefunctions spanned by the states $|p_0, p_i\rangle$. Due to the constraint, however, only three of the four momenta can be independent. It is convenient to choose p_0 as the dependent variable. States

$$|\psi\rangle_{phys} = |p_{0\,phys}, p_i\rangle \qquad p_{0\,phys} = \sqrt{p_i^2 + m^2} \tag{4.51}$$

satisfy the constraint, $C|\psi\rangle_{phys} = 0$.

To view the relativistic particle from a noiseless subsystem point of view, consider the algebra $\mathcal{A}$ generated by the constraint C and the identity operator. Then define operators $N_\lambda = 1 + \lambda C$ acting on the system Hilbert space spanned by states labeled by four-momenta. The full Hamiltonian describing the evolution of the particle coupled to the environment is defined as

$$H_{full} = 1 \otimes B + C \otimes B, \tag{4.52}$$

in analogy to (4.2) but with $H_S = 0$ due to the actual Hamiltonian of the relativistic particle being zero in the constrained dynamics picture. The particle and the environment evolve via the evolution operator $U = \exp(i\tau\, H_{full})$; the evolution is naturally parametrized by a new external time variable τ which has physical meaning as far as the environment evolution is concerned.

In the quantum information theoretic picture, a generic initial state evolves into a totally mixed background with particle-like excitations. This situation can be compared to the description of signals in liquid-state Nuclear Magnetic Resonance experiments. There, a liquid sample is viewed as consisting of many small randomly-oriented spins. When a low-frequency pulse is applied, the spins tilt slightly with the effect of generating a net magnetization in the sample. An effective density matrix can be used to describe the state of the sample which is composed of a sum of a total mixed state and a small particle contribution. Remarkably, the particle contribution actually behaves like a real particle and can even be successfully employed in experimental quantum information processing [23]. The proposal here is to view the relativistic particle in a similar manner - as an excitation over a noisy background.

Electromagnetism

As another example, consider electromagnetism with the action

$$S = -\frac{1}{4}\int d^4x\; F_{\mu\nu}F^{\mu\nu}, \tag{4.53}$$

where $F_{\mu\nu} = \partial_\mu A_\nu - \partial_\nu A_\mu$. The action is invariant under gauge transformations $A_\mu \to A_\mu + \partial_\mu \alpha$ where α is any space-time function. The momenta that are conjugate to A_μ are $\pi^0 = 0$ and $\pi^i = F^{i0}$. The Hamiltonian for the theory is

$$H = \int d^3x\; \left(\frac{1}{2}\pi_i\pi^i + \frac{1}{4}F_{ij}F^{ij} - A_0\partial_i\pi^i\right). \tag{4.54}$$

In the last term, A_0 appears as a Lagrange multiplier imposing the constraint

$$C = \partial_i \pi^i = \partial_i \partial^i A_0 - \partial_i \partial_0 A^i. \tag{4.55}$$

The effect of the constraint is to reduce the number of physical, propagating degrees of freedom in the vector potential down to two, giving electromagnetism an interpretation as a theory of massless spin one particles (photons) propagating at the speed of light.

Since electromagnetism is a theory of a four-dimensional vector field, one might expect the Hamiltonian to be a function of all four components of A_μ and their conjugate momenta, $H = H(A_0, \pi_0, A_i, \pi_i)$. The Hamiltonian above, however, is of the special form

$$H = H_S(\pi_i, A_i) - C(\pi^i, A^i)A_0 \tag{4.56}$$

whereby H_S does not depend on the scalar potential A_0 nor its momentum, and the second term is clearly split into two factors, one that depends on A_0 and another one that does not. This kind of splitting suggests writing the Hilbert space of electromagnetism as $\mathcal{H} = \mathcal{H}_S \otimes \mathcal{H}_B$, treating the the vector potential A_i as the 'system' and the scalar potential A_0 as the 'bath.' The Hamiltonian is therefore composed of a piece $H_S \otimes 1$ that evolves the system only and an interaction term $H_I = C \otimes A_0$.

To make electromagnetism match the noiseless subsystems scheme, the system part of the interaction term should act as a stabilizer on physical states. At the moment, that part of H_I annihilates physical states. Thus, the existing interaction term is replaced by $H_I \to N \otimes A_0$ where $N = 1 + C$. The effect of this exchange is to introduce a new term into the Hamiltonian:

$$H = H_S(\pi_i, A_i) - C(\pi^i, A^i)A_0 - A_0. \tag{4.57}$$

Now the noiseless states in the system part, after tracing out the scalar potential degrees of freedom, should be exactly the ones that correspond to the transverse polarizations of photons. This is what happens when longitudinal modes decouple and do not contribute to the amplitudes of scattering processes involving incoming transverse modes.

The physical picture that emerges from the noiseless subsystem framework is as follows. The full set of fields (A_0, A_i) evolves according to a Hamiltonian without constraints or Lagrange multiplier fields which treats the vector potential as the 'system' and the scalar potential as the environment. Due to the interaction term, only certain states of the vector potential are noiseless. So only those states can be expected to be preserved in the 'long term' when the environment is traced or averaged out. Presumably, these long lived states are those that can be seen/observed/detected in the laboratory - thus photons are interpreted as excitations in the noiseless sector of the vector potential.

Having experience dealing only with the noiseless states in the laboratory, the usual description of experimental results is made using a theory that is re-parametrization invariant, i.e. a gauge theory. However, if experiments could give access to the full spectrum of states as opposed only to the noise-free ones, in effect allowing us to measure the scalar potential directly, then the gauge invariance would perhaps not be a true symmetry of the full system.

The extra term in the Hamiltonian has a similar effect to introducing a gauge fixing condition. This is not a problem in the present sense because, at the same time, it is postulated that the scalar potential is not observable and focus the discussion on noiseless

states in the vector potential Hilbert space; tracing out the scalar potential gets rid of the rigidity of the fixed gauge. At the end, the quantum information theoretic description ends up with the same physical solutions as the original gauge theory. In this sense gauge invariance is an emergent property in the noiseless states.

Gravity as a Constrained System

As a final example, consider general relativity which is, like the relativistic particle, a totally constrained system [1]. The Hamiltonian in the Ashtekar variables is a sum of first-class constraints,

$$H = \int_{\Sigma} A_0^i G^i + N_a D_a + N D. \tag{4.58}$$

The integral is taken over a three-dimensional manifold Σ. The Lagrange multiplier A_0^i is of the kind appearing in the gauge theory example and implements the Gauss constraint G^i. The lapse function N that implements the Hamiltonian constraint D is akin to the Lagrange multiplier appearing in the relativistic particle example. The remaining multipliers N_a that implement the three diffeomorphism constraints D_a are characteristic to this example, but they can be treated using similar methods.

Multiple constraints in the gravity Hamiltonian can be treated in sequence and on an individual basis as follows. In general, each constraint (suppose there are n of them) can have a separate environment Hilbert space $\mathcal{H}_{Bn}$ associated with it giving $\mathcal{H}_{full} = \mathcal{H}_S \otimes \mathcal{H}_{B1} \otimes \cdots \otimes \mathcal{H}_{Bn}$. Solutions to the n-th constraint can be found in the space $\mathcal{H}_S \otimes \mathcal{H}_{B1} \otimes \cdots \otimes \mathcal{H}_{B(n-1)}$ (or its dual) as the noiseless states with respect to the appropriate coupling. After having characterized the solutions/noiseless states of this constraint, another constraint can be considered to further restrict the set of states that are of physical significance, and so on until all the constraints are taken care of. At each step, the size of the noiseless Hilbert space decreases until one finally determines the states of interest.

If the goal of studying general relativity is said to be finding the exact solutions of the constraints, it is of no significance whether the characterization of these solutions is done via standard methods or via quantum information theoretic tools. In particular, the discussion of quantum gravity in terms of noiseless subsystems can be simplified by using the well-known result that states invariant under gauge transformations and spatial diffeomeorphisms can be labeled by spin networks [1]. To formally obtain solutions to full quantum general relativity, then, these spin-networks can be coupled to an environment and an interaction Hamiltonian can be introduced to correspond to the Hamiltonian constraint. The noiseless spin networks in this scheme are the physical solutions of interest. Unfortunately, the quantum information theoretic approach does not make the problem of actually writing down simple expressions for these states any easier than in the standard Dirac quantization program. A perhaps promising feature of the noiseless subsystem approach, however, is that these physical states should appear dynamically as invariant states out of a generic initial state of a system and environment.

4.3 Implications

From the above examples, one can make some general comments on the status of symmetries in fundamental physics. The connection of physical states with noiseless subsystems brings forth some conceptual differences with the standard approach of dealing with symmetries.

Role of Symmetries

In the case of the relativistic particle, noiseless states evolve as if the Hamiltonian were zero exactly as in the original constrained system. Thus, these states exhibit an emergent time-reparametrization invariance property. However, in the noiseless subsystems picture, the 'true' Hamiltonian is actually H_{full} and is nonzero. The system evolves according to this 'true' Hamiltonian in an external time τ. There is no 'problem of time' as the evolution of the environment provides, in principle, a well defined clock to measure time flow by.

The proposed viewpoint, in a sense, is orthogonal to the much discussed relational approach (see for example [26, 27]) where the introduction of a background time is seen as something that should be avoided. For example, there is a proposal [27] that uses noiseless subsystems and quantum information theoretic tools to write a relational formulation of quantum theory that is originally expressed in terms of a background time. In contrast, the present proposal argues in the reverse direction that the relational features usually ascribed to physical systems such as time-reparametrization invariance to the relativistic particle can be understood as arising out of a non-relational theory of the system coupled to an environment.

Relationalism can be restored, however, by considering the new non-relational system as part of another even larger system. Then, density matrices would form a hierarchy

$$\rho_{rel} \hookrightarrow \rho_{non\,rel} \hookrightarrow \rho_{new\,rel} \tag{4.59}$$

where ρ_{rel}, $\rho_{non\,rel}$ and $\rho_{new\,rel}$ describe, respectively, the usual relativistic particle, the particle together with the environment, and the particle together with an environment as well as another auxiliary system (a clock). The transition between a density matrix in a large Hilbert space to a density matrix in a smaller space is performed by tracing out the redundant degrees of freedom. The bottom line is that the fixed background structure of the environment can be treated in a relational manner if relationalism is desired.

Apart from time-reparametrization invariance, gauge symmetries can also be interpreted to arise only in a particular sector of a background dependent theory. In the quantum information theoretic picture, states in the full Hilbert space spanned by the system and bath degrees of freedom act as if there was a fixed background time. Thus an observer having access to the full Hilbert space can follow the evolution of a gravity state using a set of external variables using the methods of standard quantum mechanics. It is only the process of ignoring, or tracing out the background environment that reproduces the background-independent features of general relativity. Tracing out the environment and focusing attention on the noiseless states is of course motivated by observations of a four-dimensional universe obeying the Einstein's equations to a high degree of accuracy.

Adding an environment to the universe is certainly a strange thing to do and introduces new interpretational issues. In addition, if the quantum theory of gravity is simply the

quantization of the known gravity and matter, then the whole approach is not very useful as in that case the noisy states would be regarded as "unphysical." However, the situation is different in approaches to quantum gravity such as those based on condensed matter systems in which general relativity is expected to be an effective theory describing the behavior of the low energy excitations of some other underlying system. In that case, an environment and usually a true Hamiltonian are already present in the fundamental theory and the question is how a constrained theory can arise at the effective level. There are similar questions in Causal Dynamical Triangulations, in which the full theory has a time parameter. Finally, the whole approach is reminiscent of the 'random dynamics' research program where fundamental laws and interactions of nature are assumed to be essentially random (or, too complicated to be easily determined and/or describe) and gauge and other symmetries are emergent at low energies [25].

Applications

Besides rephrasing constrained dynamics in a new language, the noiseless subsystems approach may also have some useful applications [15]. For example, in models of discrete space (or spacetime), as seen in the causal dynamical triangulation program and quantum graphity model discussed previously, where geometry is fluctuating and cannot be assumed constant, it is impossible to use standard tools to find and describe the low-lying particle like excitations. In those cases, one needs a new set of criteria that could be used to identify particle states. It has been argued [15] that the notion of noiseless subsystems could be used in those situations since the criteria for noiselessness are formulated in the quite abstract sense without reference to any underlying geometry.

Another possible application for noiseless subsystems is for simulations of constrained systems. Since states which are not noiseless decohere, one can conceive simulating a system as follows. Starting from an arbitrary initial state of the system (i.e. a state composed of a noiseless and noisy part), and a large environment, one can evolve the full system and environment unitarily according to the full Hamiltonian. At late times, the environment can be traced out. Because of the specific interaction with the environment, the noisy states of the system will drop out of the final description. Thus some insight on the constrained system might be gained without actually having to formulate explicitly the physical states. A negative feature of this idea is that it is in practice very difficult to simulate large quantum systems.

5 Particle Phenomenology

Regardless of what microscopic description one adopts for Planck scale geometry, it is generically expected that the Planck scale will have some effect on the propagation of matter. Thus while it is important to understand what the predictions of each model of Planck-scale spacetime structure are, the problem of particle phenomenology due to the Planck scale can also be studied quite generically. The simplest way to incorporate the Planck energy into a field theory, as mentioned in the introduction, is to add new terms to the standard model Lagrangian. Models constructed in this manner usually break Lorentz invariance in their very formulation. Thus, their tests are also tests of Lorentz symmetry. In recent years, these models have been extensively studied with terms of mass dimension four and five, and their free parameters have already been tightly constrained [36, 37]. However, several other proposals have also appeared in the literature. For example, there are models exhibiting decoherence, models defined on non-commutative geometries, models with non-canonical commutation relations - some of these can actually be mapped into one another [42].

One of the candidates for the resolution of the Lorentz symmetry problem is Deformed Special Relativity (DSR). Originally, the motivation for DSR was the playful question of whether it is possible to alter the postulates of special relativity so that in addition to an invariant speed c, there would also be an invariant mass κ (or length ℓ_P). Some examples of transformations satisfying this conditions were actually written down [38] and soon those transformation were found to correspond to a formalism of quantum deformations of the Poincare algebra. Also, the deformed notion of low-energy symmetry has been found to arise in the classical limit of one candidate for a full theory of quantum gravity in $2+1$ dimensions [40, 41]; a similar correspondence of DSR with quantum gravity has been conjectured to occur in the physical $3+1$ dimensional case as well.

Despite the optimism around DSR, the idea of deformed symmetry was quickly associated with several problems (see [30] or [47] for reviews). Among these, two are of importance here. First, after the original DSR models were formulated, many other apparently distinct models of DSR with different properties followed. This ambiguity problem was partially resolved when it was realized that the DSR transformations were associated with a curved momentum space, i.e. that the space of momenta of particles obeying DSR transformation rules is a de Sitter space with constant curvature. Second, the interpretation of DSR based on the work on quantum deformation of the Poincare algebra created the "soccer ball" problem: the DSR transformation seemed to imply that collections of particles would also have their energy bounded by κ in contradiction with observations. The resolution of this paradox is still debated.

The approach taken in this work relies on the observation that the momentum space of a DSR particle is de Sitter and further that de Sitter space can be seen as surface embedded in a five dimensional flat space. The embedding equation for de Sitter space is in fact the

quadratic form

$$\mathcal{H}_{5d} = P_0 P^0 - P_i P^i - P_4 P^4 + \kappa^2 = 0. \tag{5.1}$$

In the DSR context, this $\mathcal{H}_{5d}$ is interpreted as a constraint that restricts the physical momenta from to a five dimensional space to a reduced space that is actually de Sitter space $SO(4,1)/SO(3,1)$. In addition to this constraint, one can also consider a constraint $\mathcal{H}_{4d}$ which would endow the particle with a mass just like in the standard setup. Several possibilities for this constraint exist, but a convenient one that will be used here is

$$\mathcal{H}_{4d} = P_0 P^0 - P_i P^i - m^2 = 0. \tag{5.2}$$

A different way of writing this is

$$\mathcal{H}_{4d} = P_4^2 - (\kappa^2 + m^2) = 0. \tag{5.3}$$

Singling out the P_4 direction in this constraint is only a choice and has no deep explanation or physical significance. An equivalent alternative would be to define $\mathcal{H}_{4d}$ in terms of a unit vector V^A in the $5d$ space by $\mathcal{H}_{4d} = (P_A V^A)^2 - (\kappa^2 + m^2)$. Either notation shows that the mass constraint breaks the de Sitter symmetry of $\mathcal{H}_{5d}$.

The motivation for shifting attention to the higher dimensional flat space in this work is that from this perspective, DSR has many similar features to standard special relativity. To demonstrate this, the following section reviews the physics of the free particle in special relativity where there is one constraint and then extends the discussion to the DSR context where there are two [34]. Following that, a proposal for a DSR field theory is presented in section 5.2. The definition of this field theory [35] is quite different from other proposals and some of these differences, along with the conclusions of this work, are summarized in the final remarks in section 5.3.

5.1 The Free Particle

A new proposed symmetry can be studied in a variety of settings, but the simplest one is the free particle. This natural starting point is first reviewed in the context of standard special relativity and then the same techniques are applied to DSR.

The Free Particle in Special Relativity

In the Lagrangian formulation, the action for a free relativistic spinless particle of mass m is given by

$$S = \int d\tau \mathcal{L}, \qquad \mathcal{L} = m\sqrt{\dot{x}^\mu \dot{x}_\mu}. \tag{5.4}$$

It is just the line element on $4d$ space with flat metric and is parametrized by an arbitrary time variable τ; the dot means $\dot{x} = \partial x/\partial\tau$. The Euler-Lagrange equations specify the symplectic form and phase space structure. The canonical momentum is defined as

$$p_\mu = \frac{\partial \mathcal{L}}{\partial \dot{x}^\mu} = m\frac{\dot{x}_\mu}{\sqrt{\dot{x}^\mu \dot{x}_\mu}} \tag{5.5}$$

and the Poisson bracket on the phase space is canonical

$$\{x_\mu, p_\nu\} = \eta_{\mu\nu}. \tag{5.6}$$

The Lagrangian $\mathcal{L}$ can also be written as $\dot{x}^\mu p_\mu$ so that the Hamiltonian vanishes. Nevertheless, the momentum p_μ satisfies

$$\mathcal{H} = p^2 - m^2 = 0, \tag{5.7}$$

which is called the Hamiltonian constraint. Hence the free particle action can be written in the first order formalism as

$$S = \int d\tau (\dot{x}^\mu p_\mu - \lambda \mathcal{H}), \tag{5.8}$$

where λ is a Lagrange multiplier. Note that, unlike (5.4), this action can describe massless particles.

The constraint $\mathcal{H}$ defines the equations of motion through the commutators

$$\begin{array}{rcl} \delta x_\mu &=& \{x_\mu, \lambda\mathcal{H}\} = 2\lambda p_\mu, \\ \delta p_\mu &=& \{p_\mu, \lambda\mathcal{H}\} = 0. \end{array} \tag{5.9}$$

Enforcing the mass-shell condition $p_\mu p^\mu = m^2$ allows to solve for the value of the Lagrange multiplier

$$\lambda = \frac{1}{2m}\sqrt{\delta x_\mu \delta x^\mu} \tag{5.10}$$

so that the momentum is

$$p_\mu = m\frac{\delta x_\mu}{\sqrt{\delta x_\nu \delta x^\nu}} = m\frac{\dot{x}_\mu}{\sqrt{\dot{x}_\nu \dot{x}^\nu}}. \tag{5.11}$$

As a check, one can insert this expression in the action (5.8) to recover the original action (5.4) in terms of the line element.

A time variable is a phase space function that does not commute with the Hamiltonian or Hamiltonian constraint. As seen in (5.9), x_0 does not commute with $\lambda\mathcal{H}$ and so $t = x_0$ is a possible choice for the time variable. The equations of motion of the other variables in terms of t are obtained by the flow of the Hamiltonian constraint. Indeed, since $\{\lambda\mathcal{H}, x_\mu\} = -2\lambda p_\mu \neq 0$ and $\{\lambda\mathcal{H}, p_\mu\} = 0$, one has

$$\dot{x}_i = \frac{\delta x_i}{\delta x_0} = \frac{p_i}{p_0}, \qquad \dot{p}_i = 0. \tag{5.12}$$

This defines a notion of speed $v_i = \dot{x}_i = p_i/p_0$.

Substituting $t = x_0$ into the action (5.8) gives

$$S = \int dt \, \left[\dot{x}_i p_i - p_0 - \lambda(p^2 - m^2)\right]. \tag{5.13}$$

Solving the constraint gives $p_0 = \pm\sqrt{\overrightarrow{p}^2 + m^2}$ and the action reduces to

$$S = \int dt \, (\dot{x}_i p_i - H). \tag{5.14}$$

Here $H = \pm\sqrt{\overrightarrow{p}^2 + m^2}$ is a non-vanishing Hamiltonian. Its sign depends on whether the positive or negative energy branch is considered.

The choice of a time variable can be regarded as an explicit gauge fixing that breaks the symmetry of the action under time reparametrization. After gauge fixing, the symplectic form on the reduced phase space is given by the Dirac bracket. Given a constraint $\mathcal{H}$ and a gauge fixing condition $\mathcal{C}$ such that $\{\mathcal{C}, \mathcal{H}\} \neq 0$, the Dirac bracket is defined as

$$\begin{aligned}\{\phi, \psi\}_D =& \{\phi, \psi\} - \{\phi, \mathcal{C}\} \left(\frac{1}{\{\mathcal{H}, \mathcal{C}\}}\right) \{\mathcal{H}, \psi\} \\ & - \{\phi, \mathcal{H}\} \left(\frac{-1}{\{\mathcal{H}, \mathcal{C}\}}\right) \{\mathcal{C}, \psi\}.\end{aligned} \tag{5.15}$$

For the standard time choice $\mathcal{C} = x_0 - t$, where t is a free parameter, one has

$$\begin{aligned}\{x_0, p_0\}_D &= 0, \\ \{x_i, p_0\}_D &= -v_i, \\ \{x_\mu, x_\nu\}_D &= 0.\end{aligned} \tag{5.16}$$

Note that p_0 generates the usual Hamiltonian flow under the Dirac bracket and is actually the true physical Hamiltonian dictating the time evolution with respect to the clock x_0.

The Free Particle in Deformed Special Relativity

As mentioned before, the free particle in Deformed Special Relativity has a curved four dimenional momentum space characterized by the de Sitter constraint (5.1) in a five dimensional flat momentum space. In direct correspondence with (5.8), therefore, the action for a particle in DSR in the Hamiltonian formalism is written as

$$S_{5d} = \int d\tau \left[\dot{X}_A P^A - \Lambda \mathcal{H}_{5d} - \lambda \mathcal{H}_{4d}\right]. \tag{5.17}$$

The coordinates X_A and P^A form a ten dimensional phase space with the usual symplectic structure $\{X_A, P_B\} = \eta_{AB}$. The two constraints are those of (5.1) implementing the curvature in the four dimensional momentum space and (5.2) implementing the particle mass-shell condition.

The symmetries of the action are generated by those operators that commute with both of the constraints. It is straightforward to check that the angular momentum operators,

$$J_{\mu\nu} = X_\mu P_\nu - X_\nu P_\mu, \tag{5.18}$$

satisfy that condition. These $J_{\mu\nu}$'s together with the P_μ's are the generators of a ten-dimensional Lie algebra. In fact, this algebra is in direct correspondence with the Poincare algebra in four-dimensions, suggesting that the action actually describes four-dimensional physics. Note that the operators $J_{4\mu}$ do not commute with the mass-shell constraint $\mathcal{H}_{4d}$ and hence cannot be regarded as symmetries of the particle.

The proposed action S_{5d} is defined independently of any choice of "basis" or coordinate system on the reduced phase space. Standard presentations of DSR are then to be obtained

through a gauge fixing of the 5d κ-shell constraint $\mathcal{H}_{5d}$. More precisely, a gauge fixing is defined by a phase space function $\mathcal{C}_{5d}$ which does not commute with $\mathcal{H}_{5d}$,

$$\{\mathcal{H}_{5d}, \mathcal{C}_{5d}\} \neq 0. \tag{5.19}$$

The additional constraint $\mathcal{C}_{5d} = 0$ turns $\mathcal{H}_{5d}$ into a second class constraint and imposing $\mathcal{H}_{5d} = \mathcal{C}_{5d} = 0$ reduces the initial 10-dimensional phase space to a more traditional 8-dimensional phase space for a relativistic particle. The symplectic structure induced on the reduced phase space is described by the Dirac bracket defined previously.

Proper coordinates on the reduced phase will be denoted by (x_μ, p_μ). They should commute with both $\mathcal{H}_{5d}$ and $\mathcal{C}_{5d}$,

$$\{x_\mu, \mathcal{H}_{5d}\} = \{x_\mu, \mathcal{C}_{5d}\} = \{p_\mu, \mathcal{H}_{5d}\} = \{p_\mu, \mathcal{C}_{5d}\} = 0. \tag{5.20}$$

Their Dirac bracket with any phase space function is exactly equal to their Poisson bracket with that same function, i.e.

$$\{x, F\}_D = \{x, F\}, \qquad \{p, F\}_D = \{p, F\} \tag{5.21}$$

for all $F = F(X, P)$. A common convention for the coordinates p_μ is that they are dependent solely on the 5d momentum coordinates P_A; the coordinates x_μ can be a mixture of X_A and P_A. The p_μ's are a choice of coordinate system of the 4-dimensional de Sitter space, while the x_μ are the generators of the translations on this same de Sitter space. Different versions of DSR are formulated through such a choice of coordinates (x_μ, p_μ), called a choice of basis. This ambiguity is related to the choice of a gauge fixing condition, as will be seen below.

Using the eight coordinates x_μ and p_μ together with the phase space functions $\mathcal{H}_{5d}$ and $\mathcal{C}_{5d}$, it is possible to invert the relation between the 4d and the 5d coordinates. In other words, the 5d coordinates X_A and P_A can be expressed in terms of $\mathcal{H}_{5d}, \mathcal{C}_{5d}, x_\mu, p_\mu$. From the conventions for defining p and x, it follows that $\mathcal{C}_{5d}$ is not needed to express the 5d momentum coordinates P_A which are a function of p_μ and κ only. That condition is needed, however, to express the 5d coordinates X_A in terms of the 4d coordinates x_μ. Thus, the condition $\mathcal{C}_{5d}$ may be crucial to understanding the "meaning" of the fifth space-time coordinate X_4.

Some interesting properties follow from the fact that $\mathcal{H}_{5d}$ and $\mathcal{C}_{5d}$ commute with the x's and p's. For example, the x, p variables form a closed algebra under the Poisson bracket and define a true 4d phase space without having 5d variables appearing in their commutation relations. This also implies that it should be possible to understand and quantize the DSR particle as a 4d system without recourse to the 5d space. Nevertheless, perhaps quantization would be more transparent at the fully five-dimensional context without introducing any particular gauge fixing.

Apart from this rather general discussion, one can see these principles at work in several examples where the choice of gauge fixing condition $\mathcal{C}_{5d}$ can give rise to different versions of DSR. In these considerations, the mass shell constrain is mostly ignored and the analysis applies to the κ-shell constraint $\mathcal{H}_{5d}$ only.

Snyder Basis

Consider the gauge fixing condition

$$\mathcal{C}_{5d} = \mathcal{D} - T = X_A P^A - T \tag{5.22}$$

where T is an arbitrary real parameter. This is a $5d$ dilatation and in the following it is shown that the reduced phase space of the particle obtained after imposing the gauge $\mathcal{C}_{5d} = 0$ is the so called Snyder spacetime.

After some trial and error, a set of four-dimensional position and momentum variables that satisfy the conditions (5.20) are

$$\begin{aligned} p_\mu &\equiv \kappa \frac{P_\mu}{P_4}, \\ x_\mu &\equiv \frac{1}{\kappa} J_{\mu 4} = \frac{1}{\kappa}(X_\mu P_4 - X_4 P_\mu). \end{aligned} \tag{5.23}$$

In terms of these 4d variables, the kinetic part of the integrand in S_{5d} in (5.17) can be written up to boundary terms as

$$\dot{X}_A P^A = \dot{x}_\mu p^\mu - p_\mu \frac{x \cdot p}{\kappa^2 - p^2} \dot{p}^\mu. \tag{5.24}$$

In addition to the usual $\dot{x}_\mu p^\mu$ term, there is now a new term that depends on κ. Note that to arrive at the above formula, the constraint relation $\mathcal{H}_{5d} = 0$ is used.

The Poisson brackets of these 4d variables can be computed either directly from the definitions (5.23) and the 5d symplectic structure or from the kinematical part of the action given in (5.24). The resulting non-vanishing bracket relations are

$$\begin{aligned} \{x_\mu, x_\nu\} &= -\frac{1}{\kappa^2} J_{\mu\nu}, \\ \{x_\mu, p_\nu\} &= \eta_{\mu\nu} - \frac{p_\mu p_\nu}{\kappa^2}. \end{aligned} \tag{5.25}$$

Although these relations involve $J_{\mu\nu}$ defined in (5.18) in terms of the $5d$ variables, it turns out (as expected from the general discussion above) that these generators can also be written entirely in terms of the $4d$ variables:

$$J_{\mu\nu} = (X_\mu P_\nu - X_\nu P_\mu) = (x_\mu p_\nu - x_\nu p_\mu). \tag{5.26}$$

The deformed symplectic structure defines the Snyder non-commutative space-time. When κ goes to infinity, the standard phase space of the relativistic particle is recovered.

As an aside, note that the kinetic term in (5.24) can be trivialized to $x'_\mu \dot{p}^\mu$ with the new set of $4d$ position coordinates:

$$x'_\mu = x_\mu + p_\mu \frac{x \cdot p}{\kappa^2 - p^2}. \tag{5.27}$$

The symplectic structure expressed with these new coordinates is simply $\{x'_\mu, p_\nu\} = \eta_{\mu\nu}$. Since the new primed coordinates are defined only in terms of the unprimed ones, they still commute with both the Hamiltonian constraint and the gauge-fixing condition. The natural issue is the physical meaning and interpretation of these new coordinates x'_μ.

Since the 4d variables x_μ and p_μ commute with the constraint $\mathcal{H}_{5d}$, they can be interpreted as Dirac observables of the 5d system with respect to the 5d κ-shell constraint. This means that considered as operators they leave the de Sitter space invariant: the x_μ's generate the translations on the de Sitter space which has become the 4d momentum space. Since x_μ, p_μ also commute with the gauge fixing condition $\mathcal{C}_{5d}$, both expressions can be set to zero,

$\mathcal{H}_{5d} = \mathcal{C}_{5d} = 0$, in the ten-dimensional phase space without interfering with the x, p variables. This reduces the phase space to eight-dimensions and implies that the Dirac bracket of x_μ, p_μ with any function will be equal to their Poisson bracket with that function. It is also possible to invert the definition (5.23) and express the 5d coordinates X, P in terms of x, p, κ, T. The condition $\mathcal{H}_{5d} = 0$ is used to obtain the 5d momentum P_A, while the condition $\mathcal{D} = 0$ gives the expression for the 5d position X_A. Denoting these resulting functions by $\widetilde{X}$ and $\widetilde{P}$ in order to avoid confusion with the original variables X, P,

$$\begin{aligned}
\widetilde{P}_4 &= \frac{\kappa}{\sqrt{1-\frac{p^2}{\kappa^2}}}, \qquad \widetilde{P}_\mu = \frac{p_\mu}{\sqrt{1-\frac{p^2}{\kappa^2}}}, \\
\widetilde{X}_4 &= \frac{1}{\kappa\sqrt{1-\frac{p^2}{\kappa^2}}}(x\cdot p - T), \\
\widetilde{X}_\mu &= x_\mu\sqrt{1-\frac{p^2}{\kappa^2}} + \frac{p_\mu}{\kappa^2\sqrt{1-\frac{p^2}{\kappa^2}}}(x\cdot p - T).
\end{aligned} \tag{5.28}$$

The latter can also be written in a more condensed format,

$$\begin{aligned}
\widetilde{X}_4 &= \frac{\widetilde{P}_4}{\kappa^2}x\cdot p - T\frac{\widetilde{P}_4}{\kappa}, \\
\widetilde{X}_\mu &= \frac{\kappa}{\widetilde{P}_4}x'_\mu - T\frac{\widetilde{P}_\mu}{\kappa}.
\end{aligned} \tag{5.29}$$

On the one hand, the final equation explains the meaning of the x'_μ coordinates: they are the four-dimensional sector of the 5d coordinates (at $T = 0$). On the other hand, the inversion formula reveals the meaning of the fifth space-time coordinate (in the Snyder basis): it is the dilatation $D = x \cdot p$ on the 4-dimensional relativistic particle.

Finally, one can compute the Dirac brackets corresponding to the gauge fixing. They are

$$\begin{aligned}
\{X_A, X_B\}_D &= \frac{-1}{P_C P^C}J_{AB} = \frac{1}{\kappa^2}J_{AB}, \\
\{X_A, P_B\}_D &= \eta_{AB} - \frac{P_A P_B}{P_C P^C} = \eta_{AB} + \frac{P_A P_B}{\kappa^2}.
\end{aligned} \tag{5.30}$$

The four dimensional sector of these relations are, by construction, the same as the commutation relations (5.25) for x_μ and p_μ. Also, the following relations hold for the 5d variables

$$\begin{aligned}
\{\widetilde{X}_A, \widetilde{X}_B\} &= \{X_A, X_B\}_D, \\
\{\widetilde{X}_A, \widetilde{P}_B\} &= \{X_A, P_B\}_D, \\
\{\widetilde{P}_A, \widetilde{P}_B\} &= \{P_A, P_B\}_D.
\end{aligned} \tag{5.31}$$

Bicrossproduct Basis

A similar analysis can be carried out for other gauge-fixing conditions. Consider as a different example

$$\mathcal{C}_{5d} = \frac{X_0 - X_4}{P_0 - P_4} - T, \tag{5.32}$$

where T is again a free parameter. This turns out to produce the bicrossproduct version of DSR, thus showing that basis relies on a "light cone" gauge for the 5d action.

A set of 4d momentum variables that commute with both $\mathcal{H}_{5d}$ and $\mathcal{C}$ are

$$p_0 \equiv \kappa \ln \frac{P_4 - P_0}{\kappa}, \qquad p_i \equiv \frac{\kappa P_i}{P_0 - P_4}. \tag{5.33}$$

As for the position variables, one can take

$$x_0 \equiv \frac{1}{\kappa} J_{40}, \qquad x_i \equiv \frac{1}{\kappa}(J_{i0} - J_{i4}). \tag{5.34}$$

The ten variables $(\mathcal{H}_{5d}, \mathcal{C}, x_\mu, p_\mu)$ parametrize the ten-dimensional phase space. Actually, there is an implicit restriction in this basis to the sector $P_4 > P_0$. If the whole space is needed, then it should be parametrized by two sets of 4d momentum variables p_μ each defined for different signs of $P_4 - P_0$.

From here, the same calculations as those presented in the previous subsection on the Snyder gauge-fixing can be repeated. Imposing $P_A P^A + \kappa^2 = 0$, the kinetic part of the 5d action reduces to

$$\dot{X}_A P^A = p_\mu \, \dot{x}_\mu + p_i \, x_i \, \dot{p}_0. \tag{5.35}$$

This provides the 4d action principle describing the DSR particle in the bicrossproduct basis. The non-vanishing Poisson brackets are

$$\begin{aligned} &\{x_0, p_0\} = 1, \quad \{x_i, p_j\} = -\delta_{ij}, \\ &\{x_0, x_i\} = +\frac{1}{\kappa} x_i, \quad \{x_0, p_i\} = -\frac{1}{\kappa} p_i. \end{aligned} \tag{5.36}$$

This is the symplectic structure of κ-Minkowski phase space.

Solving the 5d Hamiltonian constraint $\mathcal{H}_{5d} = 0$ and fixing the gauge with $\mathcal{C}_{5d} = 0$ allows to invert (5.33) and (5.34) to obtain

$$\begin{aligned} \widetilde{P}_0 &= -\kappa \sinh \frac{p_0}{\kappa} - \frac{\overrightarrow{p}^2}{2\kappa} e^{\frac{p_0}{\kappa}}, \\ \widetilde{P}_i &= -p_i e^{\frac{p_0}{\kappa}}, \\ \widetilde{P}_4 &= \kappa \cosh \frac{p_0}{\kappa} - \frac{\overrightarrow{p}^2}{2\kappa} e^{\frac{p_0}{\kappa}}, \\ \widetilde{X}_\mu &= \kappa \frac{x_\mu}{P_0 - P_4} + T P_\mu, \\ \widetilde{X}_4 &= \kappa \frac{x_0}{P_0 - P_4} + T P_4. \end{aligned} \tag{5.37}$$

The first set of relations are just the familiar definitions of the bicrossproduct basis in terms of planar coordinates on de Sitter.

The Dirac bracket induced by the gauge fixing condition acts on the 5d variables as

$$\begin{aligned}
\{X_0, X_4\}_D &= \frac{1}{2}\frac{X_0 - X_4}{P_0 - P_4}, \\
\{X_i, P_j\}_D &= \delta_{ij}, \\
\{X_0, P_0\}_D &= -1 - \frac{1}{2}\frac{P_0}{P_0 - P_4}, \\
\{X_4, P_4\}_D &= +1 - \frac{1}{2}\frac{P_4}{P_0 - P_4}, \\
\{X_0, P_4\}_D &= -\frac{1}{2}\frac{P_0}{P_0 - P_4}, \\
\{X_4, P_0\}_D &= -\frac{1}{2}\frac{P_4}{P_0 - P_4}.
\end{aligned} \tag{5.38}$$

As earlier, the important facts about the Dirac bracket are that, first, the Dirac bracket of (x, p) with any other phase space function is exactly equal to the Poisson bracket and, second, the Poisson brackets of the $(\widetilde{X}, \widetilde{P})$ variables is equal to the Dirac bracket of the (X, P) variables computed above.

As in the Snyder case, there is an alternate system of position variables that trivializes the $4d$ symplectic structure. For the bicrossproduct basis, this is achieved by defining

$$x'_0 = x_0 - \frac{1}{\kappa} x_i p^i, \qquad \text{and} \qquad x'_i = x_i. \tag{5.39}$$

This choice of space-time coordinates is commutative and the couple (x', p) have canonical Poisson brackets. In terms of the 5d coordinates, x'_0 is given by

$$\kappa\, x'_0 = J_{40} - \frac{P_i}{P_0 - P_4}(J_{i0} - J_{i4}) \tag{5.40}$$

$$= (X_4 P_0 - X_0 P_4) - X_i P_i + P_i P_i \frac{X_0 - X_4}{P_0 - P_4}. \tag{5.41}$$

This variable is singular at $P_0 - P_4 = 0$. In terms of the 4d momentum coordinates, this singularity happens when the quantity p_0, naively interpreted as an "energy," becomes infinite. The $P_0 - P_4 = 0$ is also the singularity for the bicrossproduct momentum variables (5.33).

The symmetry generators (5.18), in terms of p_μ and x_μ coordinates, are

$$\begin{aligned}
M_{ij} &= J_{ij} = x_i p_j - x_j p_i, \\
N_i &= J_{i0} = x_i \left(\kappa e^{-\frac{p_0}{\kappa}} \sinh \frac{p_0}{\kappa} + \frac{\overrightarrow{p}^2}{2\kappa} \right) - x_0 p_i.
\end{aligned} \tag{5.42}$$

Hence the rotations appear in the usual way while the boosts are deformed in the first term. They still form an undeformed Lorentz algebra (this is possible due to the deformed symplectic structure), but their action on the space-time coordinates is deformed. More

precisely, the action of these generators on the position variables x_μ is

$$\begin{aligned}
\{N_i, x_0\} &= x_i - \frac{1}{\kappa} N_i, \\
\{N_i, x_j\} &= x_0\, \delta_{ij} - \frac{1}{\kappa} M_{ij}, \\
\{M_{ij}, x_0\} &= 0 \\
\{M_{ij}, x_k\} &= x_j\, \delta_{ik} - x_i \delta_{jk}.
\end{aligned} \tag{5.43}$$

The action of these generators on the momentum variables give the well known relations of the bicrossproduct basis

$$\begin{aligned}
\{N_i, p_0\} &= p_i, \\
\{N_i, p_j\} &= \delta_{ij} \left(\frac{\kappa}{2} \left(1 - e^{-2\hat{p}_0/\kappa} \right) + \frac{1}{2\kappa} \hat{p}_i \hat{p}^i \right) - \frac{\hat{p}_i \hat{p}_j}{\kappa}, \\
\{M_{ij}, p_0\} &= 0 \\
\{M_{ij}, p_k\} &= \delta_{ik} p_j - \delta_{jk} p_i.
\end{aligned} \tag{5.44}$$

Again, the rotation algebra does not seem deformed whatsoever while some new features appear in the boost sector.

Relativistic effects

It is natural to ask whether Given the deformed symmetry algebra can give rise to observable effects. For concreteness, the discussion of this issue below relies on the bicrossproduct variables and algebra.

One consequence of the new algebra is that the Lorentz invariant quadratic form, the "metric," is not $x_\mu x^\mu$ anymore. However a deformation of it in the form

$$L^2 = x_0^2 - \left(x_i - \frac{1}{\kappa} N_i \right)^2 \tag{5.45}$$

is invariant and thus can be thought of in principle as a new metric. However, since the quantity N_i depends on the particle momentum, the whole quadratic form is momentum-dependent. Explicitly, it is

$$L^2 = x_0^2 \left(1 - \frac{\overrightarrow{p}^2}{\kappa^2} \right) - x_i x_i f(p)^2 - \frac{2x_0}{\kappa} \overrightarrow{x} . \overrightarrow{p}\, f(p), \tag{5.46}$$

$$f(p) = 1 - e^{-\frac{p_0}{\kappa}} \sinh \frac{p_0}{\kappa} - \frac{\overrightarrow{p}^2}{2\kappa^2}. \tag{5.47}$$

From the general relativistic perspective, a particle can be expected to deform the geometry of the surrounding space-time depending on its energy-momentum tensor, so this metric may not be so strange. If DSR is, as it has been suggested, an effective description of particles in quantum gravity, then this is where this property of general relativity may be showing up in the present framework. From the point of view of special relativity, however, a deformation

of L^2 seems hard to accept on physical grounds. In fact, the metric in special relativity usually has a clear operational meaning being the measure of distances between spacetime points. What one should presumably do is to try to construct the metric operationally, in terms of physical rods and clocks, using the fact that one has at one's disposal a universal observer-independent scale of velocity. It is crucial that all inertial observers agree on a way the metric is constructed and that there exists a means to synchronize clocks and rods of observers at different points and/or observers moving with respect to each other with constant speed. The kinematical description of the particle presented here is a good starting point for such a construction.

Consider for simplicity the action of boosts along the $i = 1$ direction. Defining $\partial_\xi F = \{N_1, F\}$ for any function F, one obtains from the commutators (5.43) the differential equations

$$\begin{aligned} \partial_\xi x_0(\xi) &= x(\xi) - N_1(\xi), \\ \partial_\xi x_1(\xi) &= x_0(\xi), \\ \partial_\xi x_2(\xi) &= -M_3(\xi), \\ \partial_\xi x_3(\xi) &= +M_2(\xi). \end{aligned} \tag{5.48}$$

The functions $N_1(\xi)$, $M_{2,3}(\xi)$ are shorthand for the combinations of x, p defined in (5.42) in terms of the boost parameter. To solve this system of equations, it is worth simplifying the right hand sides. Since $\{N_1, N_1\} = 0$, the object $N_1(\xi)$ in the first equation above is actually a constant independent of ξ. Therefore, $N_1(\xi) = n_1$ can be evaluated once at a certain time in one particular reference frame (with a certain boost parameter) using (5.42), i.e.

$$n_1 = \left[x_1 \left(e^{-p_0} \sinh p_0 + \frac{p^2}{2} \right) - x_0 p_1 \right]_0 . \tag{5.49}$$

The subscript 0 on the bracket denotes that the expression is evaluated in a particular frame defined by the initial conditions.

Another trick is to find the functions $M_3(\xi)$ and $M_2(\xi)$. This can be done by considering how they themselves behave under boosts,

$$\begin{aligned} \partial_\xi M_2(\xi) &= N_3(\xi) \\ \partial_\xi N_3(\xi) &= M_2(\xi) \\ \partial_\xi M_3(\xi) &= -N_2(\xi) \\ \partial_\xi N_2(\xi) &= -M_3(\xi), \end{aligned} \tag{5.50}$$

Solutions to this set of differential equations are

$$\begin{aligned} M_2(\xi) &= m_2 \cosh\xi + n_3 \sinh\xi \\ M_3(\xi) &= m_3 \cosh\xi - n_2 \sinh\xi \\ N_2(\xi) &= n_2 \cosh\xi - m_3 \sinh\xi \\ N_3(\xi) &= n_3 \cosh\xi + m_2 \sinh\xi. \end{aligned} \tag{5.51}$$

The coefficients all denote initial values similarly as in (5.49).

These observations makes it straight-forward to write down the solutions to the system of differential equations (5.48):

$$\begin{aligned} x_0(\xi) &= x_0(0)\cosh\xi + x_1(0)\sinh\xi - n_1\sinh\xi, \\ x_1(\xi) &= x_0(0)\sinh\xi + x_1(0)\cosh\xi - n_1\cosh\xi + n_1 \\ x_2(\xi) &= x_2(0) - n_2 + n_2\cosh\xi - m_3\sinh\xi \\ x_3(\xi) &= x_3(0) - n_3 + n_3\cosh\xi + m_2\sinh\xi. \end{aligned} \tag{5.52}$$

To study relativistic effects, these equations should be supplemented by the equations of motion arising from the flow of x, p with respect to the mass shell constraint $\lambda\mathcal{H}_{4d}$. These flows are

$$\begin{aligned} \delta x_0 &= -2\lambda(\kappa\sinh\frac{p_0}{\kappa} + \frac{\overrightarrow{p}^2}{2\kappa}e^{\frac{p_0}{\kappa}}), \\ \delta x_i &= -2\lambda p_i e^{\frac{p_0}{\kappa}}, \\ \delta p_0 &= \delta p_i = 0. \end{aligned} \tag{5.53}$$

If the time variable is chosen to be $t = x_0$, then the speed is defined as usual as $v_i \equiv \delta x_i/\delta x_0$. Now the dependence of the velocity $v_i = \delta x_i/\delta x_0$ on the boost parameter can be checked explicitly. Consider a particle that is initially at rest, i.e. its initial momentum $p_i = 0$. Then, using the transformation laws of momenta p_μ [49], the result is

$$v = \tanh\xi \tag{5.54}$$

just like in special relativity. The result does not depend on the initial value of the particle's energy (rest energy or mass), thus all particles approach the speed of light $v = c = 1$ after repeated boosts.

Other relativistic effects that are worth investigating are time dilation and length contraction. The following calculations are based on an approach developed in [50] and consider a system of two particles. One particle, labeled A, is placed at $x^A = 0$ and has zero spatial momentum in some reference frame. The other particle, labeled B, is placed at $x^B = \ell$ in the 1 direction and is also stationary in that same reference frame. The equations of motion for these particles, in terms of their affine parameters s_A and s_B, are

$$\begin{aligned} x_0^A(s_A,\xi) &= s_A\sinh p_0^A\cosh\xi \\ x_1^A(s_A,\xi) &= s_A\sinh p_0^A\sinh\xi \\ x_2^A(s_A,\xi) &= 0 \\ x_3^A(s_A,\xi) &= 0 \end{aligned} \tag{5.55}$$

and

$$\begin{aligned} x_0^B(s_B,\xi) &= s_B\sinh p_0^B\cosh\xi + \ell_1\sinh\xi - n_1^B\sinh\xi. \\ x_1^B(s_B,\xi) &= s_B\sinh p_0^B\sinh\xi + \ell_1\cosh\xi - n_1^B\cosh\xi + n_1^B \\ x_2^B(s_B,\xi) &= \ell_2 - n_2 + n_2\cosh\xi \\ x_3^B(s_B,\xi) &= \ell_3 - n_3 + n_3\cosh\xi. \end{aligned} \tag{5.56}$$

In one reference frame characterized by $\xi = 0$, the 'time' along each particle's worldline may be defined as the difference of x_0 functions at different value of the affine parameter s,

$$\tau = x_0(s', 0) - x_0(s, 0). \tag{5.57}$$

One can find how these quantities transform under boosts by introducing another frame with general ξ. Then time intervals become

$$\tau' = x_0(s', \xi) - x_0(s, \xi) = \tau \cosh \xi \tag{5.58}$$

for each particle. This is time dilation in its standard (special relativistic) form.

A naive way to define distance is to consider the coordinate difference

$$d_1 = x_1^A(0, 0) - x_1^B(0, 0) = \ell_1; \tag{5.59}$$

similar expressions in the other directions give d_2 and d_3. The distance interval between the particles in the second reference frame is computed by first setting $x_0^A(s_A, \xi) = x_0^B(s_B, \xi)$ to obtain a relation between s_A and s_B, and then doing the subtraction of coordinates. The result along the direction of the boost is

$$\begin{aligned} d_1' &= x_1^A(s_A, \xi) - x_1^B(s_B, \xi) \\ &= \frac{1}{\cosh \xi} \ell_1 + n_1^B \left(\frac{\cosh \xi - 1}{\cosh \xi} \right). \end{aligned} \tag{5.60}$$

The first term gives the usual length contraction effect, whereas the second term is a correction due to the momentum space curvature. Its significance grows with the original separation ℓ and with increasing ξ values. Since n_1^B is also a function of p_0^B, the correction is also dependant on what kind of particle is being discussed. In the orthogonal directions, the distances are just $d_2 = x_2^B(s_B, \xi)$ and $d_3 = x_3^B(s_B, \xi)$. In contrast to d_1, these distances become larger as the boost parameter is increased.

The invariant quadratic form is (5.45), however, and it suggests an alternative approach for looking at length contraction by defining distances in terms of the combination $x_i - N_i$. This amounts to a shift of the coordinates by a constant. Then, one has

$$d_i = (x_i^A(0, 0) - n_i^A) - (x_i^B(0, 0) - n_i^B) = \ell_i - n_i^B. \tag{5.61}$$

In a boosted frame, the new measured distance along the direction of the boost is

$$d_1' = \frac{1}{\cosh \xi} d_1, \tag{5.62}$$

the usual length contraction. In the other directions, however, one has

$$d_2' = d_2 - n_2^B (1 - \cosh \xi). \tag{5.63}$$

It appears that directions orthogonal to the boost are slightly contracted as well. And this is not a regular standard relativistic effect.

5.2 A Proposal for Field Theory

After looking at single particles in standard and deformed special relativity, one naturally can ask whether the deformed symmetry can also be implemented in a field theory. Several attempts at formulating field theory consistent with DSR already exist in the literature [43–46]. The philosophy in this work, however, is to extend the use of the $5d$ formalism explained above to the field theory context. As in the previous subsection, the goal is to use insights gained from special relativity as much as possible when formulating the field theory for DSR.

There are several lessons to be learnt from standard special relativity that are relevant for field theory. One lesson is that the curvature in momentum space has physical consequences. In SR, that physical consequence is an upper bound on particle velocity and a velocity addition rule that is compatible with that bound. Another lesson is that, for practical purposes, it is easier to work with the higher-dimensional flat space rather than the intrinsic variables defining a curved space. In particular, calculations of scattering thresholds are easily done using linear four-momentum conservation rules whereas they are much trickier in terms of variables such as velocities that must be added in a non-trivial way. In addition to their utility for computations, the higher-dimensional variables also have a physical interpretation. As is well known, special relativity reveals a profound correlation between space and time (momentum and energy). Together, these lessons imply that field theories based on standard special relativity are usually formulated on a four-dimensional flat space.

When the DSR postulate is introduced, one is led to the five dimensional formalism where particles are described by two constraints. One of the lessons from standard special relativity suggests that momentum addition (conservation) rules on the underlying five-dimensional flat space of momenta could be linear despite the constraints. Thus, a key feature of the proposal below [35] is that all components of five-momentum, including the new p_4 component, are taken to add linearly and are assumed to be conserved in scattering processes. This key assumption sets this work apart from some of the previous works. A welcome consequence of this assumption is that particle scattering amplitudes can be computed explicitly; new features that arise because of the new postulated conservation law are super-selection rules that can be understood as imposing what is usually termed as charge conservation in the standard field theory language.

It should be stressed again that the proposal below relies heavily on the $5d$ interpretation of the DSR particle and is not the usual approach to DSR-based quantum field theory [43–46]. An alternative formulation of DSR field theory along with related criticism of the present approach is briefly presented in the discussion section 5.3.

Free Scalar Theory

The proposal [35] is to make the fundamental momentum integral five-dimensional and to select physical configurations by imposing the two constraints (5.1) and (5.2). The field expansion is defined by

$$\begin{aligned}\phi(x, x_4) = \int \frac{d^5p}{(2\pi)^5}\, \phi(p, p_4) e^{ip\cdot x} e^{-ip_4 x_4} \\ \times (2\pi)\delta^{(4)}(p^2 - m^2)\ (2\pi)\delta^{(5)}(p^2 - p_4^2 + \kappa^2).\end{aligned} \tag{5.64}$$

Integrating out the two delta-functions and selecting the solutions with positive p_0 and positive p_4, the field becomes

$$\phi(x, x_4) = \int \frac{d^3p}{(2\pi)^3} \frac{1}{2p_0} \frac{1}{2p_4} \, \phi(p) e^{ip_0 x_0} e^{-i\mathbf{p}\cdot\mathbf{x}} e^{-ip_4 x_4}, \tag{5.65}$$

where $p_0 = \sqrt{p_i^2 + m^2}$ and $p_4 = \sqrt{\kappa^2 + m^2}$. The resulting natural phase space integral for the field is

$$\int d\Pi(p) = \int \frac{d^3p}{(2\pi)^3} \frac{1}{2p_0} \frac{1}{2p_4}, \tag{5.66}$$

which is, up to a constant $(2p_4)^{-1}$, the same as in standard field theory. The extra constraint does not provide a regulator for this integral.

The normalization condition for the fields can be taken as

$$(\phi(p), \phi(p')) \propto (2\pi)^3 \, p_0 p_4 \, \delta^{(3)}(\mathbf{p} - \mathbf{p}'), \tag{5.67}$$

which is positive definite in the selected sector where both p_0 and p_4 are positive. The quantization of the field can proceed in the usual manner by setting

$$\phi(x, x_4) = \int \frac{d^3p}{(2\pi)^3} \frac{1}{\sqrt{2p_0}\sqrt{2p_4}} \, \left(a_{\mathbf{p}} e^{-ip_0 x_0} e^{i\mathbf{p}\cdot\mathbf{x}} e^{ip_4 x_4} + h.c. \right), \tag{5.68}$$

where a_p and $a_p^\dagger$ obey the usual commutators

$$[a_{\mathbf{p}}, a_{\mathbf{p}'}^\dagger] = (2\pi)^3 \delta^{(3)}(\mathbf{p} - \mathbf{p}'). \tag{5.69}$$

The interpretation of these operators is similar to the usual case: $a_p^\dagger$ creates a particle with positive energy and positive p_4 while a_p annihilates such a particle if one exists.

The two point function for the new field is

$$D\left((x, x_4) - (y, y_4)\right) = \int \frac{d^3p}{(2\pi)^3} \frac{1}{2p_0} \frac{1}{2p_4} \, e^{-ip_0(x_0 - y_0)} e^{i\mathbf{p}\cdot(\mathbf{x}-\mathbf{y})} e^{ip_4(x_4 - y_4)}. \tag{5.70}$$

From this, one can construct a propagator D_F. Since two momenta are constrained and it was assumed above that physical particles have both of these momenta positive, the ordering in the definition of this propagator involves both the x_0, y_0 and x_4, y_4 variables,

$$\begin{aligned} D_F = &\Theta(x_0 - y_0)\, \Theta(y_4 - x_4)\, D((x, x_4) - (y, y_4)) + \\ &\Theta(y_0 - x_0)\, \Theta(x_4 - y_4)\, D((y, y_4) - (x, x_4)). \end{aligned} \tag{5.71}$$

Although this is not exactly the definition of the Feynman propagator in standard quantum field theory, it is the closest to it that one can write given the new dimension and the new constraint in the present setup. Proceeding, then, this propagator can be written in terms of higher dimensional integrals with particular choices of contour integrations along the p_0 and p_4 directions. For computations with Feynman rules, this propagator will be defined as

$$D_F(p) = \frac{-1}{(p^2 - m^2 + i\epsilon)} \frac{1}{(p_4^2 - \kappa^2 - m^2 + i\epsilon)}. \tag{5.72}$$

The appearance of a new factor in the denominator reveals the propagator has poles along the p_4 axis which implement the κ-shell constraint. The placement of these new poles on the axis of the extra dimension (as opposed to the p_0 axis) will become important in the discussion of unitarity below.

Interactions

An interacting theory and scattering amplitudes for processes can be defined perturbatively through Feynman diagrams. To obtain an analog of ϕ^4 theory, the vertices can be made four-valent and proportional to a small coupling constant $-i\lambda$. The distinctive features of interactions in this framework are that momentum conservation is required in all five dimensions, and that momentum integrals arising in a loop diagrams are also five dimensional.

Using these Feynman rules, it is straight-forward to see that the amplitude for the first order scattering of two incoming scalar fields into two outgoing scalar fields can be set up to be $|\mathcal{M}_\kappa|^2 = \lambda^2$ just like in standard ϕ^4 theory. This amplitude has the same form as in the standard theory partly because the overall momentum conservation δ-function for any two-particle to two-particle process is trivially satisfied in the extra dimension because all particles have $p_4 = \sqrt{\kappa^2 + m^2}$. However, any process that takes two incoming particles to four or more outgoing particles is kinematically forbidden by p_4 conservation. Since such processes are allowed in standard ϕ^4 theory, the theory presented in this section makes some very different predictions from the standard theory at higher orders in the perturbation expansion. (In light of the discussion and results of the next section on fermions, however, it is conceivable to arrange for this kind of discrepancy to be removed in the case where the field is complex and ϕ and ϕ^* carry opposite signs of the momentum p_4.) It is therefore clear that the requirement for the momentum in an extra dimension to be fixed at a set value, which may at first seem like a small modification to the usual QFT framework, can in fact have significant effects on processes amplitudes.

Unitarity

A prescription for writing transition amplitudes from Feynman diagrams as defined above can only be called self-consistent if the resulting model is unitary. The following discussion mirrors Ref. [56] and shows that unitarity is preserved in the proposed interacting model to λ^2 order.

Consider a process whereby two particles with momenta p, p_4 and p', p'_4 interact to produce two other particles with momenta k, k_4 and k', k'_4. The S-matrix is defined as $S = 1 + iT$ where T is related to the process amplitude $\mathcal{M}_\kappa$ by

$$\begin{aligned}\langle kk_4,\, k'k'_4|T|pp_4,\, p'p'_4\rangle = i\mathcal{M}_\kappa(pp_4,\, p'p'_4 \to kk_4,\, k'k'_4)\\ \times (2\pi)^5\, \delta^{(5)}(p + p' - k - k').\end{aligned} \tag{5.73}$$

Note that, as already mentioned earlier, the condition $p_4 + p'_4 - k_4 - k'_4 = 0$ is automatically satisfied because all these components are fixed to $\sqrt{\kappa^2 + m^2}$. The theory is unitary if the S-matrix satisfies $SS^\dagger = 1$; in terms of the T-matrix, this translates into

$$-i(T - T^\dagger) = T^\dagger T. \tag{5.74}$$

The unitarity condition can be checked to first non-trivial order in perturbation theory

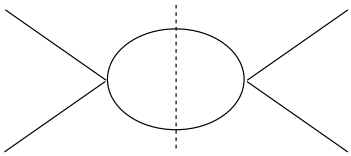

Figure 11: A one-loop diagram with indicated cut.

by considering a one-loop diagram. Its amplitude is

$$\begin{aligned} & i\mathcal{M}_\kappa\, \delta^{(5)}(p+p'-k-k') \\ & \quad = \frac{\lambda^2}{2}\int \frac{d^5q}{(2\pi)^5}\int \frac{d^5q'}{(2\pi)^5}\ (f_0 f_4) \\ & \qquad \times (2\pi)^5\delta^{(5)}(p+p'-q-q')\delta^{(5)}(q+q'-k-k'), \end{aligned} \tag{5.75}$$

where

$$\begin{aligned} f_0 &= \left(\frac{1}{q^2-m^2+i\epsilon}\right)\left(\frac{1}{q'^2-m^2+i\epsilon}\right), \\ f_4 &= \left(\frac{1}{q_4^2-\kappa^2-m^2+i\epsilon}\right)\left(\frac{1}{q_4'^2-\kappa^2-m^2+i\epsilon}\right). \end{aligned} \tag{5.76}$$

The integration is actually over one undetermined five-momentum propagating around the loop, but it is written in terms of integrals d^5q and d^5q' and a δ-function for convenience. A useful feature is that all the dependence on the parameter κ and the extra dimensions can be neatly put in the function f_4. Thus the amplitude splits into

$$\mathcal{M}_\kappa = \mathcal{M}_s\,\mathcal{M}_4, \tag{5.77}$$

where $\mathcal{M}_s$ is the standard four-dimensional piece and $\mathcal{M}_4$ depends only on the extra dimension.

In the 'center of mass' frame, the incoming particles have momenta (p_0, p_i, p_4) and $(p_0, -p_i, p_4)$ so that the total momentum is $(2p_0, 0, 2p_4)$. The energy p_0 can be as large as desired but p_4 is fixed by the on-shell conditions. Therefore, the matrix element $\mathcal{M}_\kappa$ for this process can be taken to be a function of the energy p_0 alone, $\mathcal{M}_\kappa = \mathcal{M}_\kappa(p_0)$. The overall amplitude $\mathcal{M}_\kappa$ should be real at low energies. This implies that the four-dimensional part of the amplitude $\mathcal{M}_s$ satisfies the condition

$$\operatorname{Disc}\mathcal{M}_s(p_0) = 2i\operatorname{Im}\mathcal{M}_s(p_0+i\epsilon) \tag{5.78}$$

relating the discontinuity (due to the $+i\epsilon$ prescription in the standard part of the propagator) and the imaginary parts of the amplitude. This is useful for checking unitarity because

$$\operatorname{Im}\mathcal{M}_\kappa(p_0+i\epsilon) = (\operatorname{Im}\mathcal{M}_s(p_0+i\epsilon))\mathcal{M}_4 \tag{5.79}$$

appears on the left hand side of (5.74).

Thus checking unitarity involves computing the discontinuity of the amplitude (5.75) and then comparing that result to the right hand side of (5.74). The discontinuity can be computed using the usual cutting rules algorithm [56]. In the present case the cuts should be made along the two internal lines in the loop diagram (momenta q and q'). The cutting rule algorithm replaces all the factors in f_0 by δ-functions as follows

$$\frac{1}{(q^2 - m^2 + i\epsilon)} \to -2\pi i \delta(q^2 - m^2) \tag{5.80}$$

and similarly for the primed variables. These δ-functions allow to evaluate the integrals along the q_0, q_0' directions. As for the integrals involving f_4 in $\mathcal{M}_\kappa$, they can be evaluated directly by replacing them by the residues of the two poles along the fifth-dimension axis, for example

$$\int \frac{dq_4}{(2\pi)} \frac{1}{(q_4^2 - \kappa^2 - m^2 + i\epsilon)} \to \frac{i}{2q_4}. \tag{5.81}$$

On the right hand side, q_4 stands for the position of the pole. After these manipulations, the discontinuity of the diagram is found to be

$$\begin{aligned} \mathrm{Disc}\, i\mathcal{M}_\kappa\, \delta^{(5)} = \frac{\lambda^2}{2} \int \frac{d^3q}{(2\pi)^3} \frac{1}{2q_0} \frac{1}{2q_4} \int \frac{d^3q'}{(2\pi)^3} \frac{1}{2q_0'} \frac{1}{2q_4'} \\ \times (2\pi)^5 \delta^{(5)}(p + p' - q - q')\, \delta^{(5)}(q + q' - k - k'). \end{aligned} \tag{5.82}$$

Returning to the right hand side of (5.74) and inserting an identity operator in the middle of $TT^\dagger$ gives

$$\begin{aligned} &\langle k\, k_4,\, k'\, k_4' | T^\dagger T | p\, p_4,\, p'\, p_4' \rangle \\ &\quad = \sum_n \left(\prod \int \frac{d^3q}{(2\pi)^3} \frac{1}{2q_0} \frac{1}{2q_4} \right) \\ &\quad \times \langle k\, k_4,\, k'\, k_4' | T^\dagger | \{q\, q_4\} \rangle \langle \{q\, q_4\} | T | p\, p_4,\, p'\, p_4' \rangle. \end{aligned} \tag{5.83}$$

Here the sum is over all possible intermediate configurations and the factors in parenthesis are the one-particle phase space integrals from (5.66) (see [56] for more details on notation). For the whole expression to be of order λ^2, each of the matrix elements $\langle \cdot | T | \cdot \rangle$ on the right hand side should correspond to single-vertex diagrams which are valued λ. There is only one possible such configuration and it contains two intermediate particles. Thus (5.83) reduces to

$$\begin{aligned} &\langle k\, k_4,\, k'\, k_4' | T^\dagger T | p\, p_4,\, p'\, p_4' \rangle \\ &\quad = \lambda^2 \int \frac{d^3q}{(2\pi)^3} \frac{1}{2q_0} \frac{1}{2q_4} \int \frac{d^3q'}{(2\pi)^3} \frac{1}{2q_0'} \frac{1}{2q_4'} \\ &\quad \times (2\pi)^5 \delta^{(5)}(p + p' - q - q')\, \delta^{(5)}(q + q' - k - k'), \end{aligned} \tag{5.84}$$

which is very close to (5.82). The usual discrepancy of $1/2$ is due to the fact (5.84) should be symmetrized with respect to the intermediate particles labelled by q, q_4 and q', q_4'. The result shows that the proposed Feynman rules generate unitary amplitudes, at least to second order in the coupling constant λ.

Renormalization

Another interesting question to ask is whether the proposed model is renormalizable. To answer this question properly, one should first understand the physical meaning of the fifth dimension in momentum space. Nevertheless, a quick assessment of this issue can still be obtained by looking at the degree of superficial divergence for various Feynman diagrams that can arise.

The superficial degree of divergence D of a Feynman diagram is the difference in powers of momentum in the numerator and denominator of a Feynman diagram evaluation. In the proposed model, the separation of the momentum dependence in the propagators implies that all amplitudes $\mathcal{M}_\kappa$ can be split into a product

$$\mathcal{M}_\kappa = \mathcal{M}_s \, \mathcal{M}_4, \tag{5.85}$$

where $\mathcal{M}_s$ is the standard piece containing the usual propagators, coupling constants, and integrals over four-momenta, and $\mathcal{M}_4$ is related to the new component of momentum. The degree of divergence D_s of the first sector is just the usual one for ϕ^4 theory, $D_s = 4L - 2P$, where L is the number of loops and P is the number of propagators. Using the combinatorial relation

$$L = 1 + \frac{1}{2}P - \frac{1}{4}N, \tag{5.86}$$

where N is the number of nodes in the diagram, gives

$$D_s = 4 - N : \tag{5.87}$$

only a finite number of amplitudes diverge so that the standard sector of the theory is renormalizable. In the sector defined by $\mathcal{M}_4$, the degree of divergence is $D_4 = L - 2P$. Substituting the same combinatorial relation for L as before gives

$$D_4 = 1 - \frac{1}{4}N - \frac{3}{2}P. \tag{5.88}$$

Since all potentially divergent diagrams that contain a loop have $P > 0$, the last term in this expression guarantees that D_4 is always negative. Thus, the new sector of the model is ultra-violet finite. Put together, these observations suggest that the full scalar field theory is renormalizable. (Note that this conclusion is different from what one would have obtained from an analysis of a ϕ^4 theory in five dimensions in the usual sense, which would have suggested non-renormalizability, or from an analysis that ignored the factorization of amplitudes, which would have suggested super-renormalizability.) Given that these power-counting estimates are encouraging, the renormalization program should now be carried out systematically to verify the validity of the estimates and to find out how radiative corrections from the extra dimension affect scattering amplitudes. In what follows, however, attention is shifted to discuss how the proposed framework can be applied to quantum electrodynamics (QED).

Electrodynamics

The primary goal of any extension of QED should be to reproduce all the amplitudes of the standard theory at low energies. In the present context, it is important to ensure that conservation of the momentum in the fifth momentum component is compatible with all the standard QED processes. When extending quantum electrodynamics, a theory with many types of particles, several questions arise about the properties of the p_4 momentum. Should all particle types have the same magnitude of the constant κ? Should physical particles all have their p_4 momenta carry the same sign? To answer such questions, it is useful to consider some simple scattering experiments.

As a first example, consider the reaction $e^+e^- \to \tau^+\tau^-$. In the center of mass frame, the incoming particles both have p_4 of magnitude $\sqrt{\kappa_e^2 + m_e^2}$; the constant κ_e has a subscript e to emphasize that it is labeling the κ-shell of an electron. Suppose further that the outgoing particles both have their fifth components of momentum of magnitude $\sqrt{\kappa_\tau^2 + m_\tau^2}$. Momentum is taken to be conserved, $p_4^{e^+} + p_4^{e^-} = p_4^{\tau^+} + p_4^{\tau^-}$. From this, one can infer that if all the momenta are of the same sign, then the values of κ_e and κ_τ must be different. If, however, the momenta for particles and anti-particles have opposite signs, then the conservation equation is satisfied trivially.

As another example, consider the process $e^+e^- \to \tau^+\tau^-\tau^+\tau^-$ or any similar one in which there are more than two outgoing particles. Momentum conservation forbids such processes if all the particles have p_4 of the same sign. However, such processes can occur if particles and anti-particles carry p_4 of opposite signs. It should be concluded, therefore, that p_4 must be different for particles and anti-particles; in this sense, p_4 seems to be directly correlated with the particle charge. No conclusion can be reached on the values of κ for the different particle species. It seems reasonable at this points to set the values of κ for all species equal for simplicity.

As a final example, consider the process $e^- \to e^-\gamma\cdots\gamma$ where an electron radiates one or more photons. This process is forbidden in standard QED in vacuo; it can occur, however, in the presence of an external electric field, for example when the electron travels in a liquid. If the scale κ_γ for the photon is assumed to be non-zero, then this radiation process is forbidden due to momentum conservation in the fifth dimension. This would be a drastic modification of standard electrodynamics and would likely be met with strong experimental constraints, although these are not considered here.

In terms of particle kinematics, perhaps a less radical approach to allowing the $e^- \to e^-\gamma\cdots\gamma$ process would be to take $\kappa_\gamma = 0$. But this choice of κ_γ would pose restrictions on the possible interpretation of the proposed framework. In the DSR literature, κ is usually assumed to be remnant of quantum gravity and is thus set close to the Planck energy. Its large and non-zero size allows to define the bicrossproduct coordinates and to expand dispersion relations to in a series in $\hat{p}_0/\kappa$. If the parameter κ_γ were set to zero, it would no longer be possible to use the bicrossproduct basis to write modified dispersion relations for photons.

To summarize, the sample processes considered suggest that particles and anti-particles should have the same deformation scale κ but opposite signs of p_4. In this sense the value of the p_4 momentum is directly correlated with the particle charge (note that this allows

one to think of charge conjugation in terms of a reversal of p_4 momentum just like, say, time conjugation can be understood as a reversal in p_0). The photon is assumed to carry positive momentum p_4 dependent on a scale κ_γ which may have to be set to zero. There is no indication as to whether the values of κ for different fermions should be the same or different. The remainder of this section shows how these ideas could be implemented.

The free fermion fields can be defined in a similar fashion as done in the section on the scalar field,

$$\begin{aligned}\psi(x,x_4) = &\int \frac{d^3p}{(2\pi)^3}\frac{1}{\sqrt{2p_0}}\frac{1}{\sqrt{2p_4}} \\ &\times \sum_s \left(a^s_{\mathbf{p}} u^s(p) e^{-ip\cdot x} + b^{s\dagger}_{\mathbf{p}} v^s(p) e^{ip\cdot x}\right) e^{-ip_4 x_4}\end{aligned} \tag{5.89}$$

and similarly for $\overline{\psi}(x,x_4)$. The operators $a^s_{\mathbf{p}}, b^s_{\mathbf{p}}$, their conjugates, and the four-dimensional spinors u^s, v^s and their conjugates are the usual ones. The presence of the new scale is seen in the new phase functions $e^{\pm ip_4x_4}$ and in factors of $p_4^{-1/2}$. Operators $b^{s\dagger}$ and $a^{s\dagger}$ create particles with the same four-momentum p but with opposite values of the fifth momentum component p_4, in accordance with the insights obtained previously. The propagator for one of these fermions can be computed as in the section on the scalar field with the result

$$D_F(p) = \left(\frac{\not{p} + m}{p^2 - m^2 + i\epsilon}\right)\left(\frac{1}{p_4^2 - \kappa^2 - m^2 + i\epsilon}\right). \tag{5.90}$$

Similarly, a modification of the electromagnetic field $A(x,x_4)$ can yield

$$D_{F\mu\nu}(p) = \left(\frac{\eta_{\mu\nu}}{q^2 + i\epsilon}\right)\left(\frac{1}{q_4^2 - \kappa_\gamma^2 + i\epsilon}\right). \tag{5.91}$$

The main difference between this expression and the one used for the fermion propagator is that the energy scale is κ_γ rather than κ.

For the purpose of introducing an interaction between fermions and the photons, it is useful to have a Lagrangian or action formulation of the theory. An action for the photon field giving rise to the desired propagator could be, in Lorentz gauge,

$$S_A \propto \frac{1}{2}\int \frac{d^4q\, dq_4}{(2\pi)^5}\left[A_\mu(-q,-q_4)(q_4^2 - \kappa_\gamma^2)(q^2)A^\mu(q,q_4)\right]. \tag{5.92}$$

Similarly, from the structure of the fermion propagator, it seems reasonable to guess

$$S_\psi \propto \int \frac{d^4p\, dp_4}{(2\pi)^5}\left[\overline{\psi}(-p,-p_4)\left(p_4^2 - \kappa^2\right)(\not{p} - m)\,\psi(p,p_4)\right]. \tag{5.93}$$

In a five dimensional position-space representation, these actions would lead to a higher-derivative theory. Although this feature often implies the presence of ghost particles, the present model can be expected to preserve unitarity in a similar fashion as in the case of the scalar field. The reason behind this lies in the fact that the extra derivatives only act along the extra dimension. For convenience, it is also useful to define

$$\Psi(p,p_4) = \left(p_4^2 - \kappa^2\right)^{1/2}\psi(p,p_4) \tag{5.94}$$

in terms of which the fermion action resembles the usual form

$$S_\psi \propto \int \frac{d^4p\, dp_4}{(2\pi)^5} \left[\overline{\Psi}(-p,-p_4)\,(\not{p} - m)\,\Psi(p,p_4)\right]. \tag{5.95}$$

The simplicity of the model is now evident. The significant modification to QED arises in the interaction.

The definitions of interaction vertices and the coupling constant are usually obtained by replacing partial derivatives by covariant derivatives, $\partial_\mu \to \partial_\mu + eA_\mu$. In momentum space, this replacement roughly translates to $p_\mu \to p_\mu + eA_\mu(q)$ and a condition enforcing momentum conservation at the vertex. In the current scenario, the interaction term could be

$$\begin{aligned} S_{int} \propto e \left(\int \frac{d^4p\, dp_4}{(2\pi)^5}\right)\left(\int \frac{d^4p'\, dp'_4}{(2\pi)^5}\right)\left(\int \frac{d^4q\, dq_4}{(2\pi)^5}\right) \\ \left[\overline{\Psi}(p,p_4)\right]\left[(q_4^2 - \kappa_\gamma^2)^{1/2}\gamma^\mu A_\mu(q,q_4)\right]\left[\Psi(p',p'_4)\right] \\ \times (2\pi)^4\,\delta^{(4)}(p+p'+q)\,(2\pi)\,\delta(p_4+p'_4+q_4). \end{aligned} \tag{5.96}$$

Despite its long form, this term is not difficult to understand. The last line of (5.96) imposes momentum conservation in all five-dimensions. The first and second line express that two fermions are interacting with one photon in five dimensions. The factor e in front of the integrals is the usual coupling constant used in perturbation series. There are also some factors depending on the fifth component of momentum. These factors can be understood as arising from (5.95) by the minimal coupling prescription. The factor associated with the A field is introduced so that all three fields enter symmetrically in the expression. A consequence of this minimal coupling prescription is that diagrammatic Ward identities are automatically preserved in this model just like in standard QED.

From equations (5.95), (5.92) and the interaction term (5.96), it is clear that the structure of the five-dimensional model is very similar to standard QED. When calculating amplitudes of various Feynman diagrams, expression arising in this model split to $\mathcal{M}_\kappa = \mathcal{M}_s\mathcal{M}_4$ just like in the scalar theory. Moreover, the extra factors in the propagators (5.90) and (5.91) get cancelled by similar factors coming from the interaction term (5.96). Thus the part $\mathcal{M}_4$ of an amplitude that depends on the extra dimension is either unity or an infinite integral over undetermined momenta p_4 inside loops. It is therefore clear that the problem of ultra-violet divergences in this model is actually worse than usual. Nevertheless, it may still be possible to deal with those new divergences consistently due to their simple form, c.f. the previous comments on divergences.

5.3 Discussion

The main motivations for studying Deformed Special Relativity are the following. First, the possibility of special relativity being an approximation to a different symmetry is quite intriguing by itself. Second, the connection of deformed special relativity with non-commutative spaces and thus to certain models for the micro-structure of spacetime is also relevant to the viewpoint presented in this thesis. Third, the concrete framework where the Planck scale

plays an important role seems a promising foundation around which the phenomenology of quantum gravity could be built. There are, however, still some important open questions in DSR regarding its observable consequences and its interpretation as a physical theory [52, 53]. The results of this work offer some answers but also leave many open questions.

Results and Open Issues

Regarding the free particle, different versions of DSR can be seen as realizations of the same five dimensional constrained system via distinct gauge fixings. The formulation of the DSR particle as a five dimensional system has the advantage that it explains the non-cummutativity of spatial coordinates x as a residual effect in the $4d$ reduced phase space after gauge fixing. Also, the specific gauge fixing functions $\mathcal{C}_{5d}$ which lead to different versions of DSR can be written explicitly. Finally, and perhaps most importantly, the formulation in terms of a higher dimension brings forth the viewpoint that the proposed deformations of special relativity are an extension of standard relativity. This in turn motivates the field theory proposal discussed in section 5.2.

The aim of the proposal of section 5.2 is to investigate how the energy scale κ and the curvature equation (5.1) can be incorporated in a quantum field theory. A key step in formulating the model is the adoption a five dimensional flat space. Related to this transition is the assumption that momentum is conserved linearly in the higher dimensional space. Most of the analysis is carried out for a scalar field model. The proposed ϕ^4-like theory is simple enough so that it is possible to perturbatively compute amplitudes of scattering processes via Feynman diagrams. The amplitudes of the theory reproduce the expected results at leading order and the theory is explicitly shown to be unitary to second order in the coupling parameter. The new scale does not regularize loop integrals and the theory needs to be renormalized as usual. Nevertheless, the proposed theory differs from standard ϕ^4 theory in various ways, most notably in that certain processes become kinematically forbidden due to momentum conservation in the extra dimension; momentum conservation implements a new super-selection rule on process amplitudes.

Thinking about electrodynamics leads to several conclusions about the properties of the postulated extra dimension. If the proposed framework is to reproduce low energy phenomena like electron-positron scattering, particles and anti-particles must carry momenta p_4 of opposite sign. Thus, the momentum in the extra dimension must be correlated with the particle charge. For processes involving photons, the framework is faced with one of two options, both of which have strong implications. One possibility is that photons have $p_4 = \kappa_\gamma \neq 0$ and certain higher order processes such as $e^- \to e^-\gamma\cdots\gamma$ are kinematically suppressed. Alternatively, photons have $p_4 = \kappa_\gamma = 0$ and all processes occur as usual but the constraint (5.1) loses its original interpretation as setting a curvature in the four-dimensional momentum space of the photon. This would imply that photons may not display deformed dispersion relations. Either of these options should be interesting to explore further. In any case, it is both surprising and encouraging that certain properties of the extra dimension, which in this work should be thought of as a byproduct of modeling quantum gravity, can be deduced from low energy experiments using very simple kinematical arguments.

What does this framework say about Planck scale phenomenology? Unfortunately, this

question does not have a clear answer at this point because of the unclear interpretation of the five dimensional momentum variables and their relation to observable quantities. It may be that the physically relevant momenta are ones that, like the bicrossproduct coordinates, are coordinates on de Sitter space [53]. If so, then in order to convert the amplitudes calculated in the proposed framework to observed cross-sections, one should replace all the five-dimensional momentum variables used in the above calculations by four-dimensional coordinates on the physical space. This is a subtle point: although the amplitude $\mathcal{M}_\kappa$ would be of the same functional form as the standard amplitude $\mathcal{M}_s$, the former would give a cross section σ_κ that deviates slightly from the usual σ_s,

$$\sigma_\kappa = \sigma_s \left(1 + c_1 \frac{\hat{p_0}}{\kappa} + \dots \right), \tag{5.97}$$

where c_1 is some order-unity constant and the other terms are suppressed by further factors of $\hat{p}_0/\kappa$. Computations of scattering processes in this model would resemble the methods used in previous work on reactions in DSR [54]. It would be very useful to obtain experimental feedback on this matter.

The physical interpretation for the fifth dimension, both in momentum space and the dual position space, is one of the issues that deserve more attention. In particular, the role of the gauge-fixing function $\mathcal{C}_{5d}$ in the field theory context could be studied. Other open issues are related to the fact that the interacting field theories are defined only perturbatively through a set of Feynman rules. It would be satisfying to have their formulation in terms of an action principle from which the mechanism implementing the two constraints could be understood. This should be particularly useful in the domain of quantization of the gauge field where an action principle might be able to discriminate between the options of $\kappa_\gamma = 0$ and $\kappa_\gamma \neq 0$. With regards to the scattering amplitudes, the issue of renormalizability should be addressed systematically. A related concern is to check that loop effects and radiative corrections in the modified electrodynamics are not in contradiction with existing high-precision experiments. These technical checks provide the possibility to test or rule out the proposal.

Comparison with Other Approaches

It is both fair and appropriate to mention another viewpoint on formulating field theory based on DSR. Elsewhere, research on DSR and modified dispersion relations has been motivated by the connection of the deformed algebras of the bicrossproduct basis with Hopf algebras and quantum groups. From the algebraic point of view, the Poincare algebra cannot be deformed in the sense that any proposed deformation can be smoothly mapped back to the familiar algebra (while this is true in the mathematical sense, the work in this section shows that the deformations may have physical implications.) However, Hopf algebras based on the Poincare algebra can be deformed and consequently the literature on DSR as a Hopf algebra puts a lot of emphasis on the coalgebra related to the bicrossproduct. In brief, a Hopf algebra is a structure in which in addition to the operators N_i, M_{ij}, and p_μ, and their algebra (commutation relations) one also has addition structure. There is a coproduct Δ

which acts (in the bicrossproduct basis) as

$$\begin{aligned}\Delta(P_i) &= P_i \otimes e^{-P_0/\kappa} + 1 \otimes P_i \\ \Delta(P_0) &= P_0 \otimes 1 + 1 \otimes P_0\end{aligned} \tag{5.98}$$

and an antipode map S which is defined by

$$\begin{aligned}S(P_i) &= -e^{-P_0/\kappa} \\ S(P_0) &= -P_0.\end{aligned} \tag{5.99}$$

In addition there is a co-unit but it is not important for the current purposes. The main point is that when the coproducts (5.98) are used to define total momenta for a collection of particles, the total momenta are bounded from above by the Planck scale just as the momentum of a single particle is bounded. (This is essentially the "soccer-ball" problem mentioned earlier.) A recent review on this approach to DSR is [30].

Approaches to studying field theories that take the above Hopf structure seriously start with actions defined on a non-commutative space. For example, an action for a free scalar field [46] can be

$$S = \frac{1}{2}\int d^4\mu(x)\ \partial_\mu\phi(x)^\dagger \star \partial^\mu\phi(x) + m^2\phi(x)^\dagger \star \phi(x). \tag{5.100}$$

Field multiplication on the non-commutative space is defined through the "star-product" compatible with the relations (5.98). At the end of the day, the physics of such a model is mapped to a non-local theory with an infinite number of derivatives on a standard flat Minkowski space.

In the language presented in the previous subsections, the approach based on Hopf-algebras is based on the reduced phase space of the field rather than on the higher dimensional flat space. This may have some advantages over the proposal of section 5.2. For example, the action integral is over four spatial dimensions and so there are no issues with interpreting any new dimensions. Also, it is hoped that working on the reduced phase may have a regulatory effect on the ultraviolet behavior of scattering amplitudes. However, a large drawback of the Hopf-algebra approach is that interacting theories have not been formulated and studied in very much detail and most of the effort has focussed on free theories, the main obstacle to working with interacting theories being the appearance of new derivative terms and ambiguities associated with conservation laws. Thus those alternative works are still have not made contact with physically interesting examples of quantum field theories (QED, etc.) and experiments.

6 Conclusion

In conclusion, it is alluring to look back to the beginning, evaluate progress made on the two themes spelled out in the introduction, and reflect on the possibility for advances in quantum gravity in the near future. The two themes in the introduction were understanding the possible micro-structure of space at the Planck scale and seeing how this it might reveal itself through modifications to particle physics. While the results obtained in various subtopics related to these themes and their implications were already discussed in the previous sections, they are put into a broader context here.

With respect to the structure of spacetime at the Planck scale, results from the Causal Dynamical Triangulation models suggest there are still several subtle and delicate issues that should be studied and understood. Yet in CDT models it is hard to make progress analytically (at least in $2+1$ and $3+1$ dimensions) and hence it may be fruitful to investigate other models which are in some sense simpler, for example quantum graphity. More analytic work on that system should still be possible thanks to available techniques in condensed matter systems on infinite range interactions and symmetry breaking. Of course, just like in dynamical triangulation models, in the end computer simulations may have to be used to check the analytic results. On a different note, it would also be interesting to connect models like graphity with Einstein's equations of general relativity. Since the graphity model presented here is not directly based on Einstein's equations, the model might have to be modified for this to be possible. An approach one can try in order to achieve this might be to first map a graphity-like Hamiltonian to a dynamical triangulation or spin-foam model.

All of the issues studied here are relevant for the broad problem of the low energy limit of quantum gravity. One can hope that progress on models such as graphity might provide some insights into similar issues in other well-developed approaches to quantum gravity, such as LQG. For example, one might be able to better understand the dynamics of spin networks. Finally, an interesting question to be asked is whether quantum gravity should naturally explain the evolution of the very early universe. In other words, should a quantum theory of gravity automatically provide an inflationary or alternative mechanism to explain the observed homogeneity, flatness, and anisotropies? There are still many open question in the domain of using discrete systems as cosmological models.

In addition, thinking about Planck scale physics can also bring forth questions on foundational issues such as the role of time, matter content, and other background structure in theories of physics. These questions are interesting in the sense that they are arise in many approaches to quantum gravity. An intriguing possibility that arises from the noiseless subsystems paradigm is that relational systems may in fact be subsystems of other non-relational systems, and vice versa. Beyond providing a new perspective on the debate on background independence in physics, this kind of interdependency hints that calculational tools from one set of theories may be applicable to the other. This line of thought is still largely unexplored

and, given its different nature from the model building and scenarios discussed above, could be of interest to the quantum gravity community irrespective of what specific model turns out to be favored by observations.

Coming to particle phenomenology, one can imagine that a quantum theory of gravity will provide new definitions for low energy excitations and thus will emphasize that quantum field theory is an effective rather than a fundamental framework. One can also imagine that quantum gravity will leave some residual signs at low energies that may be detectable in future experiments. This work focussed on a proposal for such a residual effect in the form of a deformed symmetry principle - Deformed Special Relativity. Because of the various ambiguities in the formulation of Deformed Special Relativity and a lack of physical principle to fix them, there is currently some confusion on the status and interpretation of DSR. Thus at the moment DSR can only point to possible signatures of quantum gravity and not make final predictions. What is possible, however, is to study its internal structure and self-consistency so that perhaps DSR could indicate correlations between experimental signatures, if seen at all.

Beyond the discussion of unitarity presented in this work, one can also investigate for example quantum (one-loop) corrections to amplitudes. It should also be interesting to see whether the $5d$ field theoretic approach fit with the approaches based on the star-product. But perhaps most importantly, it would be extremely interesting to find out in detail how a deformed symmetry could arise in the low energy limit of some candidate for a quantum theory of gravity. This again ties to the low energy limit of quantum gravity but puts the focus on how particle properties are changed as a result of Planck scale physics.

It is reassuring that experimental data from various areas of physics are becoming increasingly available to guide work on quantum gravity. Model building should try to connect with the experiments as early in their development as possible because the goal of this kind of research is, after all, to deduce what the physics of the Planck scale might be. As the experimental evidence relevant to quantum gravity can and will be revealed in many forms, it is important to remember that insight can be obtained by combining complementary approaches; in particular it is possible that understanding will come through the reconciliation of large-scale and small-scale phenomena.

References

[1] T. Thiemann, "Lectures on loop quantum gravity," Lect. Notes Phys. **631**, 41 (2003) [arXiv:gr-qc/0210094];
C. Rovelli, *Quantum gravity*, Cambridge University Press, 2004;
L. Smolin, "An invitation to loop quantum gravity," arXiv:hep-th/0408048.

[2] G. Amelino-Camelia, J. R. Ellis, N. E. Mavromatos, D. V. Nanopoulos and S. Sarkar, "Potential Sensitivity of Gamma-Ray Burster Observations to Wave Dispersion in Vacuo," Nature **393**, 763 (1998) [arXiv:astro-ph/9712103].

[3] L. Bombelli, J. H. Lee, D. Meyer and R. Sorkin, "Space-Time As A Causal Set," Phys. Rev. Lett. **59**, 521 (1987);
R. D. Sorkin, "Causal sets: Discrete gravity," arXiv:gr-qc/0309009.

[4] J. Ambjorn, J. Jurkiewicz and R. Loll, "A non-perturbative Lorentzian path integral for gravity," Phys. Rev. Lett. **85**, 924 (2000) [arXiv:hep-th/0002050];
J. Ambjorn and R. Loll, "Non-perturbative Lorentzian quantum gravity, causality and topology change," Nucl. Phys. B **536**, 407 (1998) [arXiv:hep-th/9805108];
J. Ambjorn, J. Jurkiewicz and R. Loll, "Non-perturbative 3d Lorentzian quantum gravity," Phys. Rev. D **64**, 044011 (2001) [arXiv:hep-th/0011276];
J. Ambjorn, J. Jurkiewicz and R. Loll, "Dynamically triangulating Lorentzian quantum gravity," Nucl. Phys. B **610**, 347 (2001) [arXiv:hep-th/0105267];
J. Ambjorn, J. Jurkiewicz and R. Loll, "Emergence of a 4D world from causal quantum gravity," Phys. Rev. Lett. **93**, 131301 (2004) [arXiv:hep-th/0404156].

[5] F. Markopoulou and L. Smolin, "Gauge fixing in causal dynamical triangulations" [arXiv:hep-th/0409057].

[6] T. Konopka, "Foliations and 2+1 causal dynamical triangulation models," Phys. Rev. D **73**, 024023 (2006) [arXiv:hep-th/0505004].

[7] J. Ambjorn, M. Carfora and A. Marzuoli, "The geometry of dynamical triangulations" [arXiv:hep-th/9612069].

[8] D. Gabrielli, "Polymeric phase of simplicial quantum gravity," Phys. Lett. B **421**, 79 (1998) [arXiv:hep-lat/9710055].

[9] J. B. Hartle, "Simplicial Minisuperspace. I. General Discussion," J. Math. Phys. **26**, 804 (1985).

[10] D. P. Rideout, "Dynamics of causal sets," arXiv:gr-qc/0212064.

[11] T. Konopka, F. Markopoulou and L. Smolin, "Quantum graphity," arXiv:hep-th/0611197.

[12] X. G. Wen, "Artificial light and quantum order in systems of screened dipoles," Phys. Rev. B **68**, 115413 (2003) [arXiv:cond-mat/0210040];
X. G. Wen, "Quantum order from string condensations and origin of light and massless fermions," Phys. Rev. D **68**, 065003 (2003) [arXiv:hep-th/0302201];
M. Levin and X. G. Wen, "Fermions, strings, and gauge fields in lattice spin models," Phys. Rev. B **67**, 245316 (2003) [arXiv:cond-mat/0302460];
M. A. Levin and X. G. Wen, "String-net condensation: A physical mechanism for topological phases," Phys. Rev. B **71**, 045110 (2005) [arXiv:cond-mat/0404617].

[13] M. Levin and X. G. Wen, "Quantum ether: Photons and electrons from a rotor model," arXiv:hep-th/0507118.

[14] F. Markopoulou, "Towards gravity from the quantum," arXiv:hep-th/0604120.

[15] D. W. Kribs and F. Markopoulou, "Geometry from quantum particles," arXiv:gr-qc/0510052.

[16] J. B. Kogut and L. Susskind, "Hamiltonian Formulation Of Wilson's Lattice Gauge Theories," Phys. Rev. D **11**, 395 (1975).

[17] X. G. Wen, private communication.

[18] F. Markopoulou, "The internal description of a causal set: What the universe looks like from the inside," Commun. Math. Phys. **211**, 559 (2000) [arXiv:gr-qc/9811053];
F. Markopoulou, "Quantum causal histories," Class. Quant. Grav. **17**, 2059 (2000) [arXiv:hep-th/9904009];
F. Markopoulou, "An insider's guide to quantum causal histories," Nucl. Phys. Proc. Suppl. **88**, 308 (2000) [arXiv:hep-th/9912137];
E. Hawkins, F. Markopoulou and H. Sahlmann, "Evolution in quantum causal histories," Class. Quant. Grav. **20**, 3839 (2003) [arXiv:hep-th/0302111].

[19] V. Mukhanov, "Physical Foundations of Cosmology," Cambridge University Press, 2005.

[20] M. A. Nielsen and I. L. Chuang, *Quantum Computation and Quantum Information*, Cambridge University Press, 2000.

[21] P.Zanardi and M.Rasetti, Phys.Rev.Lett.**79** 3306 (1997);
D. A. Lidar, I. L. Chuang and K. B. Whaley, "Decoherence Free Subspaces for Quantum Computation," Phys. Rev. Lett. **81**, 2594 (1998) [arXiv:quant-ph/9807004];
E.Knill, R.Laflamme and L.Viola, Phys.Rev.Lett. **84** 2525 (2000);
J. Kempe, D. Bacon, D. A. Lidar and K. B. Whaley, "Theory of decoherence-free fault-tolerant universal quantum computation," Phys. Rev. A **63**, 042307 (2001).

[22] T. Konopka and F. Markopoulou, "Constrained mechanics and noiseless subsystems," arXiv:gr-qc/0601028.

[23] R. Laflamme, et al. "Introduction to NMR Quantum Information Processing," arXiv:quant-ph/020717.

[24] V. Husain, "Background independent duals of the harmonic oscillator," Phys. Rev. Lett. **96**, 221303 (2006) [arXiv:hep-th/0511131].

[25] D. Forster, H. B. Nielsen and M. Ninomiya, "Dynamical Stability Of Local Gauge Symmetry: Creation Of Light From Chaos," Phys. Lett. B **94**, 135 (1980).

[26] D. N. Page and W. K. Wootters, "Evolution Without Evolution: Dynamics Described By Stationary Observables," Phys. Rev. D **27**, 2885 (1983);
W. G. Unruh and R. M. Wald, "Time And The Interpretation Of Canonical Quantum Gravity," Phys. Rev. D **40**, 2598 (1989);
C. Rovelli, "Relational Quantum Mechanics," Int. J. of Theor. Phys. 35 (1996) 1637, arXiv:quant-ph/9609002;
R. Gambini, R. Porto and J. Pullin, "A relational solution to the problem of time in quantum mechanics and quantum gravity induces a fundamental mechanism for quantum decoherence," New J. Phys. **6**, 45 (2004) [arXiv:gr-qc/0402118].

[27] D. Poulin, "A Relational Formulation of Quantum Theory," arXiv:quant-ph/0505081.

[28] J. Magueijo, L. Smolin and C. R. Contaldi, "Holography and the scale-invariance of density fluctuations," arXiv:astro-ph/0611695.

[29] B. Z. Foster and T. Jacobson, "Quantum field theory on a growing lattice," JHEP **0408**, 024 (2004) [arXiv:hep-th/0407019].

[30] J. Kowalski-Glikman, "Doubly special relativity: Facts and prospects," arXiv:gr-qc/0603022. (to appear in 'Towards Quantum Gravity,' ed. D. Oriti, 2006).

[31] L. Freidel and E. R. Livine, "Ponzano-Regge model revisited. III: Feynman diagrams and effective field theory," Class. Quant. Grav. **23**, 2021 (2006) [arXiv:hep-th/0502106].

[32] T. J. Konopka and S. A. Major, "Observational limits on quantum geometry effects," New J. Phys. **4**, 57 (2002) [arXiv:hep-ph/0201184].

[33] D. Mattingly, "Modern tests of Lorentz invariance," Living Rev. Rel. **8**, 5 (2005) [arXiv:gr-qc/0502097].

[34] F. Girelli, T. Konopka, J. Kowalski-Glikman and E. R. Livine, "The free particle in deformed special relativity," Phys. Rev. D **73**, 045009 (2006) [arXiv:hep-th/0512107].

[35] T. Konopka, "A field theory model with a new Lorentz-invariant energy scale," arXiv:hep-th/0601030.

[36] D. Colladay and V. A. Kostelecky, "Lorentz-violating extension of the standard model," Phys. Rev. D **58**, 116002 (1998) [arXiv:hep-ph/9809521];
R. C. Myers and M. Pospelov, "Ultraviolet modifications of dispersion relations in effective field theory," Phys. Rev. Lett. **90**, 211601 (2003) [arXiv:hep-ph/0301124].

[37] D. Mattingly, "Modern tests of Lorentz invariance," Living Rev. Rel. **8**, 5 (2005) [arXiv:gr-qc/0502097];
T. Jacobson, S. Liberati and D. Mattingly, "Lorentz violation at high energy: Concepts, phenomena and astrophysical constraints," Annals Phys. **321**, 150 (2006) [arXiv:astro-ph/0505267];
R. Bluhm, "Overview of the SME: Implications and phenomenology of Lorentz violation," arXiv:hep-ph/0506054.

[38] G. Amelino-Camelia, "Relativity in space-times with short-distance structure governed by an observer-independent (Planckian) length scale," Int. J. Mod. Phys. D **11**, 35 (2002) [arXiv:gr-qc/0012051];
J. Magueijo and L. Smolin, "Lorentz invariance with an invariant energy scale," Phys. Rev. Lett. **88**, 190403 (2002) [arXiv:hep-th/0112090];
J. Magueijo and L. Smolin, "Generalized Lorentz invariance with an invariant energy scale," Phys. Rev. D **67**, 044017 (2003) [arXiv:gr-qc/0207085].

[39] J. Lukierski, H. Ruegg, A. Nowicki and V. N. Tolstoi, "Q deformation of Poincare algebra," Phys. Lett. B **264**, 331 (1991);
J. Lukierski, H. Ruegg and W. J. Zakrzewski, "Classical quantum mechanics of free kappa relativistic systems," Annals Phys. **243**, 90 (1995) [arXiv:hep-th/9312153];
J. Lukierski, A. Nowicki and H. Ruegg, "New quantum Poincare algebra and k deformed field theory," Phys. Lett. B **293**, 344 (1992).

[40] G. Amelino-Camelia, L. Smolin and A. Starodubtsev, "Quantum symmetry, the cosmological constant and Planck scale phenomenology," Class. Quant. Grav. **21**, 3095 (2004) [arXiv:hep-th/0306134];
F. Girelli, E. R. Livine and D. Oriti, "Deformed special relativity as an effective flat limit of quantum gravity," Nucl. Phys. B **708**, 411 (2005) [arXiv:gr-qc/0406100];
L. Smolin, "Falsifiable predictions from semiclassical quantum gravity," arXiv:hep-th/0501091;
K. Imilkowska and J. Kowalski-Glikman, "Doubly Special Relativity as a Limit of Gravity," arXiv:gr-qc/0506084.

[41] L. Freidel, J. Kowalski-Glikman and L. Smolin, "2+1 gravity and doubly special relativity," Phys. Rev. D **69**, 044001 (2004) [arXiv:hep-th/0307085];
L. Freidel and E. R. Livine, "Ponzano-Regge model revisited. III: Feynman diagrams and effective field theory," Class. Quant. Grav. **23**, 2021 (2006) [arXiv:hep-th/0502106];
L. Freidel and E. R. Livine, "Effective 3d Quantum Gravity and Non-Commutative Quantum Field Theory," arXiv:hep-th/0512113.

[42] S. Hossenfelder, "Self-consistency in theories with a minimal length," Class. Quant. Grav. **23**, 1815 (2006) [arXiv:hep-th/0510245].

[43] M. Daszkiewicz, K. Imilkowska, J. Kowalski-Glikman and S. Nowak, "Scalar field theory on kappa-Minkowski space-time and doubly special relativity," Int. J. Mod. Phys. A **20**, 4925 (2005) [arXiv:hep-th/0410058].

[44] G. Amelino-Camelia and M. Arzano, "Coproduct and star product in field theories on Lie-algebra non-commutative space-times," Phys. Rev. D **65**, 084044 (2002) [arXiv:hep-th/0105120].

[45] M. Dimitrijevic, L. Jonke, L. Moller, E. Tsouchnika, J. Wess and M. Wohlgenannt, "Deformed field theory on kappa-spacetime," Eur. Phys. J. C **31**, 129 (2003) [arXiv:hep-th/0307149];
M. Dimitrijevic, F. Meyer, L. Moller and J. Wess, "Gauge theories on the kappa-Minkowski spacetime," Eur. Phys. J. C **36**, 117 (2004) [arXiv:hep-th/0310116].

[46] L. Freidel, J. Kowalski-Glikman and S. Nowak, "From noncommutative kappa-Minkowski to Minkowski space-time," arXiv:hep-th/0612170.

[47] G. Amelino-Camelia, "Doubly special relativity," Nature **418**, 34 (2002) [arXiv:gr-qc/0207049];
J. Kowalski-Glikman, "Introduction to doubly special relativity," Lect. Notes Phys. **669**, 131 (2005) [arXiv:hep-th/0405273];
G. Amelino-Camelia, J. Kowalski-Glikman, G. Mandanici and A. Procaccini, "Phenomenology of doubly special relativity," Int. J. Mod. Phys. A **20**, 6007 (2005) [arXiv:gr-qc/0312124].

[48] J. Kowalski-Glikman, "De Sitter space as an arena for doubly special relativity," Phys. Lett. B **547**, 291 (2002) [arXiv:hep-th/0207279];
J. Kowalski-Glikman and S. Nowak, "Doubly special relativity and de Sitter space," Class. Quant. Grav. **20**, 4799 (2003) [arXiv:hep-th/0304101].

[49] N. R. Bruno, G. Amelino-Camelia and J. Kowalski-Glikman, *Deformed boost transformations that saturate at the Planck scale*, Phys. Lett. B **522** (2001) 133 [arXiv:hep-th/0107039].

[50] J. Kowalski-Glikman, *Planck-scale relativity from quantum kappa-Poincare algebra*, Mod. Phys. Lett. A **17**, 1 (2002) [arXiv:hep-th/0107054].

[51] S. Majid and H. Ruegg, "Bicrossproduct structure of kappa Poincare group and non-commutative geometry," Phys. Lett. B **334**, 348 (1994) [arXiv:hep-th/9405107].

[52] D. V. Ahluwalia-Khalilova, "A freely falling frame at the interface of gravitational and quantum realms," Class. Quant. Grav. **22**, 1433 (2005) [arXiv:hep-th/0503141];

[53] S. Liberati, S. Sonego and M. Visser, "Interpreting doubly special relativity as a modified theory of measurement," Phys. Rev. D **71**, 045001 (2005) [arXiv:gr-qc/0410113];
R. Aloisio, A. Galante, A. Grillo, S. Liberati, E. Luzio and F. Mendez, "Deformed special relativity as an effective theory of measurements on quantum gravitational backgrounds," Phys. Rev. D **73**, 045020 (2006) [arXiv:gr-qc/0511031];
F. Girelli and E. R. Livine, "Physics of deformed special relativity: Relativity principle revisited," arXiv:gr-qc/0412004;
F. Girelli and E. R. Livine, "Physics of Deformed Special Relativity," Braz. J. Phys. **35**, 432 (2005) [arXiv:gr-qc/0412079].

[54] S. Judes and M. Visser, "Conservation Laws in Doubly Special Relativity," Phys. Rev. D **68**, 045001 (2003) [arXiv:gr-qc/0205067];
D. Heyman, F. Hinteleitner and S. Major, "On reaction thresholds in doubly special relativity," Phys. Rev. D **69**, 105016 (2004) [arXiv:gr-qc/0312089];
S. Hossenfelder, M. Bleicher, S. Hofmann, J. Ruppert, S. Scherer and H. Stoecker, "Collider signatures in the Planck regime," Phys. Lett. B **575**, 85 (2003) [arXiv:hep-th/0305262].

[55] F. Girelli and E. R. Livine, "Special Relativity as a non commutative geometry: Lessons for Deformed Special Relativity," arXiv:gr-qc/0407098.

[56] M. E. Peskin and D. V. Schroeder, "An Introduction to Quantum Field Theory," Westview Press, 1995.